Zero-Delay Sequential Transmission of Markov Sources over Burst Erasure Channels

Farrokh Etezadi, Ashish Khisti and Mitchell Trott

arXiv:1410.2326v1 [cs.IT] 9 Oct 2014

***Abstract*—A setup involving zero-delay sequential transmission of a vector Markov source over a burst erasure channel is studied. A sequence of source vectors is compressed in a causal fashion at the encoder, and the resulting output is transmitted over a burst erasure channel. The destination is required to reconstruct each source vector with zero-delay, but those source sequences that are observed either during the burst erasure, or in the interval of length W following the burst erasure need not be reconstructed. The minimum achievable compression rate is called the rate-recovery function. We assume that each source vector is sampled i.i.d. across the spatial dimension and from a stationary, first-order Markov process across the temporal dimension.**

For discrete sources the case of lossless recovery is considered, and upper and lower bounds on the rate-recovery function are established. Both these bounds can be expressed as the rate for predictive coding, plus a term that decreases at least inversely with the recovery window length W. For Gauss-Markov sources and a quadratic distortion measure, upper and lower bounds on the minimum rate are established when $W = 0$. These bounds are shown to coincide in the high resolution limit. Finally another setup involving i.i.d. Gaussian sources is studied and the rate-recovery function is completely characterized in this case.

***Index Terms*—Joint Source-Channel Coding, Distributed Source Coding, Gauss-Markov Sources, Kalman Filter, Burst Erasure Channels, Multi-terminal Information Theory, Rate-distortion Theory.**

I. Introduction

Real-time streaming applications require both the sequential compression, and playback of multimedia frames under strict latency constraints. Linear predictive techniques such as DPCM have long been used to exploit the source memory in such systems. However predictive coding schemes also exhibit a significant level of error propagation in the presence of packet losses [1]. In practice one must develop transmission schemes that satisfy both the real-time constraints and are robust to channel errors.

There exists an inherent tradeoff between the underlying *transmission-rate* and the *error-propagation* at the receiver in all video streaming applications. Commonly used video compression formats such as H.264/MPEG and HEVC use a combination of intra-coded and predictively-coded frames to limit the amount of error propagation. The predictively-coded frames are used to improve the compression efficiency whereas the intra-coded frames limit the amount of error propagation. Other techniques including forward error correction codes [2], leaky DPCM [3] and distributed video coding [4] can also be used to trade off the transmission rate with error propagation. Despite this, such a tradeoff is not well understood even in the case of a single isolated packet loss [5].

In this paper we study the information theoretic tradeoff between the transmission rate and error propagation in a simple source-channel model. We assume that the channel introduces an isolated erasure burst of a certain maximum length, say B. The encoder observes a sequence of vector sources and compresses them in a causal fashion. The decoder is required to reconstruct each source vector with zero delay, except those that occur during the error propagation window. The decoder can declare a *don't-care* for all the source sequences that occur in this window. We assume that is period spans the duration of the erasure burst, as well an interval of length W immediately following it. We study the minimum rate required $R(B, W)$, and define it as the *rate-recovery function*.

We first consider the case of discrete sources and lossless reconstruction and establish upper and lower bounds on the minimum rate. Both these bounds can be expressed as the rate of the predictive coding scheme, plus an additional term that decreases at-least as $H(\mathsf{s})/(W + 1)$ where $H(\mathsf{s})$ denotes the entropy of the source symbol. Our lower bound is obtained through connection to a certain multi-terminal source coding problem that captures the tension in encoding a source sequence during the error-propagation period, and outside it. The upper bound is based on a natural random-binning scheme. We also consider the case of Gauss-Markov sources and a quadratic distortion measure. We again establish upper and lower bounds on the minimum rate when $W = 0$, i.e., when instantaneous recovery following the burst erasure is imposed. We observe that our upper and lower bounds coincide in the high resolution limit, thus establishing the rate-recovery function in this regime. Finally we consider a different setup involving i.i.d. Gaussian sources, and a special recovery constraint, and obtain an exact characterization of the rate-recovery function in this special case. Many of our results also naturally extend to the case when the channel introduces multiple erasure bursts.

The remainder of the paper is organized as follows. We discuss related literature in Section II. The problem setup is described in Section III and a summary of the main results is provided in Section IV. We treat the case of discrete sources and lossless recovery in Section V and establish upper and lower bounds on the minimum rate. The optimality of binning for the special case of symmetric sources and memoryless encoders is established in Section VI. In Section VII we

Manuscript submitted June 2013, revised December 2013.

Farrokh Etezadi (fetezadi@comm.utoronto.ca) and Ashish Khisti (akhisti@comm.utoronto.ca) are with the University of Toronto, Toronto, ON, Canada, Mitchell Trott was with HP Labs, Palo Alto, USA. This work was supported by an NSERC Discovery Research Grant, a Hewlett-Packard Innovation Research Program award and an Ontario Early Research Award. This work was presented in parts at the 2012 IEEE Data Compression Conference and the 2012 Allerton Conference on Communication, Control and Computing.

consider the case of Gauss-Markov source with a quadratic distortion constraint. Section IX studies another setup involving independent Gaussian sources and a sliding window recovery constraint, where an exact characterization of the minimum rate is obtained. Conclusions appear in Section X.

Notations: Throughout this paper we represent the Euclidean norm operator by $||\cdot||$ and the expectation operator by $E[\cdot]$. The notation "log" is used for the binary logarithm, and rates are expressed in bits. The operations $H(.)$ and $h(.)$ denote the entropy and the differential entropy, respectively. The "slanted sans serif" font a and the normal font a represent random variables and their realizations respectively. The notation $\mathsf{a}_i^n = \{\mathsf{a}_{i,1}, \ldots, \mathsf{a}_{i,n}\}$ represents a length-n sequence of symbols at time i. The notation $[f]_i^j$ for $i < j$ represents $f_i, f_{i+1}, \ldots, f_j$.

II. Related Works

Problems involving real-time coding and compression have been studied from many different perspectives in related literature. The compression of a Markov source, with zero encoding and decoding delays, was studied in an early work by Witsenhausen [6]. In this setup, the encoder must sequentially compress a (scalar) Markov source and transmit it over an ideal channel. The decoder must reconstruct the source symbols with zero-delay and under an average distortion constraint. It was shown in [6] that for a k-th order Markov source model, an encoding rule that only depends on the k most recent source symbols, and the decoder's memory, is sufficient to achieve the optimal rate. Similar structural results have been obtained in a number of followup works, see e.g., [7] and references therein. The authors in [8] considered real-time communication of a memoryless source over memoryless channels, with or without the presence of unit-delay feedback. The encoding and decoding is sequential with a fixed finite lookahead at the encoder. The authors propose conditions under which symbol-by-symbol encoding and decoding, without lookahead, is optimal and more generally characterize the optimal encoder as a solution to a dynamic programming problem.

In another line of work, the problem of sequential coding of correlated vector sources in a multi-terminal source coding framework was introduced by Viswanathan and Berger [9]. In this setup, a set of correlated sources must be sequentially compressed by the encoder, whereas the decoder at each stage is required to reconstruct the corresponding source sequence, given all the encoder outputs up to that time. It is noted in [9] that the correlated source sequences can model consecutive video frames and each stage at the decoder maps to sequential reconstruction of a particular source frame. This setup is an extension of the well-known successive refinement problem in source coding [10]. In followup works, in reference [11] the authors consider the case where the encoders at each time have access to previous encoder outputs rather than previous source frames. Reference [12] considers an extension where the encoders and decoders can introduce non-zero delays. All these works assume ideal channel conditions. Reference [13] considers an extension of [9] where at any given stage the decoder has either all the previous outputs, or only the present output. A robust extension of the predictive coding scheme is proposed and shown to achieve the minimum sum-rate. However this setup does not capture the effect of packet losses over a channel, where the destination has access to all the non erased symbols. To our knowledge, only reference [3] considers the setting of sequential coding over a random packet erasure channel. The source is assumed to be Gaussian, spatially i.i.d. and temporally autoregressive. A class of linear predictive coding schemes is studied and an optimal scheme within this class, with respect to the excess distortion ratio metric is proposed. Our proposed coding scheme is qualitatively different from [3], [13] and involves a random binning based approach, which is inherently robust to the side-information at the decoder.

In other related works, the joint source-channel coding of a vector Gaussian source over a vector Gaussian channel with zero reconstruction delay has also been extensively studied. While optimal analog mappings are not known in general, a number of interesting approaches have been proposed in e.g. [14], [15] and related references. Reference [16] studies the problem of sequential coding of the scalar Gaussian source over a channel with random erasures. In [5], the authors consider a joint source-channel coding setup and propose the use of distributed source coding to compensate the effect of channel losses. However no optimality results are presented for the proposed scheme. Sequential random binning techniques for streaming scenarios have been proposed in e.g. [17], [18] and the references therein.

To the best of our knowledge, there has been no prior work that studies an information theoretic tradeoff between error-propagation and compression efficiency in real-time streaming systems.

III. Problem Statement

In this section we introduce our source and channel models and the associated definition of the rate-recovery function.

We assume that the communication spans the interval $i \in [-1, \mathcal{L}]$. At each time i, a source vector $\{\mathsf{s}_i^n\}$ is sampled, whose symbols are drawn independently across the spatial dimension, and from a first-order Markov chain across the temporal dimension, i.e.,

$$\Pr(\ \mathsf{s}_i^n = s_i^n \mid \mathsf{s}_{i-1}^n = s_{i-1}^n,\ \mathsf{s}_{i-2}^n = s_{i-2}^n, \ldots, \mathsf{s}_{-1}^n = s_{-1}^n) = \prod_{k=1}^{n} p_1(s_{i,k}|s_{i-1,k}), \qquad 0 \le i \le \mathcal{L}. \quad (1)$$

The underlying random variables $\{\mathsf{s}_i\}$ constitute a time-invariant, stationary and a first-order Markov chain with a common marginal distribution denoted by $p_{\mathsf{s}}(\cdot)$ over an alphabet $\mathcal{S}$. The sequence s_{-1}^n is sampled i.i.d. from $p_{\mathsf{s}}(\cdot)$ and revealed to both the encoder and decoder before the start of the communication. It plays the role of a synchronization frame.

A rate-R encoder computes an index $\mathsf{f}_i \in [1, 2^{nR}]$ at time i, according to an encoding function

$$\mathsf{f}_i = \mathcal{F}_i\left(\mathsf{s}_{-1}^n, \mathsf{s}_0^n, ..., \mathsf{s}_i^n\right), \qquad 0 \le i \le \mathcal{L}. \quad (2)$$

Note that the encoder in (2) is a causal function of the source sequences. A *memoryless* encoder satisfies $\mathcal{F}_i(\cdot) = \mathcal{F}_i(\mathsf{s}_i^n)$

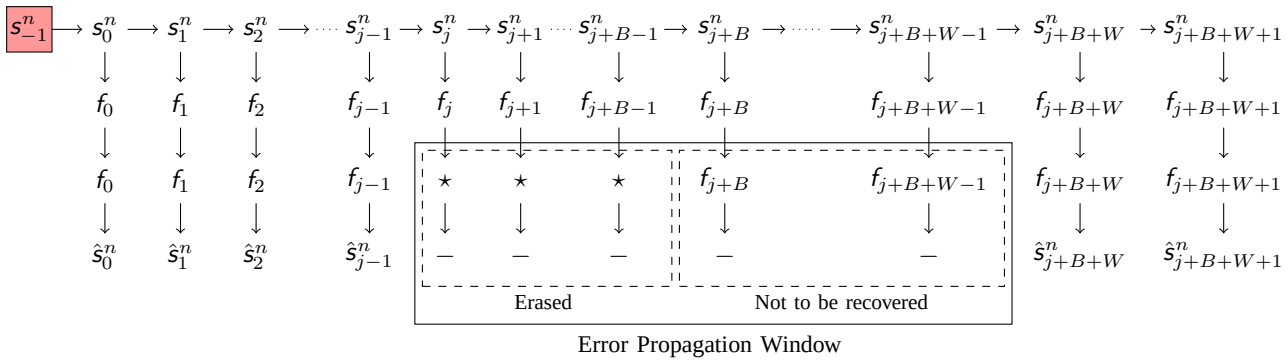

Fig. 1: Problem Setup: The encoder output f_i is a function of all the past source sequences. The channel introduces a burst erasure of length up to B. The decoder produces $\hat{s}_i^n$ upon observing the channel outputs up to time i. As indicated, the decoder is not required to produce those source sequences that are observed either during the burst erasure, or a period of W following it. The first sequence, s_{-1}^n is a synchronization frame available to both the source and destination.

i.e., the encoder does not use the knowledge of the past sequences. Naturally a memoryless encoder is very restrictive, and we will only use it to establish some special results.

The channel takes each f_i as input and either outputs $g_i = f_i$ or an erasure symbol i.e., $g_i = \star$. We consider the class of burst erasure channels. For some particular $j \geq 0$, it introduces a burst erasure such that $g_i = \star$ for $i \in \{j, j+1, ..., j+B'-1\}$ and $g_i = f_i$ otherwise i.e.,

$$g_i = \begin{cases} \star, & i \in [j, j+1, \ldots, j+B'-1] \\ f_i, & \text{else,} \end{cases} \tag{3}$$

where the burst length B' is upper bounded by B.

Upon observing the sequence $\{g_i\}_{i\geq 0}$, the decoder is required to reconstruct each source sequence with zero delay i.e.,

$$\hat{s}_i^n = \mathcal{G}_i(g_0, g_1, \ldots, g_i, s_{-1}^n), \quad i \notin \{j, \ldots, j+B'+W-1\} \tag{4}$$

where $\hat{s}_i^n$ denotes the reconstruction sequence and j denotes the time at which burst erasure starts in (3). The destination is not required to produce the source vectors that appear either during the burst erasure or in the period of length W following it. We call this period the error propagation window. Fig. 1 provides a schematic of the causal encoder (2), the channel model (3), and the decoder (4).

A. Rate-Recovery Function

We define the rate-recovery function under lossless and lossy reconstruction constraints.

1) Lossless Rate-Recovery Function: We first consider the case when the reconstruction in (4) is required to be lossless. We assume that the source alphabet is discrete and the entropy $H(s)$ is finite. A rate $R_{\mathcal{L}}(B, W)$ is feasible if there exists a sequence of encoding and decoding functions and a sequence ϵ_n that approaches zero as $n \to \infty$ such that, $\Pr(s_i^n \neq \hat{s}_i^n) \leq \epsilon_n$ for all source sequences reconstructed as in (4). We seek the minimum feasible rate $R_{\mathcal{L}}(B, W)$, which is the *lossless rate-recovery* function. In this paper, we will focus on infinite-horizon case, $R(B, W) = \lim_{\mathcal{L}\to\infty} R_{\mathcal{L}}(B, W)$, which will be called the rate-recovery function for simplicity.

TABLE I: Summary of notation used in the paper.

Source Parameters	Source Symbol	s
	Source Reproduction	$\hat{s}$
	Temporal Correlation Coefficient of Gauss-Markov Source Model	ρ
Channel Parameters	Channel Input	f
	Channel Output	g
	Maximum Burst Length	B
	Guard Length between Consecutive Bursts	L
System Parameters	Length of Source Sequences	n
	Communication Duration	$\mathcal{L}$
	Recovery Window Length	W
Performance Metrics	Rate	R
	Average Distortion	D

2) Lossy Rate-Recovery Function: We also consider the case where reconstruction in (4) is required to satisfy an average distortion constraint:

$$\limsup_{n\to\infty} E\left[\frac{1}{n}\sum_{k=1}^{n} d(s_{i,k}, \hat{s}_{i,k})\right] \leq D \tag{5}$$

for some distortion measure $d : \mathbb{R}^2 \to [0, \infty)$. The rate R is feasible if a sequence of encoding and decoding functions exists that satisfies the average distortion constraint. The minimum feasible rate $R_{\mathcal{L}}(B, W, D)$, is the *lossy rate-recovery function*. The study of lossy rate-recovery function for the general case appears to be quite challenging. In this paper we will focus on the class of Gaussian-Markov sources, with quadratic distortion measure, i.e. $d(s, \hat{s}) = (s - \hat{s})^2$, where the analysis simplifies. We will again focus on infinite-horizon case, $R(B, W, D) = \lim_{\mathcal{L}\to\infty} R_{\mathcal{L}}(B, W, D)$ which we simply call the rate-recovery function. Table I summarizes the notation used throughout the paper.

Remark 1. *Note that our proposed setup only considers a*

single burst erasure during the entire duration of communication. When we consider lossless recovery at the destination our results immediately extend to channels involving multiple burst erasures with a certain guard interval separating consecutive bursts. When we consider Gauss-Markov sources with a quadratic distortion measure, we will explicitly treat the channel with multiple burst erasures and compare the achievable rates with that of a single burst erasure channel.

B. Practical Motivation

Note that our setup assumes that the size of both the source frames and channel packets is sufficiently large. A relevant application for the proposed setup is video streaming. Video frames are generated at a rate of approximately 60 Hz and each frame typically contains several hundred thousand pixels. The inter-frame interval is thus $\Delta_s \approx 17$ ms. Suppose that the underlying broadband communication channel has a bandwidth of $W_s = 2.5$ MHz. Then in the interval of Δ_s the number of symbols transmitted using ideal synchronous modulation is $N = 2\Delta_s W_s \approx 84,000$. Thus the block length between successive frames is sufficiently long that capacity achieving codes could be used and the erasure model and large packet sizes is justified. The assumption of spatially i.i.d. frames could reasonably approximate the video *innovation process* generated by applying suitable transform on original video frames. Such models have been also used in earlier works e.g., [3], [9], [11]–[13].

Possible applications of the burst loss model considered in our setup include fading wireless channels and congestion in wired networks. We note that the present paper does not consider a statistical channel model but instead considers a worst case channel model. As mentioned before even the effect of such a single burst loss has not been well understood in the video streaming setup and therefore our proposed setup is a natural starting point. Furthermore while the statistical models are used to capture the typical behaviour of channel errors, the atypical behaviour is often modelled (see e.g., [19, Sec. 6.10]) using a worst-case approach. Therefore in low-latency applications where the local channel dynamics are relevant such models are often used (see e.g., [20]–[23]). Finally we note that earlier works (see e.g., [3]) that consider statistical channel models, also ultimately simplify the system by analyzing the effect of each burst erasure separately in steady state.

IV. Main Results

We summarize the main results of this paper. We note in advance that throughout the paper, the upper bound on the rate-recovery function indicates the rate achievable by a proposed coding scheme and the lower bound corresponds to a necessary condition that the rate-recovery function of any feasible coding scheme has to satisfy. Section IV-A treats the lossless rate-recovery function and presents lower and upper bounds in Theorem 1. Corollary 2 presents the lossless rate-recovery function for a special case of symmetric sources, when restricted to memoryless encoders. Section IV-B treats the lossy rate-recovery function for the class of Gauss-Markov sources. Prop. 1 presents a lower bound, whereas Prop. 2 and Prop. 3 present upper bounds on lossy rate-recovery function for the single and multiple burst erasure channel models respectively. Our bounds coincide in the high resolution limit, as stated in Corollary 3. Finally Section IV-C treats another setup involving independent Gaussian sources, with a sliding window recovery constraint, and establishes the associated rate-recovery function.

A. Lossless Rate-Recovery Function

Theorem 1. *(Lossless Rate-Recovery Function) For the stationary, first-order Markov, discrete source process, the lossless rate-recovery function satisfies the following upper and lower bounds:* $R^-(B,W) \le R(B,W) \le R^+(B,W)$, *where*

$$R^+(B,W) = H(\mathsf{s}_1|\mathsf{s}_0) + \frac{1}{W+1} I(\mathsf{s}_B; \mathsf{s}_{B+1}|\mathsf{s}_0), \tag{6}$$

$$R^-(B,W) = H(\mathsf{s}_1|\mathsf{s}_0) + \frac{1}{W+1} I(\mathsf{s}_B; \mathsf{s}_{B+W+1}|\mathsf{s}_0). \tag{7}$$

□

Notice that the upper and lower bounds (6) and (7) coincide for $W = 0$ and $W \to \infty$, yielding the rate-recovery function in these cases. We can interpret the term $H(\mathsf{s}_1|\mathsf{s}_0)$ as the amount of uncertainty in s_i when the past sources are perfectly known. This term is equivalent to the rate associated with ideal predictive coding in absence of any erasures. The second term in both (6) and (7) is the additional penalty that arises due to the recovery constraint following a burst erasure. Notice that this term decreases at-least as $H(\mathsf{s})/(W+1)$, thus the penalty decreases as we increase the recovery period W. Note that the mutual information term associated with the lower bound is $I(\mathsf{s}_B; \mathsf{s}_{B+W+1}|\mathsf{s}_0)$ while that in the upper bound is $I(\mathsf{s}_B; \mathsf{s}_{B+1}|\mathsf{s}_0)$. Intuitively this difference arises because in the lower bound we only consider the reconstruction of s_{B+W+1}^n following an erasure bust in $[1, B]$ while, as explained below in Corollary 1 the upper bound involves a binning based scheme that reconstructs all sequences $(\mathsf{s}_{B+1}^n, \ldots, \mathsf{s}_{B+W+1}^n)$ at time $t = B + W + 1$.

A proof of Theorem 1 is provided in Section V. The lower bound involves a connection to a multi-terminal source coding problem. This model captures the different requirements imposed on the encoder output following a burst erasure and in the steady state. The following Corollary provides an alternate expression for the achievable rate and makes the connection to the binning technique explicit.

Corollary 1. *The upper bound in* (6) *is equivalent to the following expression*

$$R^+(B,W) = \frac{1}{W+1} H(\mathsf{s}_{B+1}, \mathsf{s}_{B+2}, \ldots, \mathsf{s}_{B+W+1}|\mathsf{s}_0). \tag{8}$$

□

The proof of Corollary 1 is provided in Appendix A. We make several remarks. First, the entropy term in (8) is equivalent to the sum-rate constraint associated with the Slepian-Wolf coding scheme in simultaneously recovering $\{\mathsf{s}_{B+1}^n, \mathsf{s}_{B+2}^n, \ldots, \mathsf{s}_{B+W+1}^n\}$ when s_0^n is known. Note that due to the stationarity of the source process, the rate expression in

(8) suffices for recovering from any burst erasure of length up to B, spanning an arbitrary interval. Second, note that in (8) we amortize over a window of length $W+1$ as $\{s_{B+1}^n, \ldots, s_{B+W+1}^n\}$ are recovered simultaneously at time $t = B+W+1$. Note that this is the maximum window length over which we can amortize due to the decoding constraint. Third, the results in Theorem 1 immediately apply when the channel introduces multiple bursts with a guard spacing of at least $W+1$. This property arises due to the Markov nature of the source. Given a source sequence at time i, all the future source sequences $\{s_t^n\}_{t>i}$ are independent of the past $\{s_t^n\}_{t<i}$ when conditioned on s_i^n. Thus when a particular source sequence is reconstructed at the destination, the decoder becomes oblivious to past erasures. Finally, while the results in Theorem 1 are stated for the rate-recovery function over an infinite horizon, upon examining the proof of Theorem 1, it can be verified that both the upper and lower bounds hold for the finite horizon case, i.e. $R_{\mathcal{L}}(B,W)$, when $\mathcal{L} \geq B+W$.

A *symmetric* source is defined as a Markov source such that the underlying Markov chain is also reversible i.e., the random variables satisfy $(s_0, \ldots, s_l) \stackrel{\mathrm{d}}{=} (s_l, \ldots, s_0)$, where the equality is in the sense of distribution [24]. Of particular interest to us is the following property satisfied for each t:

$$p_{s_{t+1},s_t}(s_a, s_b) = p_{s_{t-1},s_t}(s_a, s_b), \quad \forall s_a, s_b \in \mathcal{S} \tag{9}$$

i.e., we can "exchange" the source pair (s_{t+1}^n, s_t^n) with (s_{t-1}^n, s_t^n) without affecting the joint distribution. An example of a symmetric source is the binary symmetric source: $s_t^n = s_{t-1}^n \oplus z_t^n$, where $\{z_t^n\}_{t\geq 0}$ is an i.i.d. binary source process (in both temporal and spatial dimensions) with the marginal distribution $\Pr(z_{t,i}=0) = p$, the marginal distribution $\Pr(s_{t,i}=0) = \Pr(s_{t,i}=1) = \frac{1}{2}$ and $\oplus$ denotes modulo-2 addition.

Corollary 2. *For the class of symmetric Markov sources that satisfy* (9)*, the lossless rate-recovery function when restricted to the class of memoryless encoders i.e., $f_i = \mathcal{F}_i(s_i^n)$, is given by*

$$R(B,W) = \frac{1}{W+1} H(s_{B+1}, s_{B+2}, \ldots, s_{B+W+1} | s_0). \tag{10}$$

□

The proof of Corollary 2 is presented in Section VI. The converse is obtained by again using a multi-terminal source coding problem, but obtaining a tighter bound by exploiting the memoryless property of the encoders and the symmetric structure (9).

B. Gauss-Markov Sources

We study the lossy rate-recovery function when $\{s_i^n\}$ is sampled i.i.d. from a zero-mean Gaussian distribution, $\mathcal{N}(0,\sigma_s^2)$, along the spatial dimension and forms a first-order Markov chain across the temporal dimension i.e.,

$$s_i = \rho s_{i-1} + n_i \tag{11}$$

where $\rho \in (0,1)$ and $n_i \sim \mathcal{N}(0, \sigma_s^2(1-\rho^2))$. Without loss of generality we assume $\sigma_s^2 = 1$. We consider the quadratic distortion measure $d(s_i, \hat{s}_i) = (s_i - \hat{s}_i)^2$ between the source symbol s_i and its reconstruction $\hat{s}_i$. In this paper we focus on the special case of $W=0$, where the reconstruction must begin immediately after the burst erasure. We briefly remark about the case when $W>0$ at the end of Section VII-B. As stated before unlike the lossless case, the results of Gauss-Markov sources for single burst erasure channels do not readily extend to the multiple burst erasures case. Therefore, we treat the two cases separately.

1) Channels with Single Burst Erasure: In this channel model, as stated in (3), we assume that the channel can introduce a single burst erasure of length up to B during the transmission period. Define $R_{\text{GM-SE}}(B,D) \triangleq R(B, W=0, D)$ as the lossy rate-recovery function of Gauss-Markov sources with single burst erasure channel model.

Proposition 1 (Lower Bound–Single Burst)**.** *The lossy rate-recovery function of the Gauss-Markov source for single burst erasure channel model when $W=0$ satisfies*

$$R_{\textit{GM-SE}}(B,D) \geq R^{-}_{\textit{GM-SE}}(B,D) \triangleq \frac{1}{2}\log\left(\frac{D\rho^2 + 1 - \rho^{2(B+1)} + \sqrt{\Delta}}{2D}\right) \tag{12}$$

where $\Delta \triangleq (D\rho^2 + 1 - \rho^{2(B+1)})^2 - 4D\rho^2(1-\rho^{2B})$. □

The proof of Prop. 1 is presented in Section VII-A. The proof considers the recovery of a source sequence s_t^n, given a burst erasure in the interval $[t-B, t-1]$ and extends the lower bounding technique in Theorem 1 to incorporate the distortion constraint.

Proposition 2 (Upper Bound–Single Burst)**.** *The lossy rate-recovery function of the Gauss-Markov source for single burst erasure channel model when $W=0$ satisfies*

$$R_{\textit{GM-SE}}(B,D) \leq R^{+}_{\textit{GM-SE}}(B,D) \triangleq I(s_t; u_t | \tilde{s}_{t-B}) \tag{13}$$

where $u_t \triangleq s_t + z_t$, and z_t is sampled i.i.d. from $\mathcal{N}(0,\sigma_z^2)$. Also $\tilde{s}_{t-B} \triangleq s_{t-B} + e$ and $e \sim \mathcal{N}\left(0, \Sigma(\sigma_z^2)/(1-\Sigma(\sigma_z^2))\right)$ with

$$\Sigma(\sigma_z^2) \triangleq \frac{1}{2}\sqrt{(1-\sigma_z^2)^2(1-\rho^2)^2 + 4\sigma_z^2(1-\rho^2)} + \frac{1-\rho^2}{2}(1-\sigma_z^2), \tag{14}$$

is independent of all other random variables. The test channel noise $\sigma_z^2 > 0$ is chosen to satisfy

$$\left[\frac{1}{\sigma_z^2} + \frac{1}{1-\rho^{2B}(1-\Sigma(\sigma_z^2))}\right]^{-1} \leq D. \tag{15}$$

This is equivalent to σ_z^2 satisfying

$$E\left[(s_t - \hat{s}_t)^2\right] \leq D, \tag{16}$$

where $\hat{s}_t$ denotes the minimum mean square estimate (MMSE) of s_t from $\{\tilde{s}_{t-B}, u_t\}$. □

The following alternative rate expression for the achievable rate in Prop. 2, provides a more explicit interpretation of the

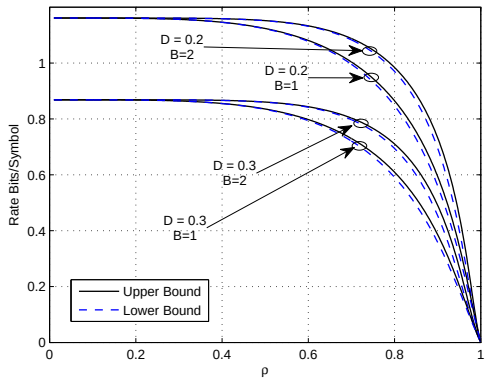

Fig. 2: Lower and upper bounds of lossy rate-recovery function $R_{\text{GM-SE}}(B, D)$ versus ρ for $D = 0.2$, $D = 0.3$ and $B = 1$, $B = 2$.

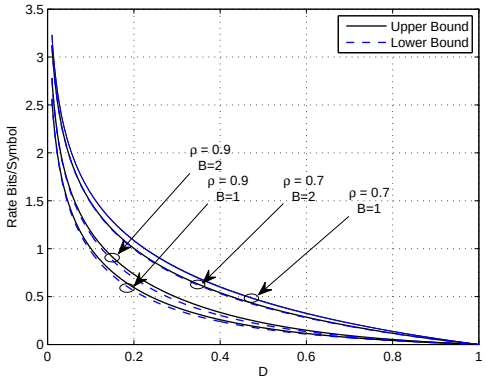

Fig. 3: Lower and upper bounds of lossy rate-recovery function $R_{\text{GM-SE}}(B, D)$ versus D for $\rho = 0.9$, $\rho = 0.7$ and $B = 1$, $B = 2$.

coding scheme.

$$R^{+}_{\text{GM-SE}}(B, D) = \lim_{t\to\infty} I(s_t; u_t | [u]_0^{t-B-1}) \tag{17}$$

where the random variables u_t are obtained using the same test channel in Prop. 2. Notice that the test channel noise $\sigma_z^2 > 0$ is chosen to satisfy $E\left[(s_t - \hat{s}_t)^2\right] \leq D$ where $\hat{s}_t$ denotes the MMSE of s_t from $\{[u]_0^{t-B-1}, u_t\}$ in steady state, i.e. $t \to \infty$. Notice that (17) is based on a quantize and binning scheme when the receiver has side information sequences $\{u_0^n, \ldots, u_{t-B-1}^n\}$. The proof of Prop. 2 which is presented in Section VII-B also involves establishing that the worst case erasure pattern during the recovery of $\hat{s}_t^n$ spans the interval $[t - B - 1, t - 1]$. The proof is considerably more involved as the reconstruction sequences $\{u_t^n\}$ do not form a Markov chain.

As we will show subsequently, the upper and lower bounds in Prop. 1 and Prop. 2 coincide in the high resolution limit. Numerical evaluations suggest that the bounds are close for a wide range of parameters. Fig. 2 and Fig. 3 illustrate some sample comparison plots.

2) Channels with Multiple Burst Erasures: We also consider the case where the channel can introduce multiple burst erasures, each of length no greater than B and with a guard interval of length at-least L separating consecutive bursts. The encoder is defined as in (2). We again only consider the case when $W = 0$. Upon observing the sequence $\{g_i\}_{i\geq 0}$, the decoder is required to reconstruct each source sequence with zero delay, i.e.,

$$\hat{s}_i^n = \mathcal{G}_i(g_0, g_1, \ldots, g_i, s_{-1}^n), \qquad \text{whenever } g_i \neq \star \tag{18}$$

such that the reconstructed source sequence $\hat{s}_i^n$ satisfies an average mean square distortion of D. The destination is not required to produce the source vectors that appear during any of the burst erasures. The rate $R(L, B, D)$ is feasible if a sequence of encoding and decoding functions exists that satisfies the average distortion constraint. The minimum feasible rate $R_{\text{GM-ME}}(L, B, D)$, is the lossy rate-recovery function.

Proposition 3 (Upper Bound–Multiple Bursts)**.** *The lossy rate-recovery function $R_{\text{GM-ME}}(L, B, D)$ for Gauss-Markov sources over the multiple burst erasures channel satisfies the following upper bound:*

$$R_{\text{GM-ME}}(L, B, D) \leq R^{+}_{\text{GM-ME}}(L, B, D) \triangleq I(u_t; s_t | \tilde{s}_{t-L-B}, [u]_{t-L-B+1}^{t-B-1}) \tag{19}$$

where $\tilde{s}_{t-L-B} = s_{t-L-B} + e$, where $e \sim \mathcal{N}(0, D/(1-D))$. Also for any i, $u_i \triangleq s_i + z_i$ and z_i is sampled i.i.d. from $\mathcal{N}(0, \sigma_z^2)$ and the noise in the test channel, $\sigma_z^2 > 0$ satisfies

$$E\left[(s_t - \hat{s}_t)^2\right] \leq D \tag{20}$$

and $\hat{s}_t$ denotes the MMSE estimate of s_t from $\{\tilde{s}_{t-L-B}, [u]_{t-L-B+1}^{t-B-1}, u_t\}$. □

The proof of Prop. 3 presented in Section VII-C is again based on quantize-and-binning technique and involves characterizing the worst-case erasure pattern by the channel. Note also that the rate expression in (19) depends on the minimum guard spacing L, the maximum burst erasure length B and distortion D, but is not a function of time index t, as the test channel is time invariant and the source process is stationary. An expression for computing σ_z^2 is provided in Section VII-C. While we do not provide a lower bound for $R_{\text{GM-ME}}(L, B, D)$ we remark that the lower bound in Prop. 1 also applies to the multiple burst erasures setup.

Fig. 4 provides numerical evaluation of the achievable rate for different values of L. We note that even for L as small as 4, the achievable rate in Prop. 3 is virtually identical to the rate for single burst erasure in Prop. 2. This strikingly fast convergence to the single burst erasure rate appears due to the exponential decay in the correlation coefficient between source samples as time-lag increases.

3) High Resolution Regime: For both the single and multiple burst erasures models, the upper and lower bounds on lossy rate-recovery function for $W = 0$ denoted by $R(L, B, D)$ coincide in the high resolution limit as stated below.

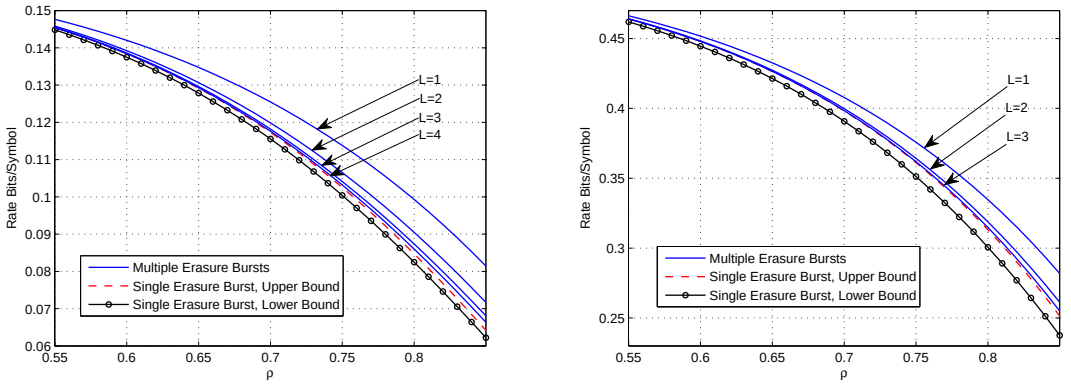

(a) $D = 0.8$ (b) $D = 0.5$

Fig. 4: Achievable rates for multiple burst erasures model for different values of guard length L separating burst erasures comparing to single burst erasure. As L grows, the rate approaches the single erasure case. The lower bound for single erasure case is also plotted for comparison ($B = 1$).

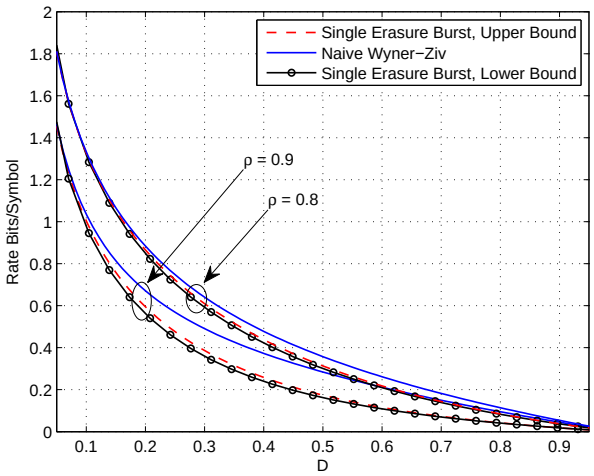

Fig. 5: A comparison of achievable rates for the Gauss-Markov source ($B = 1$).

Corollary 3. *In the high resolution limit, the Gauss-Markov lossy rate-recovery function satisfies the following:*

$$R(L, B, D) = \frac{1}{2} \log \left(\frac{1 - \rho^{2(B+1)}}{D} \right) + o(D). \tag{21}$$

where $\lim_{D \to 0} o(D) = 0$. □

The proof of Corollary 3 is presented in Section VIII. It is based on evaluating the asymptotic behaviour of the lower bound in (12) and the upper bound in Prop. 3, in high resolution regime. Notice that the rate expression in (21) does not depend on the guard separation L. The intuition behind this is as follows. In the high resolution regime, the output of the test channel, i.e. u_t, becomes very close to the original source s_t. Therefore the Markov property of the original source is approximately satisfied by these auxiliary random variables and hence the past sequences are not required. The rate in (21) can also be approached by a *Naive Wyner-Ziv* coding scheme that only makes use of the most recently available sequence at the decoder [25]. The rate of this scheme is given by:

$$R_{\text{NWZ}}(B, D) \triangleq I(s_t; u_t | u_{t-B-1}) \tag{22}$$

where for each i, $u_i = s_i + z_i$ and $z_i \sim \mathcal{N}(0, \sigma_z^2)$ and σ_z^2 satisfies the following distortion constraint

$$E[(s_t - \hat{s}_t)^2] \leq D \tag{23}$$

where $\hat{s}_t$ is the MMSE estimate of s_t from $\{u_{t-B-1}, u_t\}$.

Fig. 5 reveals that while the rate in (22) is near optimal in the high resolution limit, it is in general sub-optimal when compared to the rates in (19) when $\rho = 0.9$. As we decrease ρ, the performance loss associated with this scheme appears to reduce.

C. Gaussian Sources with Sliding Window Recovery Constraints

In this section we consider a specialized source model and distortion constraint, where it is possible to improve upon the binning based upper bound. Our proposed scheme attains the rate-recovery function for this special case and is thus optimal. This example illustrates that the binning based scheme can be sub-optimal in general.

1) Source Model: We consider a sequence of i.i.d. Gaussian source sequences i.e., at time i, s_i^n is sampled i.i.d. according to a zero mean unit variance Gaussian distribution $\mathcal{N}(0, 1)$, independent of the past sources. At each time we associate an auxiliary source

$$\mathbf{t}_i^n = \left(s_i^n \; s_{i-1}^n \; \dots \; s_{i-K}^n \right) \tag{24}$$

which is a collection of the past $K + 1$ source sequences. Note that $\mathbf{t}_i^n$ constitutes a first-order Markov chain. We will define a reconstruction constraint with the sequence $\mathbf{t}_i^n$.

2) Encoder: The (causal) encoder at time i generates an output given by $f_i = \mathcal{F}_i(s_{-1}^n, \dots, s_i^n) \in [1, 2^{nR}]$.

3) Channel Model: The channel can introduce a burst erasure of length up to B in an arbitrary interval $[j, j + B - 1]$.

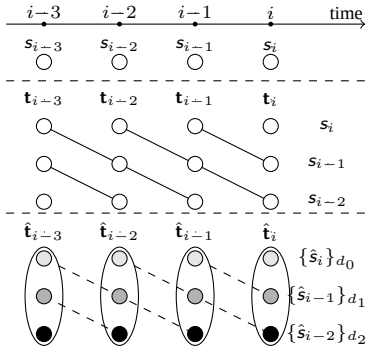

Fig. 6: Schematic of the Gaussian sources with sliding window recovery constraints for $K = 2$. The source s_i, drawn as white circles, are independent sources and $\mathbf{t}_i$ is defined as a collection of $K + 1 = 3$ most recent sources. The source symbols along the diagonal lines are the same. The decoder at time i recovers s_i, s_{i-1} and s_{i-2} within distortions d_0, d_1 and d_2, respectively where $d_0 \leq d_1 \leq d_2$. In figure the colour density of the circle represents the amount of reconstruction distortion.

4) Decoder: At time i the decoder is interested in reproducing a collection of past $K + 1$ sources[1] within a distortion vector $\mathbf{d} = (d_0, d_1, \cdots, d_K)$ i.e., at time i the decoder is interested in reconstructing $(\hat{s}_i^n, \ldots, \hat{s}_{i-K}^n)$ where $E\left[||s_{i-l}^n - \hat{s}_{i-l}^n||^2\right] \leq nd_l$ must be satisfied for $l \in [0, K]$. We assume throughout that $d_0 \leq d_1 \leq \ldots \leq d_K$ which corresponds to the requirement that the more recent source sequences must be reconstructed with a smaller average distortion.

In Fig. 6, the source symbols s_i are shown as white circles. The symbols $\mathbf{t}_i$ and $\hat{\mathbf{t}}_i$ are also illustrated for $K = 2$. The different shading for the sub-symbols in $\hat{\mathbf{t}}_i$ corresponds to different distortion constraints.

If a burst erasure spans the interval $[j, j+B-1]$, the decoder is not required to output a reproduction of the sequences $\mathbf{t}_i^n$ for $i \in [j, j + B + W - 1]$.

The *lossy rate-recovery function* denoted by $R(B, W, \mathbf{d})$ is the minimum rate required to satisfy these constraints.

Remark 2. *One motivation for considering the above setup is that the decoder might be interested in computing a function of the last $K + 1$ source sequences at each time e.g.,, $v_i = \sum_{j=0}^{K} \alpha^j s_{i-j}$. A robust coding scheme, when the coefficient α is not known to the encoder is to communicate s_{i-j}^n with distortion d_j at time i to the decoder.*

Theorem 2. *For the proposed Gaussian source model with a non-decreasing distortion vector $\mathbf{d} = (d_0, \ldots, d_K)$ with $0 < d_i \leq 1$, the lossy rate-recovery function is given by*

$$R(B, W, \mathbf{d}) = \frac{1}{2}\log\left(\frac{1}{d_0}\right) + \frac{1}{W+1}\sum_{k=1}^{\min\{K-W,B\}} \frac{1}{2}\log\left(\frac{1}{d_{W+k}}\right). \quad (25)$$

□

The proof of Theorem 2 is provided in Section IX. The coding scheme for the proposed model involves using a successive refinement codebook for each sequence s_i^n to produce $B + 1$ layers and carefully assigning the sequence of layered codewords to each channel packet. A simple quantize and binning scheme in general does not achieve the rate-recovery function in Theorem 2. A numerical comparison of the lossy rate-recovery function with other schemes is presented in Section IX.

This completes the statement of the main results in this paper.

V. General Upper and Lower Bounds on Lossless Rate-Recovery Function

In this section we present the proof of Theorem 1. In particular, we show that the rate-recovery function satisfies the following lower bound.

$$R \geq R^-(B, W) = H(s_1|s_0) + \frac{1}{W+1} I(s_B, s_{B+W+1}|s_0). \quad (26)$$

which is inspired by a connection to a multi-terminal source coding problem introduced in Section V-A. Based on this connection, the proof of the lower bound in general form in (26) is presented in Section V-B. Then by proposing a coding scheme based on random binning, we show in Section V-C that the following rate is achievable.

$$R \geq R^+(B, W) = H(s_1|s_0) + \frac{1}{W+1} I(s_B, s_{B+1}|s_0). \quad (27)$$

A. Connection to Multi-terminal Source Coding Problem

We first present a multi-terminal source coding setup which captures the tension inherent in the streaming setup. We focus on the special case when $B = 1$ and $W = 1$. At any given time j the encoder output f_j must satisfy two objectives simultaneously: 1) if j is outside the error propagation period then the decoder should use f_j and the past sequences to reconstruct s_j^n; 2) if j is within the recovery period then f_j must only help in the recovery of a future source sequence.

Fig. 7 illustrates the multi-terminal source coding problem with one encoder and two decoders that captures these constraints. The sequences (s_j^n, s_{j+1}^n) are revealed to the encoder and produces outputs f_j and f_{j+1}. Decoder 1 needs to recover s_j^n given f_j and s_{j-1}^n while decoder 2 needs to recover s_{j+1}^n given s_{j-2}^n and (f_j, f_{j+1}). Thus decoder 1 corresponds to the steady state of the system when there is no loss while decoder 2 corresponds to the recovery immediately after an erasure when $B = 1$ and $W = 1$. We note in advance that the multi-terminal source coding setup does not directly correspond to

[1]In this section it is sufficient to assume that any source sequence with a time index $j < -1$ is a constant sequence.

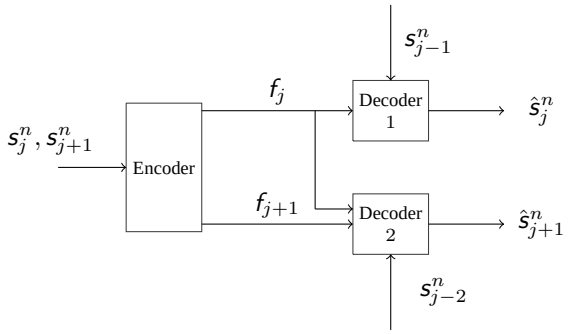

Fig. 7: Multi-terminal problem setup associated with our proposed streaming setup when $W = B = 1$. The erasure at time $t = j - 1$ leads to two virtual decoders with different side information as shown.

providing genie-aided side information in the streaming setup. In particular this setup does not account for the fact that the encoder has access to all previous source sequences and the decoders have access to past channel outputs. Nevertheless the main steps of the lower bound developed in the multi-terminal setup are then generalized rather naturally in the formal proof of the lower bound in the next sub-section.

For the above multi-terminal problem, we establish a lower bound on the sum rate as follows:

$$\begin{aligned}
&n(R_1+R_2)\\
&\geq H(f_j, f_{j+1})\\
&\geq H(f_j, f_{j+1}|s_{j-2}^n)\\
&= H(f_j, f_{j+1}, s_{j+1}^n|s_{j-2}^n) - H(s_{j+1}^n|f_j, f_{j+1}, s_{j-2}^n)\\
&= H(f_j, s_{j+1}^n|s_{j-2}^n) + H(f_{j+1}|f_j, s_{j-2}^n, s_{j+1}^n)\\
&\quad - H(s_{j+1}^n|f_j, f_{j+1}, s_{j-2}^n) \qquad (28)\\
&\geq H(f_j, s_{j+1}^n|s_{j-2}^n) - n\varepsilon_n \qquad (29)\\
&= H(s_{j+1}^n|s_{j-2}^n) + H(f_j|s_{j+1}^n, s_{j-2}^n) - n\varepsilon_n\\
&\geq H(s_{j+1}^n|s_{j-2}^n) + H(f_j|s_{j+1}^n, s_{j-1}^n, s_{j-2}^n) - n\varepsilon_n \qquad (30)\\
&\geq H(s_{j+1}^n|s_{j-2}^n) + H(s_j^n|s_{j+1}^n, s_{j-1}^n, s_{j-2}^n) - 2n\varepsilon_n \qquad (31)\\
&= H(s_{j+1}^n|s_{j-2}^n) + H(s_j^n|s_{j+1}^n, s_{j-1}^n) - 2n\varepsilon_n \qquad (32)\\
&= nH(s_3|s_0) + nH(s_1|s_2, s_0) - 2n\varepsilon_n \qquad (33)
\end{aligned}$$

where (28) follows from the chain rule of entropy, (29) follows from the fact that s_{j+1}^n must be recovered from $\{f_j, f_{j+1}, s_{j-2}^n\}$ at decoder 2 hence Fano's inequality applies and (30) follows from the fact that conditioning reduces entropy. Eq. (31) follows from Fano's inequality applied to decoder 1 and (32) follows from the Markov chain associated with the source process. Finally (33) follows from the fact that the source process is memoryless. Dividing throughout by n in (33) and taking $n \to \infty$ yields

$$R_1 + R_2 \geq H(s_1|s_0, s_2) + H(s_3|s_0). \qquad (34)$$

Tightness of Lower Bound: As a side remark, we note that the sum-rate lower bound in (34) can be achieved if Decoder 1 is further revealed s_{j+1}^n. Note that the lower bound (34) also applies in this case since the Fano's Inequality applied to decoder 1 in (31) has s_{j+1}^n in the conditioning. We claim that $R_1 = H(s_j|s_{j+1}, s_{j-1})$ and $R_2 = H(s_{j+1}|s_{j-2})$ are achievable. The encoder can achieve R_1 by random binning of source s_j^n with $\{s_{j-1}^n, s_{j+1}^n\}$ as decoder 1's side information and achieve R_2 by random binning of source s_{j+1}^n with s_{j-2}^n as decoder 2's side information. Thus revealing the additional side information of s_{j+1}^n to decoder 1, makes the link connecting f_j to decoder 2 unnecessary.

Also note that the setup in Fig. 7 reduces to the source coding problem in [26] if we set $s_{j-2}^n = \phi$. It is also a successive refinement source coding problem with different side information at the decoders and special distortion constraints at each of the decoders. However to the best of our knowledge the multi-terminal problem in Fig. 7 has not been addressed in the literature nor has the connection to our proposed streaming setup been considered in earlier works.

In the streaming setup, the symmetric rate i.e., $R_1 = R_2 = R$ is of interest. Setting this in (34) we obtain:

$$R \geq \frac{1}{2}H(s_1|s_0, s_2) + \frac{1}{2}H(s_3|s_0). \qquad (35)$$

It can be easily shown that the expression in (35) and the right hand side of the general lower bound in (7) for $B = W = 1$ are the equivalent using a simple calculation.

$$\begin{aligned}
&R^-(B=1, W=1)\\
&= H(s_1|s_0) + \frac{1}{2}I(s_1; s_3|s_0)\\
&= H(s_1|s_0) + \frac{1}{2}H(s_3|s_0) - \frac{1}{2}H(s_3|s_0, s_1)\\
&= \frac{1}{2}H(s_1, s_2|s_0) + \frac{1}{2}H(s_3|s_0) - \frac{1}{2}H(s_3|s_1) \qquad (36)\\
&= \frac{1}{2}H(s_2|s_0) + \frac{1}{2}H(s_1|s_0, s_2) + \frac{1}{2}H(s_3|s_0) - \frac{1}{2}H(s_3|s_1) \qquad (37)\\
&= \frac{1}{2}H(s_1|s_0, s_2) + \frac{1}{2}H(s_3|s_0) \qquad (38)
\end{aligned}$$

where the first term in (36) follows from the Markov Chain property $s_0 \to s_1 \to s_2$, the last term in (36) follows from the Markov Chain property $s_1 \to s_2 \to s_3$ and (38) follows from the fact that the source model is stationary, thus the first and last term in (37) are the same.

As noted before the above proof does not directly apply to the streaming setup as it does not take into account that the decoders have access to all the past encoder outputs, and that the encoder has access to all the past source sequences. We next provide a formal proof of the lower bound that shows that this additional information does not help.

B. Lower Bound on Lossless Rate-Recovery Function

For any sequence of $(n, 2^{nR})$ codes we show that there is a sequence ε_n that vanishes as $n \to \infty$ such that

$$R \geq H(s_1|s_0) + \frac{1}{W+1}I(s_{B+W+1}; s_B|s_0) - \varepsilon_n. \qquad (39)$$

We consider that a burst erasure of length B spans the interval $[t - B - W, t - W - 1]$ for some $t \geq B + W$. It suffices to lower bound the rate for this erasure pattern. By

considering the interval $[t-W,t]$, following the burst erasure we have the following.

$$\begin{aligned}(W+1)nR &\geq H([f]_{t-W}^{t}) \\ &\geq H([f]_{t-W}^{t}|[f]_{0}^{t-B-W-1}, s_{-1}^{n}) \qquad (40)\end{aligned}$$

where (40) follows from the fact that conditioning reduces the entropy. By definition, the source sequence s_t^n must be recovered from $\{[f]_0^{t-B-W-1}, [f]_{t-W}^{t}, s_{-1}^{n}\}$ Applying Fano's inequality we have that

$$H(s_t^n|[f]_0^{t-B-W-1}, [f]_{t-W}^{t}, s_{-1}^{n}) \leq n\varepsilon_n. \qquad (41)$$

Therefore we have

$$\begin{aligned}&H([f]_{t-W}^{t} \mid [f]_0^{t-B-W-1}, s_{-1}^{n}) \\ &= H(s_t^n, [f]_{t-W}^{t} \mid [f]_0^{t-B-W-1}, s_{-1}^{n}) \\ &\quad - H(s_t^n|[f]_0^{t-B-W-1}, [f]_{t-W}^{t}, s_{-1}^{n}) \qquad (42)\\ &\geq H(s_t^n \mid [f]_0^{t-B-W-1}, s_{-1}^{n}) \\ &\quad + H([f]_{t-W}^{t} \mid s_t^n, [f]_0^{t-B-W-1}, s_{-1}^{n}) - n\varepsilon_n. \qquad (43)\end{aligned}$$

where (42) and the first two terms of (43) follow from the application of chain rule and the last term in (43) follows form (41). Now we bound each of the two terms in (43). First we note that:

$$\begin{aligned}&H(s_t^n|[f]_0^{t-B-W-1}, s_{-1}^{n}) \\ &\quad \geq H(s_t^n|[f]_0^{t-B-W-1}, s_{t-B-W-1}^{n}, s_{-1}^{n}) \qquad (44)\\ &\quad = H(s_t^n|s_{t-B-W-1}^{n}) \qquad (45)\\ &\quad = H(s_{B+W+1}^{n}|s_0^n) \qquad (46)\\ &\quad = nH(s_{B+W+1}|s_0), \qquad (47)\end{aligned}$$

where (44) follows from the fact that conditioning reduces entropy and (45) follows from the Markov relation

$$(s_{-1}^{n}, [f]_0^{t-B-W-1}) \to s_{t-B-W-1}^{n} \to s_t^n.$$

Eq. (46) and (47) follow from the stationary and memoryless source model.

Furthermore the second term in (43) can be lower bounded using the following series of inequalities.

$$\begin{aligned}&H\left([f]_{t-W}^{t} \mid s_t^n, [f]_0^{t-B-W-1}, s_{-1}^{n}\right) \\ &\geq H\left([f]_{t-W}^{t-1} \mid s_t^n, [f]_0^{t-W-1}, s_{-1}^{n}\right) \qquad (48)\\ &= H\left([f]_{t-W}^{t-1}, s_{t-W}^{n}, \ldots, s_{t-1}^{n}|s_t^n, [f]_0^{t-W-1}, s_{-1}^{n}\right) \\ &\quad - H\left(s_{t-W}^{n}, \ldots, s_{t-1}^{n}\big|s_t^n, [f]_0^{t-1}, s_{-1}^{n}\right) \\ &\geq H\left([f]_{t-W}^{t-1}, s_{t-W}^{n}, \ldots, s_{t-1}^{n}|s_t^n, [f]_0^{t-W-1}, s_{-1}^{n}\right) - Wn\varepsilon_n \qquad (49)\\ &\geq H\left(s_{t-W}^{n}, \ldots, s_{t-1}^{n}\big|s_t^n, [f]_0^{t-W-1}, s_{-1}^{n}\right) - Wn\varepsilon_n \\ &\geq H\left(s_{t-W}^{n}, \ldots, s_{t-1}^{n}\big|s_t^n, [f]_0^{t-W-1}, s_{t-W-1}^{n}, s_{-1}^{n}\right) - Wn\varepsilon_n \\ &= H\left(s_{t-W}^{n}, s_{t-W+1}^{n}, \ldots, s_{t-1}^{n}\big|s_t^n, s_{t-W-1}^{n}\right) - Wn\varepsilon_n \qquad (50)\\ &= nH(s_{B+1}, s_{B+2}, \ldots, s_{B+W}|s_B, s_{B+W+1}) - Wn\varepsilon_n \qquad (51)\\ &= nH(s_{B+1}, s_{B+2}, \ldots, s_{B+W}, s_{B+W+1}|s_B) \\ &\quad - nH(s_{B+W+1}|s_B) - Wn\varepsilon_n \\ &= n(W+1)H(s_1|s_0) - nH(s_{B+W+1}|s_B) - Wn\varepsilon_n \qquad (52)\end{aligned}$$

Note that in (48), in order to lower bound the entropy term, we reveal the codewords $[f]_{t-B-W}^{t-W-1}$ which is not originally available at the decoder and exploit the fact that conditioning reduces the entropy. This step in deriving the lower bound may not be necessarily tight, however it is the best lower bound we have for the general problem. Also (49) follows from the fact that according to the problem setup $\{s_{t-W}^n, \ldots, s_{t-1}^n\}$ must be decoded when s_{-1}^n and all the channel codewords before time t, i.e. $[f]_0^{t-1}$, are available at the decoder, Hence Fano's inequality again applies. The expression above (50) also follows from conditioning reduces entropy. Eq. (50) follows from the fact that

$$(s_{-1}^{n}, [f]_0^{t-W-1}) \to s_{t-W-1}^{n} \to (s_{t-W}^{n}, \ldots, s_{t-1}^{n}). \qquad (53)$$

Eq. (51) and (52) follow from memoryless and stationarity of the source sequences. Combining (43), (47) and (52) we have that

$$\begin{aligned}&H\left([f]_{t-W}^{t} \;\middle|\; [f]_0^{t-B-W-1}, s_{-1}^{n}\right) \geq nH(s_{B+W+1}|s_0) + \\ &\quad n(W+1)H(s_1|s_0) - nH(s_{B+W+1}|s_B) - (W+1)n\varepsilon_n \qquad (54)\end{aligned}$$

Finally from (54) and (40) we have that,

$$\begin{aligned}nR &\geq nH(s_1|s_0) + \\ &\quad \frac{n}{W+1}\left[H(s_{B+W+1}|s_0) - H(s_{B+W+1}|s_B) - (W+1)\varepsilon_n\right] \\ &= nH(s_1|s_0) + \\ &\frac{n}{W+1}\left[H(s_{B+W+1}|s_0) - H(s_{B+W+1}|s_B, s_0) - (W+1)\varepsilon_n\right] \\ &= nH(s_1|s_0) + \frac{n}{W+1}I(s_{B+W+1}; s_B|s_0) - n\varepsilon_n \qquad (55)\end{aligned}$$

where the second step above follows from the Markov condition $s_0 \to s_B \to s_{B+W+1}$. As we take $n \to \infty$ we recover (39). This completes the proof of the lower bound in Theorem 1.

We remark that the derived lower bound holds for any $t \geq B+W$. Therefore, the lower bound (39) on lossless rate-recovery function also holds for finite-horizon rate-recovery function whenever $\mathcal{L} \geq B+W$.

Finally we note that in our setup we are assuming a peak rate constraint on f_t. If we assume the average rate constraint across f_t the lower bound still applies with minor modifications in the proof.

C. Upper Bound on Lossless Rate-Recovery Function

In this section we establish the achievability of $R^+(B,W)$ in Theorem 1 using a binning based scheme. At each time the encoding function f_i in (2) is the bin-index of a Slepian-Wolf codebook [27], [28]. Following a burst erasure in $[j, j+B-1]$, the decoder collects $f_{j+B}, \ldots, f_{j+W+B}$ and attempts to jointly recover all the underlying sources at $t = j+W+B$. Using Corollary 1 it suffices to show that

$$R^+ = \frac{1}{W+1}H(s_{B+1}, \ldots, s_{B+W+1}|s_0) + \varepsilon \qquad (56)$$

is achievable for any arbitrary $\varepsilon > 0$.

We use a codebook $\mathcal{C}$ which is generated by randomly partitioning the set of all typical sequences $T_\varepsilon^n(s)$ into 2^{nR^+} bins. The partitions are revealed to the decoder ahead of time.

Upon observing s_i^n the encoder declares an error if $\mathsf{s}_i^n \notin T_\varepsilon^n(\mathsf{s})$. Otherwise it finds the bin to which s_i^n belongs to and sends the corresponding bin index f_i. We separately consider two possible scenarios at the decoder.

First suppose that the sequence s_{i-1}^n has already been recovered. Then the destination attempts to recover s_i^n from $(\mathsf{f}_i, \mathsf{s}_{i-1}^n)$. This succeeds with high probability if $R^+ > H(\mathsf{s}_1|\mathsf{s}_0)$, which is guaranteed via (56). If we define probability of the error event $\mathcal{E}_i \triangleq \{\hat{\mathsf{s}}_i^n \neq \mathsf{s}_i^n\}$ conditioned on the correct recovery of s_{i-1}^n, i.e. $\overline{\mathcal{E}}_{i-1}$, as follows

$$P_{e,1}^{(n)} \triangleq P(\mathcal{E}_i|\overline{\mathcal{E}}_{i-1}) \tag{57}$$

then for the rates satisfying $R^+ > H(\mathsf{s}_1|\mathsf{s}_0)$ and in particular for R^+ in (56), it is guaranteed that

$$\lim_{n\to\infty} P_{e,1}^{(n)} = 0. \tag{58}$$

Next consider the case where s_i^n is the first sequence to be recovered after the burst erasure. In particular the burst erasure spans the interval $[i-B'-W, i-W-1]$ for some $B' \leq B$. The decoder thus has access to $\mathsf{s}_{i-B'-W-1}^n$, before the start of the burst erasure. Upon receiving $\mathsf{f}_{i-W}, \ldots, \mathsf{f}_i$ the destination simultaneously attempts to recover $(\mathsf{s}_{i-W}^n, \ldots, \mathsf{s}_i^n)$ given $(\mathsf{s}_{i-B'-W-1}^n, \mathsf{f}_{i-W}, \ldots, \mathsf{f}_i)$. This succeeds with high probability if,

$$\begin{aligned}(W+1)nR &= \sum_{j=i-W}^{i} H(\mathsf{f}_j) && (59)\\ &> nH(\mathsf{s}_{i-W}, \ldots, \mathsf{s}_i|\mathsf{s}_{i-B'-W-1}) && (60)\\ &= nH(\mathsf{s}_{B'+1}, \ldots, \mathsf{s}_{B'+W+1}|\mathsf{s}_0) && (61)\end{aligned}$$

where (61) follows from the fact that the sequence of variables s_i is a stationary process. Whenever $B' \leq B$ it immediately follows that (61) is also guaranteed by (56). Define $P_{e,2}^{(n)}$ as the probability of error in s_i^n given $(\mathsf{s}_{i-B-W-1}^n, \mathsf{f}_{i-W}, \ldots, \mathsf{f}_i)$, i.e.

$$P_{e,2}^{(n)} \triangleq P(\mathcal{E}_i|\overline{\mathcal{E}}_{i-B-W-1}). \tag{62}$$

For rate satisfying (61), which is satisfied through (56), it is guaranteed that

$$\lim_{n\to\infty} P_{e,2}^{(n)} = 0. \tag{63}$$

Analysis of the Streaming Decoder: As described in problem setup, the decoder is interested in recovering all the source sequences outside the error propagation window with vanishing probability of error. Assume a communication duration of $\mathcal{L}$ and a single burst erasure of length $0 < B' \leq B$ spanning the interval $[j, j+B'-1]$, for $0 \leq j \leq \mathcal{L}$. The decoder fails if at least one source sequences outside the error propagation window is erroneously recovered, i.e. $\hat{\mathsf{s}}_i^n \neq \mathsf{s}_i^n$ for some $i \in [0, j-1] \cup [j+B'+W+1, \mathcal{L}]$. For this particular channel erasure pattern, the probability of decoder's failure, denoted by $P_{\mathrm{F}}^{(n)}$, can be bounded as follows.

$$\begin{aligned}P_{\mathrm{F}}^{(n)} &\leq \sum_{k=0}^{j-1} P(\mathcal{E}_k|\overline{\mathcal{E}}_0, \overline{\mathcal{E}}_1, \ldots, \overline{\mathcal{E}}_{k-1}) + \\ &\quad P(\mathcal{E}_{j+B'+W+1}|\overline{\mathcal{E}}_0, \ldots, \overline{\mathcal{E}}_{j-1}) + \\ &\quad \sum_{k=j+B'+W+2}^{\mathcal{L}} P(\mathcal{E}_k|\overline{\mathcal{E}}_0, \ldots, \overline{\mathcal{E}}_{j-1}, \overline{\mathcal{E}}_{j+B'+W+1}, \ldots, \overline{\mathcal{E}}_{k-1}) && (64)\\ &= (\mathcal{L}-B'-W)P_{e,1}^{(n)} + P_{e,2}^{(n)} \leq \mathcal{L}P_{e,1}^{(n)} + P_{e,2}^{(n)} && (65)\end{aligned}$$

where $P_{e,1}^{(n)}$ and $P_{e,2}^{(n)}$ are defined in (57) and (62). Eq. (65) follows from the fact that, because of the Markov property of the source model, all the terms in the first and the last summation in (64) are the same and equal to $P_{e,1}^{(n)}$.

According to (58) and (63), for any rate satisfying (56) and for any $\mathcal{L}$, n can be chosen large enough such that the upper bound on $P_{\mathrm{F}}^{(n)}$ in (65) approaches zero. Thus the decoder fails with vanishing probability for any fixed $\mathcal{L}$. This in turn establishes the upper bound on $R(B,W)$, when $\mathcal{L} \to \infty$. This completes the justification of the upper bound.

VI. Symmetric Sources: Proof of Corollary 2

In this section we establish that the lossless rate-recovery function for symmetric Markov sources restricted to class of memoryless encoders is given by

$$R(B,W) = \frac{1}{W+1} H(\mathsf{s}_{B+1}, \ldots, \mathsf{s}_{B+W+1}|\mathsf{s}_0). \tag{66}$$

The achievability follows from Theorem 1 and Corollary 1. We thus only need to prove the converse to improve upon the general lower bound in (7). The lower bound for the special case when $W = 0$ follows directly from (7) and thus we only need to show the lower bound for $W \geq 1$. For simplicity in exposition we illustrate the case when $W = 1$. Then we need to show that

$$R(B, W=1) \geq \frac{1}{2} H(\mathsf{s}_{B+1}, \mathsf{s}_{B+2}|\mathsf{s}_0) \tag{67}$$

The proof for general $W > 1$ will follow along similar lines and will be sketched thereafter.

Assume that a burst erasure spans time indices $j-B, \ldots, j-1$. The decoder must recover

$$\hat{\mathsf{s}}_{j+1}^n = \mathcal{G}_{j+1}\left([\mathsf{f}]_0^{j-B-1}, \mathsf{f}_j, \mathsf{f}_{j+1}, \mathsf{s}_{-1}^n\right). \tag{68}$$

Furthermore if there is no erasure until time j then

$$\hat{\mathsf{s}}_j^n = \mathcal{G}_j\left([\mathsf{f}]_0^j, \mathsf{s}_{-1}^n\right) \tag{69}$$

must hold. Our aim is to establish the following lower bound on the sum-rate.

$$2R \geq H(\mathsf{s}_{j+1}|\mathsf{s}_j) + H(\mathsf{s}_j|\mathsf{s}_{j-B-1}). \tag{70}$$

The lower bound (67) then follows since

$$\begin{aligned}R &\geq \frac{1}{2}(H(\mathsf{s}_{j+1}|\mathsf{s}_j) + H(\mathsf{s}_j|\mathsf{s}_{j-B-1}))\\ &= \frac{1}{2}(H(\mathsf{s}_{j+1}|\mathsf{s}_j, \mathsf{s}_{j-B-1}) + H(\mathsf{s}_j|\mathsf{s}_{j-B-1})) && (71)\\ &= \frac{1}{2}H(\mathsf{s}_{j+1}, \mathsf{s}_j|\mathsf{s}_{j-B-1}) = \frac{1}{2}H(\mathsf{s}_{B+1}, \mathsf{s}_{B+2}|\mathsf{s}_0), && (72)\end{aligned}$$

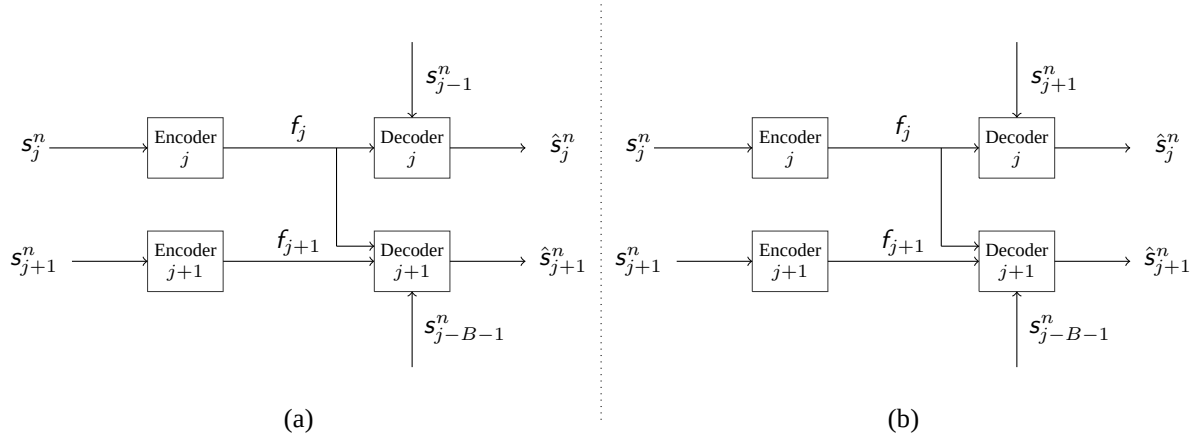

Fig. 8: Connection between the streaming problem and the multi-terminal source coding problem. The setup on the right is identical to the setup on the left, except with the side information sequence s_{j-1}^n replaced with s_{j+1}^n. However the rate region for both problems are identical for symmetric Markov sources.

where (71) follows from the Markov chain property $s_{j-B-1} \to s_j \to s_{j+1}$, and the last step in (72) follows from stationarity of the source model.

To establish (70) we make a connection to a multi-terminal source coding problem in Fig. 8(a). We accomplish this in several steps as outlined below.

A. Multi-Terminal Source Coding

Consider the multi-terminal source coding problem with side information illustrated in Fig. 8(a). In this setup there are four source sequences drawn i.i.d. from a joint distribution $p(s_{j+1}, s_j, s_{j-1}, s_{j-B-1})$. The two source sequences s_j^n and s_{j+1}^n are revealed to the encoders j and $j+1$ respectively and the two sources s_{j-1}^n and s_{j-B-1}^n are revealed to the decoders j and $j+1$ respectively. The encoders operate independently and compress the source sequences to f_j and f_{j+1} at rates R_j and R_{j+1} respectively. Decoder j has access to (f_j, s_{j-1}^n) while decoder $j+1$ has access to $(f_j, f_{j+1}, s_{j-B-1}^n)$. The two decoders are required to reconstruct

$$\tilde{s}_j^n = \tilde{\mathcal{G}}_j(f_j, s_{j-1}^n) \tag{73}$$

$$\tilde{s}_{j+1}^n = \tilde{\mathcal{G}}_{j+1}(f_j, f_{j+1}, s_{j-B-1}^n) \tag{74}$$

respectively such that $\Pr(s_i^n \neq \tilde{s}_i^n) \leq \varepsilon_n$ for $i = \{j, j+1\}$.

Note that the multi-terminal source coding setup in Fig. 8(a) is similar to the setup in Fig. 7, except that the encoders do not cooperate and $f_i = \mathcal{F}_i(s_i^n)$, due to the memoryless property. We exploit this property to directly show that a lower bound on the multi-terminal source coding setup in Fig. 8(a) also constitutes a lower bound on the rate of the original streaming problem.

Lemma 1. *For the class of memoryless encoding functions, i.e. $f_j = \mathcal{F}_j(s_j^n)$, the decoding functions $\hat{s}_j^n = \mathcal{G}_j([f]_0^j, s_{-1}^n)$ and $\hat{s}_{j+1}^n = \mathcal{G}_{j+1}([f]_0^{j-2}, f_j, f_{j+1}, s_{-1}^n)$ can be replaced by the following decoding functions*

$$\tilde{s}_j^n = \tilde{\mathcal{G}}_j(f_j, s_{j-1}^n) \tag{75}$$

$$\tilde{s}_{j+1}^n = \tilde{\mathcal{G}}_{j+1}(f_j, f_{j+1}, s_{j-2}^n,) \tag{76}$$

such that

$$\Pr(\tilde{s}_j^n \neq s_j^n) \leq \Pr(\hat{s}_j^n \neq s_j^n) \tag{77}$$

$$\Pr(\tilde{s}_{j+1}^n \neq s_{j+1}^n) \leq \Pr(\hat{s}_{j+1}^n \neq s_{j+1}^n). \tag{78}$$

□

Proof: Assume that the extra side-informations s_{j-1}^n is revealed to the decoder j. Now define the maximum a posteriori probability (MAP) decoder as follow.

$$\tilde{s}_j^n = \overline{\mathcal{G}}_j([f]_0^j, s_{-1}^n, s_{j-1}^n) \triangleq \underset{s_j^n}{\operatorname{argmax}} \quad p(s_j^n | [f]_0^j, s_{-1}^n, s_{j-1}^n) \tag{79}$$

where we dropped the subscript in conditional probability density for sake of simplicity. It is known that the MAP decoder is optimal and minimizes the decoding error probability, therefore

$$\Pr(\tilde{s}_j^n \neq s_j^n) \leq \Pr(\hat{s}_j^n \neq s_j^n) \tag{80}$$

Also note that

$$\tilde{s}_j^n = \overline{\mathcal{G}}_j([f]_0^j, s_{-1}^n, s_{j-1}^n) = \underset{s_j^n}{\operatorname{argmax}} \quad p(s_j^n | [f]_0^j, s_{-1}^n, s_{j-1}^n) \tag{81}$$

$$= \underset{s_j^n}{\operatorname{argmax}} \quad p(s_j^n | f_j, s_{j-1}^n) \tag{82}$$

$$\triangleq \tilde{\mathcal{G}}_j(f_j, s_{j-1}^n) \tag{83}$$

where (82) follows form the following Markov property.

$$\left([f]_0^{j-1}, s_{-1}^n\right) \to (f_j, s_{j-1}^n) \to s_j^n. \tag{84}$$

It can be shown through similar steps that the decoder defined in (76) exists with the error probability satisfying (78). This completes the proof. ■

The conditions in (75) and (76) show that any rate that is achievable in the streaming problem in Fig. 1 is also achieved in the multi-terminal source coding setup in Fig. 8(a). Hence a lower bound to this source network also constitutes a lower bound to the original problem. In the next section we find a lower bound on the rate for the setup in Fig. 8(a).

B. Lower Bound for Multi-terminal Source Coding Problem

In this section, we establish a lower bound on the sum-rate of the multi-terminal source coding setup in Fig. 8(a) i.e., $R \geq \frac{1}{2}H(s_{B+1}, s_{B+2}|s_0)$. To this end, we observe the equivalence between the setup in Fig. 8(a) and Fig. 8(b) as stated below.

Lemma 2. *The set of all achievable rate-pairs (R_j, R_{j+1}) for the problem in Fig. 8(a) is identical to the set of all achievable rate-pairs for the problem in Fig. 8(b) where the side information sequence s_{j-1}^n at decoder 1 is replaced by the side information sequence s_{j+1}^n.*

The proof of Lemma 2 follows by observing that the capacity region for the problem in Fig. 8(a) depends on the joint distribution $p(s_j, s_{j+1}, s_{j-1}, s_{j-B-1})$ only via the *marginal* distributions $p(s_j, s_{j-1})$ and $p(s_{j+1}, s_j, s_{j-B-1})$. Indeed the decoding error at decoder j depends on the former whereas the decoding error at decoder $j+1$ depends on the latter. When the source is symmetric, the joint distributions $p(s_j, s_{j-1})$ and $p(s_j, s_{j+1})$ are identical and thus exchanging s_{j-1}^n with s_{j+1}^n does not change the error probability at decoder j and leaves the functions at all other terminals unchanged. The formal proof is straightforward and will be omitted.

Thus it suffices to lower bound the achievable sum-rate for the problem in Fig. 8(b). First note that

$$\begin{aligned} nR_{j+1} &= H(f_{j+1}) \\ &\geq I(f_{j+1}; s_{j+1}^n | s_{j-B-1}^n, f_j) \\ &= H(s_{j+1}^n | s_{j-B-1}^n, f_j) - H(s_{j+1}^n | s_{j-B-1}^n, f_j, f_{j+1}) \\ &\geq H(s_{j+1}^n | s_{j-B-1}^n, f_j) - n\varepsilon_n \qquad (85) \end{aligned}$$

where (85) follows by applying Fano's inequality for decoder $j+1$ in Fig. 8(b) since s_{j+1}^n can be recovered from $(s_{j-B-1}^n, f_j, f_{j+1})$. To bound R_j

$$\begin{aligned} nR_j &= H(f_j) \\ &\geq I(f_j; s_j^n | s_{j-B-1}^n) \\ &= H(s_j^n | s_{j-B-1}^n) - H(s_j^n | s_{j-B-1}^n, f_j) \\ &\geq nH(s_j | s_{j-B-1}) - H(s_j^n | s_{j-B-1}^n, f_j) \\ &\quad + H(s_j^n | s_{j-B-1}^n, s_{j+1}^n, f_j) - n\varepsilon_n \qquad (86) \\ &= nH(s_j | s_{j-B-1}) - I(s_j^n; s_{j+1}^n | s_{j-B-1}^n, f_j) - n\varepsilon_n \\ &= nH(s_j | s_{j-B-1}) - H(s_{j+1}^n | s_{j-B-1}^n, f_j) \\ &\quad + H(s_{j+1}^n | s_{j-B-1}^n, s_j^n, f_j) - n\varepsilon_n \\ &= nH(s_j | s_{j-B-1}) - H(s_{j+1}^n | s_{j-B-1}^n, f_j) \\ &\quad + nH(s_{j+1} | s_j) - n\varepsilon_n \qquad (87) \end{aligned}$$

where (86) follows by applying Fano's inequality for decoder j in Fig. 8(b) since s_j^n can be recovered from (s_{j+1}^n, f_j) and hence $H(s_j^n | s_{j-B-1}^n, s_{j+1}^n, f_j) \leq n\varepsilon_n$ holds and (87) follows from the Markov relation $s_{j+1}^n \to s_j^n \to (f_j, s_{j-B-1}^n)$. By summing (85) and (87) and using $R_j = R_{j+1} = R$, we have

$$\begin{aligned} R_j + R_{j+1} &\geq H(s_{j+1}|s_j) + H(s_j|s_{j-B-1}) \qquad (88) \\ &= H(s_j, s_{j+1}|s_{j-B-1}). \qquad (89) \end{aligned}$$

which is equivalent to (70).

Remark 3. *One way to interpret the lower bound in* (89) *is by observing that the decoder $j+1$ in Fig. 8(b) is able to recover not only s_{j+1}^n but also s_j^n. In particular, the decoder $j+1$ first recovers s_{j+1}^n. Then, similar to decoder j, it also recovers s_j^n from f_j and s_{j+1}^n as side information. Hence, by only considering decoder $j+1$ and following standard source coding argument, the lower bound on the sum-rate satisfies* (89).

C. Extension to Arbitrary $W > 1$

To extend the result for arbitrary W, we use the following result which is a natural generalization of Lemma 1.

Lemma 3. *Consider memoryless encoding functions $f_k = \mathcal{F}_k(s_k^n)$ for $k \in \{j, \ldots, j+W\}$. Any set of decoding functions*

$$\hat{s}_k^n = \mathcal{G}_k([f]_0^k, s_{-1}^n) \qquad k \in \{j, \ldots, j+W-1\} \qquad (90)$$

$$\hat{s}_{j+W}^n = \mathcal{G}_{j+W}([f]_0^{j-B-1}, [f]_j^{j+W}, s_{-1}^n) \qquad (91)$$

can be replaced by a new set of decoding functions as

$$\tilde{s}_k^n = \tilde{\mathcal{G}}_k(f_k, s_{k-1}^n) \qquad k \in \{j, \ldots, j+W-1\} \qquad (92)$$

$$\tilde{s}_{j+W}^n = \tilde{\mathcal{G}}_{j+W}(s_{j-B-1}^n, [f]_j^{j+W}) \qquad (93)$$

where

$$\Pr(\tilde{s}_l^n \neq s_l^n) \leq \Pr(\hat{s}_l^n \neq s_l^n) \qquad j \leq l \leq j+W. \qquad (94)$$

□

The proof is an immediate extension of Lemma 1 and is excluded here. The lemma suggests a natural multi-terminal problem for establishing the lower bound with $W+1$ encoders and decoders. For concreteness we discuss the case when $W = 2$. Consider three encoders $t \in \{j, j+1, j+2\}$. Encoder t observes s_t^n and compresses it into an index $f_t \in [1, 2^{nR_t}]$. s_{t-1}^n for $t \in \{j, j+1\}$ are revealed to the corresponding decoders and s_{j-B-1}^n is revealed to the decoder $j+2$. Using an argument analogous to Lemma 2 the rate region is equivalent to the case when s_{j+1}^n and s_{j+2}^n are instead revealed to decoders j and $j+1$ respectively. For this new setup we can argue that decoder $j+2$ can always reconstruct $(s_j^n, s_{j+1}^n, s_{j+2}^n)$ given $(s_{j-B-1}^n, f_j, f_{j+1}, f_{j+2})$. In particular, following the same argument in Remark 3, the decoder $j+2$ first recovers s_{j+2}^n, then using $\{f_{j+1}, s_{j+2}^n\}$ recovers s_{j+1}^n and finally using $\{f_j, s_{j+1}^n\}$ recovers s_j^n. And hence if we only consider decoder $j+2$ with side information s_{j-B-1}^n the sum-rate must satisfy:

$$3R = R_j + R_{j+1} + R_{j+2} \geq H(s_j, s_{j+1}, s_{j+2}|s_{j-B-1}). \qquad (95)$$

Using Lemma 3 for $W = 2$ it follows that the proposed lower bound also continues to hold for the original streaming problem. This completes the proof. The extension to any arbitrary W is completely analogous.

VII. Lossy Rate-Recovery for Gauss-Markov Sources

We establish lower and upper bounds on the lossy rate-recovery function of Gauss-Markov sources when an immediate recovery following the burst erasure is required i.e., $W = 0$. For the single burst erasure case, the proof of the lower bound in Prop. 1 is presented in Section VII-A whereas the proof of the upper bound in Prop. 2 is presented in Section VII-B. The proof of Prop. 3 for the multiple burst erasures case is presented in Section VII-C. Finally the proof of Corollary 3, which establishes the lossy rate-recovery function in the high resolution regime is presented in Section VIII.

A. Lower Bound: Single Burst Erasure

Consider any rate R code that satisfies an average distortion of D as stated in (5). For each $i \geq 0$ we have

$$\begin{aligned} nR &\geq H(f_i) \\ &\geq H(f_i|[f]_0^{i-B-1}, s_{-1}^n) \quad (96) \\ &= I(s_i^n; f_i|[f]_0^{i-B-1}, s_{-1}^n) + H(f_i|s_i^n, [f]_0^{i-B-1}, s_{-1}^n) \\ &\geq h(s_i^n|[f]_0^{i-B-1}, s_{-1}^n) - h(s_i^n|f_i, [f]_0^{i-B-1}, s_{-1}^n) \quad (97) \end{aligned}$$

where (96) follows from the fact that conditioning reduces the entropy.

We now present an upper bound for the second term and a lower bound for the first term in (97). We first establish an upper bound for the second term in (97). Suppose that the burst erasure occurs in the interval $[i-B, i-1]$. The reconstruction sequence $\hat{s}_i^n$ must be a function of $(f_i, [f]_0^{i-B-1}, s_{-1}^n)$. Thus we have

$$\begin{aligned} h(s_i^n|[f]_0^{i-B-1}, f_i, s_{-1}^n) &= h(s_i^n - \hat{s}_i^n \mid [f]_0^{i-B-1}, f_i, s_{-1}^n) \\ &\leq h(s_i^n - \hat{s}_i^n) \\ &\leq \frac{n}{2}\log(2\pi e D), \quad (98) \end{aligned}$$

where the last step uses the fact that the expected average distortion between s_i^n and $\hat{s}_i^n$ is no greater than D, and applies standard arguments [29, Ch. 13].

To lower bound the first term in (97), we successively use the Gauss-Markov relation (11) to express:

$$s_i = \rho^{(B+1)} s_{i-B-1} + \tilde{n} \quad (99)$$

for each $i \geq B$ and $\tilde{n} \sim \mathcal{N}(0, 1-\rho^{2(B+1)})$ is independent of s_{i-B-1}. Using the Entropy Power Inequality [29] we have

$$\begin{aligned} &2^{\frac{2}{n}h(s_i^n|[f]_0^{i-B-1}, s_{-1}^n)} \geq \\ &\qquad 2^{\frac{2}{n}h(\rho^{B+1}s_{i-B-1}^n|[f]_0^{i-B-1}, s_{-1}^n)} + 2^{\frac{2}{n}h(\tilde{n}^n)} \quad (100) \end{aligned}$$

This further reduces to

$$\begin{aligned} &h(s_i^n \mid [f]_0^{i-B-1}, s_{-1}^n) \geq \\ &\frac{n}{2}\log\left(\rho^{2(B+1)}2^{\frac{2}{n}h(s_{i-B-1}^n|[f]_0^{i-B-1}, s_{-1}^n)} + 2\pi e(1-\rho^{2(B+1)})\right). \quad (101) \end{aligned}$$

It remains to lower bound the entropy term in the right hand side of (101). We show the following in Appendix B.

Lemma 4. *For any $k \geq 0$*

$$2^{\frac{2}{n}h(s_k^n|[f]_0^k, s_{-1}^n)} \geq \frac{2\pi e(1-\rho^2)}{2^{2R}-\rho^2}\left(1 - \left(\frac{\rho^2}{2^{2R}}\right)^k\right) \quad (102)$$

□

Upon substituting, (102), (101), and (98) into (97) we obtain that for each $i \geq B+1$

$$\begin{aligned} R \geq \frac{1}{2}\log\Bigg[&\frac{\rho^{2(B+1)}(1-\rho^2)}{D(2^{2R}-\rho^2)}\left(1 - \left(\frac{\rho^2}{2^{2R}}\right)^{i-B-1}\right) \\ &+ \frac{1-\rho^{2(B+1)}}{D}\Bigg]. \quad (103) \end{aligned}$$

Selecting the largest value of i, i.e. $\mathcal{L}$, yields the tightest lower bound. As mentioned earlier, we are interested in infinite horizon when $\mathcal{L} \to \infty$, which yields the tightest lower bound, we have

$$R \geq \frac{1}{2}\log\left(\frac{\rho^{2(B+1)}(1-\rho^2)}{D(2^{2R}-\rho^2)} + \frac{1-\rho^{2(B+1)}}{D}\right) \quad (104)$$

Rearranging (104) we have that

$$D2^{4R} - (D\rho^2 + 1 - \rho^{2(B+1)})2^{2R} + \rho^2(1-\rho^{2B}) \geq 0 \quad (105)$$

Since (105) is a quadratic equation in 2^{2R}, it can be easily solved. Keeping the root that yields $R > 0$ results in the lower bound in (12) in Prop. 1. This completes the proof.

Remark 4. *Upon examining the proof of the lower bound of Prop. 1, we note that it applies to any source process that satisfies* (11) *and where the additive noise is i.i.d. $\mathcal{N}(0, 1-\rho^2)$. We do not use the fact that the source process is itself a Gaussian process.*

B. Coding Scheme: Single Burst Erasure

The achievable rate is based on quantization and binning. For each $i \geq 0$, we consider the test channel

$$u_i = s_i + z_i, \quad (106)$$

where $z_i \sim \mathcal{N}(0, \sigma_z^2)$ is independent Gaussian noise. At time i we sample a total of $2^{n(I(u_i;s_i)+\varepsilon)}$ codeword sequences i.i.d. from $\mathcal{N}(0, 1+\sigma_z^2)$. The codebook at each time is partitioned into 2^{nR} bins. The encoder finds the codeword sequence u_i^n typical with the source sequence s_i^n and transmits the bin index f_i assigned to u_i^n.

The decoder, upon receiving f_i attempts to decode u_i^n at time i, using all the previously recovered codewords $\{u_j^n : 0 \leq j \leq i-1, g_j \neq \star\}$ and the source sequence s_{-1}^n as side information. The reconstruction sequence $\hat{s}_i^n$ is the minimum mean square error (MMSE) estimate of s_i^n given u_i^n and the past sequences. The coding scheme presented here is based on binning, similar to lossless case discussed in Section V-C. The main difference in the analysis is that, unlike the lossless case, neither the recovered sequences u_i^n nor reconstructed source sequences $\hat{s}_i^n$ inherit the Markov property of the original source sequences s_i^n. Therefore, unlike the lossless case, the

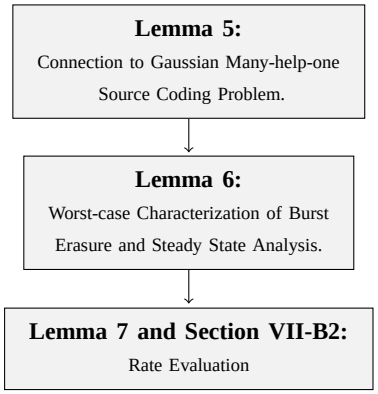
Lemma 5:
Connection to Gaussian Many-help-one Source Coding Problem.
Lemma 6:
Worst-case Characterization of Burst Erasure and Steady State Analysis.
Lemma 7 and Section VII-B2:
Rate Evaluation

Fig. 9: Flowchart summarizing the proof steps of Prop. 2.

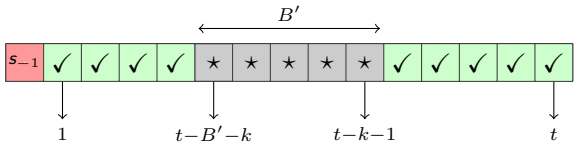

Fig. 10: Schematic of single burst erasure channel model. The channel inputs in the interval $[t-B'-k, t-k-1]$ is erased for some $0 \le B' \le B$ and $k \in [0, t-B']$. The rest are available at the decoder, as shown by check mark in the figure.

decoder does not reset following a burst erasure, once the error propagation is completed. Since the effect of a burst erasure persists throughout, the analysis of achievable rate is significantly more involved.

Fig. 9 summarizes the main steps in proving Prop. 2. In particular, in Lemma 5, we first derive necessary parametric rate constraints associated with every possible erasure pattern. Second, through the Lemma 6, we characterize the the worst-case erasure pattern that dominates the rate and distortion constraints. Finally in Lemma 7 and Section VII-B2, we evaluate the achievable rate to complete the proof of Prop. 2.

1) Analysis of Achievable Rate: Given a collection of random variables $\mathcal{V}$, we let the MMSE estimate of s_i be denoted by $\hat{s}_i(\mathcal{V})$, and its associated estimation error is denoted by $\sigma_i^2(\mathcal{V})$, i.e.,

$$\hat{s}_i(\mathcal{V}) = E\left[s_i \mid \mathcal{V}\right] \tag{107}$$

$$\sigma_i^2(\mathcal{V}) = E[(s_i - \hat{s}_i(\mathcal{V}))^2]. \tag{108}$$

We begin with a parametric characterization of the achievable rate.

Lemma 5. *A rate-distortion pair (R, D) is achievable, if for every $t \ge 0$, $B' \in [0, B]$ and $k \in [0, t-B']$ we have*

$$R \ge \lambda_t(k, B') \triangleq I(s_t; u_t \mid [u]_0^{t-B'-k-1}, [u]_{t-k}^{t-1}, s_{-1}), \tag{109}$$

and the test-channel (106) *satisfies*

$$\gamma_t(k, B') \triangleq E\left[\left(s_t - \hat{s}_t([u]_0^{t-B'-k-1}, [u]_{t-k}^{t}, s_{-1})\right)^2\right] = \sigma_t^2([u]_0^{t-B'-k-1}, [u]_{t-k}^{t}, s_{-1}) \le D. \tag{110}$$

where $\sigma_t^2(\cdot)$ and $\hat{s}_t(\cdot)$ are defined in (108) *and* (107) *respectively.* □

Proof: Consider the decoder at any time $t \ge 0$ outside the error propagation window. Assume that a single burst erasure of length $B' \in [0, B]$ spans the interval $[t-B'-k, t-k-1]$ for some $k \in [0, t-B']$ i.e.,

$$g_j = \begin{cases} \star, & j \in \{t-B'-k, \ldots, t-k-1\} \\ f_j, & \text{else.} \end{cases} \tag{111}$$

The schematic of the erasure channel is illustrated in Fig. 10. Notice that $k = 0$ represents the case of the most recent burst erasure spanning the interval $[t-B'-1, t-1]$. The decoder is interested in first successfully recovering u_t^n and then reconstructing s_t^n within distortion D by performing MMSE estimation of s_t^n from all the previously recovered sequences u_i^n where $i \le t$ and $g_i \ne \star$. The decoder succeeds with high probability if the rate constraint satisfies (109) (see e.g., [30]) and the distortion constraint satisfies (110). If these constraints hold for all the possible triplets (t, B', k), the decoder is guaranteed to succeed in reproducing any source sequence within desired distortion D.

Finally in the streaming setup, we can follow the argument similar to that in Section V-C to argue that the decoder succeeds in the entire horizon of $\mathcal{L}$ provided we select the source length n to be sufficiently large. The formal proof is omitted here. ■

As a result of Lemma 5, in order to compute the achievable rate, we need to characterize the worst case values of (t, k, B') that simultaneously maximize $\lambda_t(k, B)$ and $\gamma_t(k, B)$. We present such a characterization next.

Lemma 6. *The functions $\lambda_t(k, B)$ and $\gamma_t(k, B)$ satisfy the following properties:*

1) *For all $t \ge B'$ and $k \in [0, t-B']$, $\lambda_t(k, B') \le \lambda_t(0, B')$ and $\gamma_t(k, B') \le \gamma_t(0, B')$, i.e. the worst-case erasure pattern contains the burst erasure in the interval $[t-B, t-1]$.*
2) *For all $t \ge B$ and $0 \le B' \le B$, $\lambda_t(0, B') \le \lambda_t(0, B)$ and $\gamma_t(0, B') \le \gamma_t(0, B)$, i.e. the worse-case erasure pattern includes maximum burst length.*
3) *For a fixed B, the functions $\lambda_t(0, B)$ and $\gamma_t(0, B)$ are both increasing with respect to t, for $t \ge B$, i.e. the worse-case erasure pattern happens in steady state (i.e., $t \to \infty$) of the system.*
4) *For all $t < B$, $0 \le B' \le t$ and $k \in [0, t-B']$, $\lambda_t(k, B') \le \lambda_B(0, B)$ and $\gamma_t(k, B') \le \gamma_B(0, B)$ i.e., the burst erasure spanning $[0, B-1]$ dominates all burst erasures that terminate before time $B-1$.*

□

Proof: Before establishing the proof, we state two inequalities which are established in Appendix C. For each

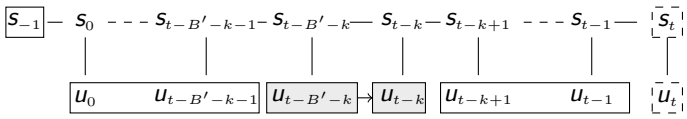

Fig. 11: Replacing $u_{t-B'-k}$ by u_{t-k} improves the estimate of s_t and u_t.

$k \in [1 : t - B']$ we have that:

$$h(u_t|[u]_0^{t-B'-k-1}, [u]_{t-k}^{t-1}, s_{-1}) \leq h(u_t|[u]_0^{t-B'-k}, [u]_{t-k+1}^{t-1}, s_{-1}), \quad (112)$$

$$h(s_t|[u]_0^{t-B'-k-1}, [u]_{t-k}^{t}, s_{-1}) \leq h(s_t|[u]_0^{t-B'-k}, [u]_{t-k+1}^{t}, s_{-1}). \quad (113)$$

The above inequalities state that the conditional differential entropy of u_t and s_t is reduced if the variable $u_{t-B'-k}$ is replaced by u_{t-k} in the conditioning and the remaining variables remain unchanged. Fig. 11 provides a schematic interpretation of the above inequalities. The proof in Appendix C exploits the specific structure of the Gaussian test channel (106) and Gaussian sources to establish these inequalities.

In the remainder of the proof, we establish each of the four properties separately.

1) We show that both $\lambda_t(k, B')$ and $\gamma_t(k, B')$ are decreasing functions of k for $k \in [1 : t - B']$.

$$\begin{aligned}\lambda_t(k, B') &= I(s_t; u_t|[u]_0^{t-B'-k-1}, [u]_{t-k}^{t-1}, s_{-1}) \\ &= h(u_t|[u]_0^{t-B'-k-1}, [u]_{t-k}^{t-1}, s_{-1}) - h(u_t|s_t) \\ &\leq h(u_t|[u]_0^{t-B'-k}, [u]_{t-k+1}^{t-1}, s_{-1}) - h(u_t|s_t) \quad (114) \\ &= I(s_t; u_t|[u]_0^{t-B'-k}, [u]_{t-k+1}^{t-1}, s_{-1}) \\ &= \lambda_t(k-1, B') \quad (115)\end{aligned}$$

where (114) follows from using (112). In a similar fashion since

$$\gamma_t(k, B') = \sigma_t^2\left([u]_0^{t-B'-k}, [u]_{t-k+1}^{t}, s_{-1}\right)$$

is the MMSE estimation error of s_t given $\left([u]_0^{t-B'-k}, [u]_{t-k+1}^{t}, s_{-1}\right)$, we have

$$\begin{aligned}\frac{1}{2}\log\left(2\pi e \cdot \gamma_t(k, B')\right) &= h(s_t|[u]_0^{t-B'-k-1}, [u]_{t-k}^{t}, s_{-1}) \\ &\leq h(s_t|[u]_0^{t-B'-k}, [u]_{t-k+1}^{t}, s_{-1}) \quad (116) \\ &= \frac{1}{2}\log\left(2\pi e \cdot \gamma_t(k-1, B')\right) \quad (117)\end{aligned}$$

where (116) follows from using (113). Since $f(x) = \frac{1}{2}\log(2\pi e x)$ is a monotonically increasing function it follows that $\gamma_t(k, B') \leq \gamma_t(k-1, B')$. By recursively applying (115) and (117) until $k = 1$, the proof of property (1) is complete.

2) We next show that the worst case erasure pattern also has the longest burst. This follows intuitively since the decoder can just ignore some of the symbols received over the channel. Thus any rate achieved with the longest burst is also achieved for the shorter burst. The formal justification is as follows. For any $B' \leq B$ we have,

$$\begin{aligned}\lambda_t(0, B') &= I(s_t; u_t|[u]_0^{t-B'-1}, s_{-1}) \\ &= h(u_t|[u]_0^{t-B'-1}, s_{-1}) - h(u_t|s_t) \quad (118) \\ &= h(u_t|[u]_0^{t-B-1}, [u]_{t-B}^{t-B'-1}, s_{-1}) - h(u_t|s_t) \\ &\leq h(u_t|[u]_0^{t-B-1}, s_{-1}) - h(u_t|s_t) \quad (119) \\ &= I(s_t; u_t|[u]_0^{t-B-1}, s_{-1}) \quad (120) \\ &= \lambda_t(0, B) \quad (121)\end{aligned}$$

where (118) and (120) follows from the Markov chain property

$$u_t \to s_t \to \{[u]_0^{t-j-1}, s_{-1}\}, \quad j \in \{B, B'\} \quad (122)$$

and (119) follows from the fact that conditioning reduces differential entropy. In a similar fashion the inequality $\gamma_t(0, B') \leq \gamma_t(0, B)$ follows from the fact that the estimation error can only be reduced by having more observations.

3) We show that both $\lambda_t(0, B)$ and $\gamma_t(0, B)$ are increasing functions with respect to t. Intuitively as t increases the effect of having s_{-1} at the decoder vanishes and hence the required rate increases. Consider

$$\begin{aligned}\lambda_{t+1}(0, B) &= I(s_{t+1}; u_{t+1}|[u]_0^{t-B}, s_{-1}) \\ &= h(u_{t+1}|[u]_0^{t-B}, s_{-1}) - h(u_{t+1}|s_{t+1}) \\ &= h(u_{t+1}|[u]_0^{t-B}, s_{-1}) - h(u_t|s_t) \quad (123) \\ &\geq h(u_{t+1}|[u]_0^{t-B}, s_{-1}, s_0) - h(u_t|s_t) \quad (124) \\ &= h(u_{t+1}|[u]_1^{t-B}, s_0) - h(u_t|s_t) \quad (125) \\ &= h(u_t|[u]_0^{t-B-1}, s_{-1}) - h(u_t|s_t) \quad (126) \\ &= I(s_t; u_t|[u]_0^{t-B-1}, s_{-1}) \\ &= \lambda_t(0, B) \quad (127)\end{aligned}$$

where (123) and (126) follow from time-invariant property of the source model and the test channel, (124) follows from the fact that conditioning reduces differential entropy and (125) uses the following Markov chain property

$$\{u_0, s_{-1}\} \to \{[u]_1^{t-B}, s_0\} \to u_{t+1}. \quad (128)$$

Similarly,

$$\begin{aligned}\frac{1}{2}\log\left(2\pi e \cdot \gamma_{t+1}(0, B)\right) &= h(s_{t+1}|[u]_0^{t-B}, u_{t+1}, s_{-1}) \\ &\geq h(s_{t+1}|[u]_0^{t-B}, u_{t+1}, s_0, s_{-1}) \\ &= h(s_{t+1}|[u]_1^{t-B}, u_{t+1}, s_0) \quad (129) \\ &= h(s_t|[u]_0^{t-B-1}, u_t, s_{-1}) \\ &= \frac{1}{2}\log\left(2\pi e \cdot \gamma_t(0, B)\right) \quad (130)\end{aligned}$$

where (129) follows from the following Markov chain property

$$\{u_0, s_{-1}\} \to \{[u]_1^{t-B}, u_{t+1}, s_0\} \to s_{t+1}. \quad (131)$$

Since (127) and (130) hold for every $t \geq B$ the proof of property (3) is complete.

4) Note that for $t < B$ we have $0 \le B' \le t$ and thus we can write

$$\begin{aligned}
\lambda_t(k, B') &\le \lambda_t(0, B') && (132)\\
&\le \lambda_t(0, t) && (133)\\
&= h(u_t|s_{-1}) - h(u_t|s_t)\\
&= h(u_t|s_{-1}) - h(u_B|s_B)\\
&= h(u_B|s_{B-t-1}) - h(u_B|s_B)\\
&\le h(u_B|s_{-1}) - h(u_B|s_B) && (134)\\
&= \lambda_B(0, B) && (135)
\end{aligned}$$

where (132) follows from part 1 of the lemma, (133) is based on the fact that the worse-case erasure pattern contains most possible erasures and follows from the similar steps used in deriving (121) and using the fact that if $t < B$, the burst erasure length is at most t. Eq. (134) follows from the fact that whenever $t < B$ the relation $s_{-1} \to s_{B-t-1} \to u_B$ holds since $t < B$ is assumed. In a similar fashion we can show that $\gamma_t(k, B') \le \gamma_B(0, B)$.

This completes the proof of lemma 6. ∎

Following the four parts of Lemma 6, it follows that the worst-case erasure pattern happens at steady state i.e. $t \to \infty$ when there is a burst of length B which spans $[t - B, t - 1]$. According to this and Lemma 5, any pair (R, D) is achievable if

$$R \ge \lim_{t\to\infty} \lambda_t(0, B) \quad (136)$$

$$D \ge \lim_{t\to\infty} \gamma_t(0, B) \quad (137)$$

Lemma 7. *Consider $u_i = s_i + z_i$ and suppose the noise variance σ_z^2 satisfies*

$$\Gamma(B, \sigma_z^2) \triangleq \lim_{t\to\infty} E\left[\left(s_t - \hat{s}_t([u]_0^{t-B-1}, u_t)\right)^2\right] \quad (138)$$

$$= \lim_{t\to\infty} \sigma_t^2\left([u]_0^{t-B-1}, u_t\right) \le D. \quad (139)$$

The following rate is achievable:

$$R = \Lambda(B, \sigma_z^2) \triangleq \lim_{t\to\infty} I(s_t; u_t|[u]_0^{t-B-1}). \quad (140)$$

□

Proof: It suffices to show that any test channel satisfying (139) also implies (137) and any rate satisfying (140) implies (136). These relations can be established in a straightforward manner as shown below.

$$\begin{aligned}
R = \Lambda(B, \sigma_z^2) &= \lim_{t\to\infty} I(s_t; u_t|[u]_0^{t-B-1})\\
&= \lim_{t\to\infty} \left(h(u_t|[u]_0^{t-B-1}) - h(u_t|s_t)\right) && (141)\\
&\ge \lim_{t\to\infty} \left(h(u_t|[u]_0^{t-B-1}, s_{-1}) - h(u_t|s_t)\right) && (142)\\
&= \lim_{t\to\infty} \lambda_t(0, B) && (143)
\end{aligned}$$

and

$$\begin{aligned}
D \ge \Gamma(B, \sigma_z^2) &= \lim_{t\to\infty} E\left[\left(s_t - \hat{s}_t([u]_0^{t-B-1}, u_t)\right)^2\right] && (144)\\
&\ge \lim_{t\to\infty} E\left[\left(s_t - \hat{s}_t([u]_0^{t-B-1}, u_t, s_{-1})\right)^2\right] && (145)\\
&= \lim_{t\to\infty} \gamma_t(0, B) && (146)
\end{aligned}$$

∎

We conclude that $\Gamma(B, \sigma_z^2) = D$, the rate $R^+_{\text{GM-SE}}(B, D) = \Lambda(B, \sigma_z^2)$ is achievable.

2) Numerical Evaluation: We derive an expression for numerically evaluating the noise variance σ_z^2 in (106) and also establish (13) and (16).

To this end it is helpful to consider the following single-variable discrete-time Kalman filter for $i \in [0, t - B - 1]$,

$$s_i = \rho s_{i-1} + n_i, \qquad n_i \sim N(0, 1 - \rho^2) \quad (147)$$

$$u_i = s_i + z_i, \qquad z_i \sim N(0, \sigma_z^2). \quad (148)$$

Note that s_i can be viewed as the state of the system updated according a Gauss-Markov model and u_i as the output of the system at each time i, which is a noisy version of the state s_i. Consider the system in steady state i.e. $t \to \infty$. The MMSE estimation error of s_{t-B} given *all* the previous outputs up to time $t - B - 1$ i.e. $[u]_0^{t-B-1}$ is expressed as (see, e.g., [31, Example V.B.2]):

$$\Sigma(\sigma_z^2) \triangleq \lim_{t\to\infty} \sigma^2_{t-B}([u]_0^{t-B-1}) \quad (149)$$

$$= \frac{1}{2}\sqrt{(1 - \sigma_z^2)^2(1 - \rho^2)^2 + 4\sigma_z^2(1 - \rho^2)} + \frac{1 - \rho^2}{2}(1 - \sigma_z^2) \quad (150)$$

Also using the orthogonality principle for MMSE estimation we have

$$[u]_0^{t-B-1} \to \hat{s}_{t-B}([u]_0^{t-B-1}) \to s_{t-B} \to s_t \quad (151)$$

Thus we can express

$$s_{t-B} = \hat{s}_{t-B}([u]_0^{t-B-1}) + \hat{e} \quad (152)$$

where the noise $\hat{e} \sim \mathcal{N}(0, \Sigma\left(\sigma_z^2\right))$ is independent of the observation set $[u]_0^{t-B-1}$. Equivalently we can express (see e.g. [32])

$$\hat{s}_{t-B}([u]_0^{t-B-1}) = \tilde{\alpha} s_{t-B} + \tilde{e} \quad (153)$$

where

$$\tilde{\alpha} \triangleq 1 - \Sigma\left(\sigma_z^2\right) \quad (154)$$

and $\tilde{e} \sim \mathcal{N}\left(0, \Sigma\left(\sigma_z^2\right)\left(1 - \Sigma\left(\sigma_z^2\right)\right)\right)$ is independent of s_{t-B}. Thus we have

$$\begin{aligned}
\Lambda(B, \sigma_z^2) &= \lim_{t\to\infty} I(s_t; u_t|[u]_0^{t-B-1})\\
&= \lim_{t\to\infty} I(s_t; u_t|\hat{s}_{t-B}([u]_0^{t-B-1}))\\
&= \lim_{t\to\infty} I(s_t; u_t|\tilde{\alpha} s_{t-B} + \tilde{e})\\
&= \lim_{t\to\infty} I(s_t; u_t|s_{t-B} + e)\\
&= I(s_t; u_t|\tilde{s}_{t-B}) && (155)
\end{aligned}$$

where we have used (153) and $e \sim \mathcal{N}(0, \Sigma\left(\sigma_z^2\right)/(1 - \Sigma\left(\sigma_z^2\right)))$. This establishes (13)

in Prop. 2. In a similar manner,

$$\begin{aligned}\Gamma(B,\sigma_z^2) &= \lim_{t\to\infty} \sigma_t^2([u]_0^{t-B-1}, u_t)\\ &= \lim_{t\to\infty} \sigma_t^2(\hat{s}_{t-B}([u]_0^{t-B-1}), u_t)\\ &= \lim_{t\to\infty} \sigma_t^2(\tilde{\alpha} s_{t-B} + \tilde{e}, , u_t)\\ &= \lim_{t\to\infty} \sigma_t^2(s_{t-B} + e, u_t)\\ &= \sigma_t^2(\tilde{s}_{t-B}, u_t) \end{aligned} \tag{156}$$

which establishes (16). Furthermore since

$$s_t = \rho^B s_{t-B} + \tilde{n} \tag{157}$$

where $\tilde{n} \sim \mathcal{N}(0, 1-\rho^{2B})$,

$$\Gamma(B,\sigma_z^2) = \sigma_t^2(\tilde{s}_{t-B}, u_t) \tag{158}$$

$$= \left[\frac{1}{\sigma_z^2} + \frac{1}{1-\rho^{2B}\left(1-\Sigma(\sigma_z^2)\right)}\right]^{-1} \tag{159}$$

where (159) follows from the application of MMSE estimator and using (157), (152) and the definition of the test channel in (106). Thus the noise σ_z^2 in the test channel (106) is obtained by setting

$$\Gamma(B,\sigma_z^2) = D. \tag{160}$$

This completes the proof of Prop. 2.

Remark 5. *When $W > 0$, the generalization of Lemma 6 appears to involve a rate-region corresponding to the Berger-Tung inner bound [33] and the analysis is considerably more involved. Furthermore hybrid schemes involving predictive coding and binning may lead to an improved performance over the binning-only scheme. Thus the scope of this problem is well beyond the results in this paper.*

C. Coding Scheme: Multiple Burst Erasures with Guard Intervals

We study the achievable rate using the quantize and binning scheme with test channel (106) when the channel introduces multiple burst erasures each of length no greater than B and with a guard interval of at-least L symbols separating consecutive burst erasures. While the coding scheme is the same as the single burst erasure channel model and is based on quantize and binning and MMSE estimation at the decoder, characterizing the worst case erasure pattern of the channel is main challenge and requires some additional steps.

1) Analysis of Achievable Rate: We introduce the following notation in our analysis. Let Ω_t denote the set of time indices up to time $t-1$ when the channel packets are not erased i.e.,

$$\Omega_t = \{i : 0 \le i \le t-1, g_i \neq \star\}, \tag{161}$$

and let us define

$$\mathbf{s}_\Omega = \{s_i : i \in \Omega\}, \tag{162}$$

$$\mathbf{u}_\Omega = \{u_i : i \in \Omega\}. \tag{163}$$

Given the erasure sequence Ω_t, and given $g_t = f_t$, the decoder can reconstruct u_t^n provided that the test channel is selected such that the rate satisfies (see e.g., [30])

$$R \ge \lambda_t(\Omega_t) \triangleq I(s_t; u_t | \mathbf{u}_{\Omega_t}, s_{-1}). \tag{164}$$

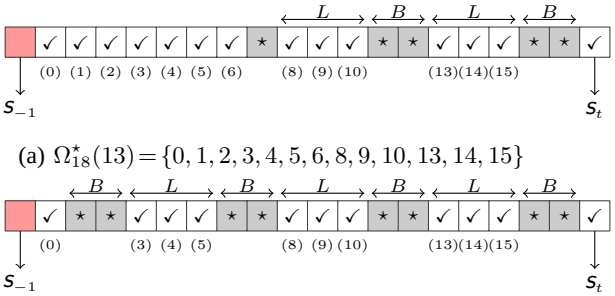

(a) $\Omega_{18}^\star(13) = \{0,1,2,3,4,5,6,8,9,10,13,14,15\}$

(b) $\Omega_{18}^\star = \{0,3,4,5,8,9,10,13,14,15\}$

Fig. 12: Schematic of the erasure patterns in Lemma 9 for $t = 18$, $L = 3$ and $B = 2$. Fig. 12a illustrates, $\Omega_t^\star(\theta)$ in part 1 of Lemma 9. The non-erased symbols are denoted by checkmarks. Fig. 12b illustrates $\Omega_t^\star$ as stated in part 2 of Lemma 9.

and the distortion constraint satisfies

$$\begin{aligned}\gamma_t(\Omega_t) &\triangleq E\left[\left(s_t - \hat{s}_t(\mathbf{u}_{\Omega_t}, u_t, s_{-1})\right)^2\right]\\ &= \sigma_t^2\left(\mathbf{u}_{\Omega_t}, u_t, s_{-1}\right) \le D \end{aligned} \tag{165}$$

for each $t \ge 0$ and each feasible set Ω_t. Thus we are again required to characterize the Ω_t for each value of t corresponding to the worst-case erasure pattern. The following two lemmas are useful towards this end.

Lemma 8. *Consider the two sets $A, B \subseteq \mathbb{N}$ each of size r as $A = \{a_1, a_2, \cdots, a_r\}$, $B = \{b_1, b_2, \cdots, b_r\}$ such that $1 \le a_1 < a_2 < \cdots < a_r$ and $1 \le b_1 < b_2 < \cdots < b_r$ and for any $i \in \{1, \ldots, r\}$, $a_i \le b_i$. Then the test channel* (106) *satisfies the following:*

$$h(s_t|\mathbf{u}_A, s_{-1}) \ge h(s_t|\mathbf{u}_B, s_{-1}), \quad \forall t \ge b_r \tag{166}$$

$$h(u_t|\mathbf{u}_A, s_{-1}) \ge h(u_t|\mathbf{u}_B, s_{-1}), \quad \forall t > b_r. \tag{167}$$

□

The proof of Lemma 8 is available in Appendix D.

Lemma 9. *Assume that at time t, $g_t = f_t$ and let Ω_t be as defined in* (161) .

1) *Among all feasible sets Ω_t of size $|\Omega_t| = \theta$, $\lambda_t(\Omega_t)$ and $\gamma_t(\Omega_t)$ are maximized by a set $\Omega_t^\star(\theta)$ where all the erasures happen in the closest possible locations to time t.*
2) *For each fixed t, both $\lambda_t(\Omega_t^\star(\theta))$ and $\gamma_t(\Omega_t^\star(\theta))$ are maximized by the minimum possible value of θ. Equivalently, the maximizing set, denoted by $\Omega_t^\star$, corresponds to the erasure pattern with maximum number of erasures.*
3) *Both $\lambda_t(\Omega_t^\star)$ and $\gamma_t(\Omega_t^\star)$ are increasing functions with respect to t.*

□

The proof of Lemma 9 is presented in Appendix E. We present an example in Fig. 12 to illustrate Lemma 9. We assume $t = 18$. The total number of possible erasures up to time $t = 18$ is restricted to be 5, or equivalently the number of non-erased packets is $\theta = 13$ in Fig 12a. The set $\Omega_{18}^\star(13)$ indicates the set of non-erased indices associated with

the worst case erasure pattern. Based on part 2 of Lemma 9, Fig. 12b shows the worst case erasure pattern for time $t = 18$, which includes the maximum possible erasures.

Following the three steps in Lemma 9 a rate-distortion pair (R, D) is achievable if

$$R \geq \lim_{t\to\infty} \lambda_t(\Omega_t^\star) \tag{168}$$

$$D \geq \lim_{t\to\infty} \gamma_t(\Omega_t^\star) \tag{169}$$

Lemma 10. *Any test channel noise σ_z^2 satisfying* (19) *and* (20) *in Prop. 3, i.e.*

$$R \geq I(\mathsf{s}_t; \mathsf{u}_t|\tilde{\mathsf{s}}_{t-L-B}, [\mathsf{u}]_{t-L-B+1}^{t-B-1}) \tag{170}$$

$$D \geq \sigma_t^2(\tilde{\mathsf{s}}_{t-L-B}, [\mathsf{u}]_{t-L-B+1}^{t-B-1}, \mathsf{u}_t) \tag{171}$$

where $\tilde{\mathsf{s}}_{t-L-B} = \mathsf{s}_{t-L-B} + \mathsf{e}$, where $\mathsf{e} \sim \mathcal{N}(0, D/(1-D))$, also satisfies (168) *and* (169)*.*

Proof: See Appendix F. ∎

This completes the proof of Prop 3.

2) Numerical Evaluation: We derive the expression for numerically evaluating σ_z^2. To this end, first note that the estimation error of estimating s_{t-B-1} from $\{\tilde{\mathsf{s}}_{t-L-B}, [\mathsf{u}]_{t-L-B+1}^{t-B-1}\}$ can be computed as follows.

$$\begin{aligned}\eta(\sigma_z^2) &\triangleq \sigma_{t-B-1}^2(\tilde{\mathsf{s}}_{t-L-B}, [\mathsf{u}]_{t-L-B+1}^{t-B-1}) \\ &= E\left[\mathsf{s}_{t-B-1}^2\right] - E\left[\mathsf{s}_{t-B-1}\mathsf{U}\right]\left(E\left[\mathsf{U}^T\mathsf{U}\right]\right)^{-1} E\left[\mathsf{s}_{t-B-1}\mathsf{U}^T\right] \qquad (172)\\ &= 1 - A_1(A_2)^{-1}A_1^T \qquad (173)\end{aligned}$$

where we define

$$\mathsf{U} \triangleq \begin{bmatrix}\mathsf{u}_{t-B-1} & \mathsf{u}_{t-B-2} & \dots & \mathsf{u}_{t-L-B+1} & \tilde{\mathsf{s}}_{t-L-B}\end{bmatrix}$$

and $(.)^T$ denotes the transpose operation. Also note that A_1 and A_2 can be computed as follows.

$$A_1 = (1, \rho, \rho^2, \cdots, \rho^{L-1}) \tag{174}$$

$$A_2 = \begin{pmatrix} 1+\sigma_z^2 & \rho & \cdots & \rho^{L-2} & \rho^{L-1} \\ \rho & 1+\sigma_z^2 & \cdots & \rho^{L-3} & \rho^{L-2} \\ \vdots & \vdots & \ddots & \vdots & \vdots \\ \rho^{L-2} & \rho^{L-3} & \cdots & 1+\sigma_z^2 & \rho \\ \rho^{L-1} & \rho^{L-2} & \cdots & \rho & 1+\frac{D}{1-D} \end{pmatrix} \tag{175}$$

According to (171) we can write

$$\begin{aligned} D &= \sigma_t^2(\tilde{\mathsf{s}}_{t-L-B}, [\mathsf{u}]_{t-L-B+1}^{t-B-1}, \mathsf{u}_t) \qquad (176)\\ &= \sigma_t^2\left(\hat{\mathsf{s}}_{t-B-1}(\tilde{\mathsf{s}}_{t-L-B}, [\mathsf{u}]_{t-L-B+1}^{t-B-1}), \mathsf{u}_t\right) \\ &= \left[\frac{1}{\sigma_z^2} + \frac{1}{1-\rho^{2(B+1)}(1-\eta(\sigma_z^2))}\right]^{-1} \qquad (177)\end{aligned}$$

Therefore by solving (177) the expression for σ_z^2 can be obtained. Finally the achievable rate is computed as:

$$\begin{aligned} R_{\text{GM-ME}}^+(L,B,D) &= I(\mathsf{s}_t; \mathsf{u}_t|\tilde{\mathsf{s}}_{t-L-B}, [\mathsf{u}]_{t-L-B+1}^{t-B-1}) \\ &= h(\mathsf{s}_t|\tilde{\mathsf{s}}_{t-L-B}, [\mathsf{u}]_{t-L-B+1}^{t-B-1}) - h(\mathsf{s}_t|\tilde{\mathsf{s}}_{t-L-B}, [\mathsf{u}]_{t-L-B+1}^{t-B-1}, \mathsf{u}_t) \\ &= h\left(\mathsf{s}_t|\hat{\mathsf{s}}_{t-B-1}(\tilde{\mathsf{s}}_{t-L-B}, [\mathsf{u}]_{t-L-B+1}^{t-B-1})\right) - \frac{1}{2}\log(2\pi e D) \\ &= \frac{1}{2}\log\left(2\pi e\left(1-\rho^{2(B+1)}(1-\eta(\sigma_z^2))\right)\right) - \frac{1}{2}\log(2\pi e D) \\ &= \frac{1}{2}\log\left(\frac{1-\rho^{2(B+1)}(1-\eta(\sigma_z^2))}{D}\right). \qquad (178)\end{aligned}$$

VIII. High Resolution Asymptotic

We investigate the behavior of the lossy rate-recovery functions for Gauss-Markov sources for single and multiple burst erasure channel models, i.e. $R_{\text{GM-SE}}(B,D)$ and $R_{\text{GM-ME}}(L,B,D)$, in the high resolution regime and establish Corollary 3. The following inequalities can be readily verified.

$$\begin{aligned} R_{\text{GM-SE}}^-(B,D) \leq R_{\text{GM-SE}}(B,D) \leq \\ R_{\text{GM-ME}}(L,B,D) \leq R_{\text{GM-ME}}^+(L,B,D) \end{aligned} \tag{179}$$

The first and the last inequalities in (179) are by definition and the second inequality follows from the fact that the rate achievable for multiple erasure model is also achievable for single burst erasure as the decoder can simply ignore the available codewords in reconstructing the source sequences. According to (179), it suffices to characterize the high resolution limit of $R_{\text{GM-SE}}^-(B,D)$ and $R_{\text{GM-ME}}^+(L,B,D)$ in Prop. 1 and Prop. 3 respectively.

For the lower bound note that as $D \to 0$ the expression for Δ in (12) satisfies

$$\Delta \triangleq (D\rho^2+1-\rho^{2(B+1)})^2 - 4D\rho^2(1-\rho^{2B}) \to (1-\rho^{2(B+1)})^2.$$

Upon direct substitution in (12) we have that

$$\lim_{D\to 0}\left\{R_{\text{GM-SE}}^-(B,D) - \frac{1}{2}\log\left(\frac{1-\rho^{2(B+1)}}{D}\right)\right\} = 0, \tag{180}$$

as required.

To establish the upper bound note that according to Prop. 3 we can write

$$\begin{aligned} &R_{\text{GM-ME}}^+(L,B,D) \\ &= I(\mathsf{s}_t; \mathsf{u}_t|\tilde{\mathsf{s}}_{t-L-B}, [\mathsf{u}]_{t-L-B+1}^{t-B-1}) \\ &= h(\mathsf{s}_t|\tilde{\mathsf{s}}_{t-L-B}, [\mathsf{u}]_{t-L-B+1}^{t-B-1}) - h(\mathsf{s}_t|\tilde{\mathsf{s}}_{t-L-B}, [\mathsf{u}]_{t-L-B+1}^{t-B-1}, \mathsf{u}_t) \\ &= h(\mathsf{s}_t|\tilde{\mathsf{s}}_{t-L-B}, [\mathsf{u}]_{t-L-B+1}^{t-B-1}) - \frac{1}{2}\log(2\pi e D) \qquad (181)\end{aligned}$$

where the last term follows from the definition of $\tilde{\mathsf{s}}_{t-L-B}$ in Prop. 3. Also we have

$$h(\mathsf{s}_t|\mathsf{s}_{t-B-1}) \leq h(\mathsf{s}_t|\tilde{\mathsf{s}}_{t-L-B}, [\mathsf{u}]_{t-L-B+1}^{t-B-1}) \leq h(\mathsf{s}_t|\mathsf{u}_{t-B-1}) \tag{182}$$

where the left hand side inequality in (182) follows from the following Markov property,

$$\{\tilde{\mathsf{s}}_{t-L-B}, [\mathsf{u}]_{t-L-B+1}^{t-B-1}\} \to \mathsf{s}_{t-B-1} \to \mathsf{s}_t \tag{183}$$

and the fact that conditioning reduces the differential entropy. Also, the right hand side inequality in (182) follows from the latter fact. By computing the upper and lower bounds in (182) we have

$$\begin{aligned} \frac{1}{2}\log\left(2\pi e(1-\rho^{2(B+1)})\right) \leq \\ h(\mathsf{s}_t|\tilde{\mathsf{s}}_{t-L-B}, [\mathsf{u}]_{t-L-B+1}^{t-B-1}) \leq \\ \frac{1}{2}\log\left(2\pi e\left(1-\frac{\rho^{2(B+1)}}{1+\sigma_z^2}\right)\right) \end{aligned} \tag{184}$$

Now note that

$$D \geq \sigma_t^2(\hat{s}_{t-L-B}, [u]_{t-L-B+1}^{t-B-1}, u_t) \geq \sigma_t^2(u_t, s_{t-1}) \tag{185}$$

$$= \left(\frac{1}{\sigma_z^2} + \frac{1}{1-\rho^2}\right)^{-1}. \tag{186}$$

which equivalently shows that if $D \to 0$ we have that $\sigma_z^2 \to 0$. By computing the limit of the upper and lower bounds in (184) as $D \to 0$, we can see that

$$\lim_{D\to 0} \Big\{ h(s_t|\tilde{s}_{t-L-B}, [u]_{t-L-B+1}^{t-B-1}) - \frac{1}{2}\log\left(2\pi e(1-\rho^{2(B+1)})\right)\Big\} = 0 \tag{187}$$

Finally (187) and (181) results in

$$\lim_{D\to 0}\left\{ R_{\text{GM-ME}}^{+}(L,B,D) - \frac{1}{2}\log\left(\frac{1-\rho^{2(B+1)}}{D}\right)\right\} = 0 \tag{188}$$

as required. Equations (180), (188) and (179) establishes the results of Corollary 3.

IX. Independent Gaussian Sources with Sliding Window Recovery: Proof of Theorem 2

In this section we study the memoryless Gaussian source model discussed in Section IV-C. The source sequences are drawn i.i.d. both in spatial and temporal dimension according to a unit-variance, zero-mean, Gaussian distribution $\mathcal{N}(0,1)$. The rate-R causal encoder sequentially compresses the source sequences and sends the codewords through the burst erasure channel. The channel erases a single burst of maximum length B and perfectly reveals the rest of the packets to the decoder. The decoder at each time i reconstructs $K+1$ past source sequences, i.e. $(s_i^n, s_{i-1}^n, \ldots, s_{i-K}^n)$ within a vector distortion measure $\mathbf{d} = (d_0, \ldots, d_K)$. More recent source sequences are required to be reconstructed within less distortion, i.e. $d_0 \leq d_1 \leq \ldots \leq d_K$. The decoder however is not interested in reconstructing the source sequences during the error propagation window, i.e. during the burst erasure and a window of length W after the burst erasure ends.

For this setup, we establish the rate-recovery function stated in Theorem 2. We do this by presenting the coding scheme in Section IX-B and the converse in Section IX-C. We also study some baseline schemes and compare their performance with the rate-recovery function at the end of this section.

Remark 6. *Our coding scheme in this section builds upon the technique introduced in [34] for lossless recovery of deterministic sources. The example involving deterministic sources in [34] established that the lower bound in Theorem 1 can be attained for a certain class of deterministic sources. The binning based scheme is suboptimal in general. The present paper does not include this example, but the reader is encouraged to see [34].*

A. Sufficiency of $K = B + W$

In our analysis we only consider the case $K = B + W$. The coding scheme can be easily extended to a general K as follows. If $K < B + W$, we can assume that the decoder, instead of recovering the source $\mathbf{t}_i = (s_i, s_{i-1}, \ldots, s_{i-K})^T$ at time i within distortion $\mathbf{d}$, aims to recover the source $\mathbf{t}_i' = (s_i, ..., s_{i-K'})^T$ within distortion $\mathbf{d}'$ where $K' = B + W$ and

$$d_j' = \begin{cases} d_j & \text{for } j \in \{0, 1, ..., K\} \\ 1 & \text{for } j \in \{K+1, ..., K'\}, \end{cases} \tag{189}$$

and thus this case is a special case of $K = B + W$. Note that layers $K+1, \ldots, K'$ require zero rate as the source sequences have unit variance.

If $K > B + W$, for each $j \in \{B + W + 1, \ldots, K\}$ the decoder is required to reconstruct s_{i-j}^n within distortion d_j. However we note the rate associated with these layers is again zero. In particular there are two possibilities during the recovery at time i. Either, $\hat{\mathbf{t}}_{i-1}^n$ or, $\hat{\mathbf{t}}_{i-B-W-1}^n$ are guaranteed to have been reconstructed. In the former case $\{\hat{s}_{i-j}^n\}_{d_{j-1}}$ is[2] available from time $i-1$ and $d_{j-1} \leq d_j$. In the latter case $\{\hat{s}_{i-j}^n\}_{d_{j-W-B-1}}$ is available from time $i-B-W-1$ and again $d_{j-W-B-1} \leq d_j$. Thus the reconstruction of any layer $j \geq B + W$ does not require any additional rate and it again suffices to assume $K = B + W$.

B. Coding Scheme

Throughout our analysis, we assume the source sequences are of length $n \cdot r$ where both n and r will be assumed to be arbitrarily large. The block diagram of the scheme is shown in Fig. 13. We partition $s_i^{n\cdot r}$ into r blocks each consisting of n symbols $(s_i^n)_l$. We then apply a successive refinement quantization codebook to each such block to generate $B+1$ indices $\left(\{m_{i,j}\}_{j=0}^{B}\right)_l$ as discussed in section IX-B1. Thereafter these indices are carefully rearranged in time to generate $(\mathbf{c}_i)_l$ as discussed in Section IX-B2. At each time we thus have a length r sequence $\mathbf{c}_i^r \triangleq \{(\mathbf{c}_i)_1, \ldots, (\mathbf{c}_i)_r\}$ We transmit the bin index of each sequence over the channel as in Section V-C. At the receiver the sequence $\hat{\mathbf{c}}_i^r$ is first reconstructed by the inner decoder. Thereafter upon rearranging the refinement layers in each packet, the required reconstruction sequences are produced. We provide the details of the encoding and decoding below.

1) Successive Refinement (SR) Encoder: The encoder at time i, first partitions the source sequence s_i^{nr} into r source sequences $(s_i^n)_l, l \in [1, r]$. As shown in Fig. 14, we encode each source signal $(s_i^n)_l$ using a $(B+1)$-layer successive refinement codebook [10], [35] to generate $(B+1)$ codewords whose indices are given by $\{(m_{i,0})_l, (m_{i,1})_l, \ldots, (m_{i,B})_l\}$ where $(m_{i,j})_l \in \{1, 2, \ldots, 2^{n\tilde{R}_j}\}$ for $j \in \{0, 1, \ldots, B\}$ and

$$\tilde{R}_j = \begin{cases} \frac{1}{2}\log(\frac{d_{W+1}}{d_0}) & \text{for } j = 0 \\ \frac{1}{2}\log(\frac{d_{W+j+1}}{d_{W+j}}) & \text{for } j \in \{1, 2, \ldots, B-1\} \\ \frac{1}{2}\log(\frac{1}{d_{W+B}}) & \text{for } j = B, \end{cases} \tag{190}$$

[2]The notation $\{\hat{s}_i^n\}_d$ indicates the reconstruction of $\hat{s}_i^n$ within average distortion d.

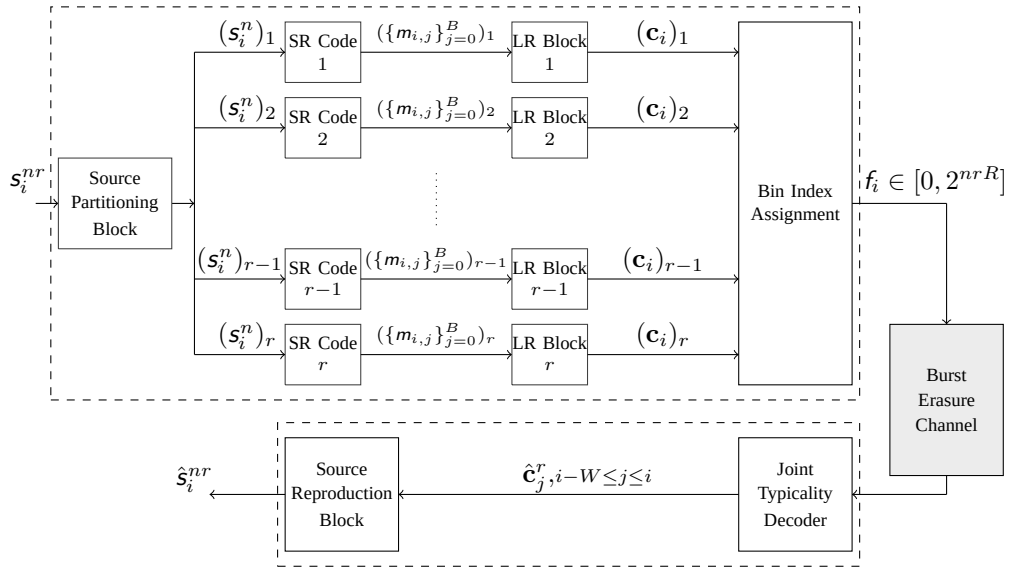

Fig. 13: Schematic of encoder and decoder for i.i.d. Gaussian with sliding window recovery constraint. SR and LR indicate successive refinement and layer rearrangement (Sections IX-B1 and IX-B2), respectively.

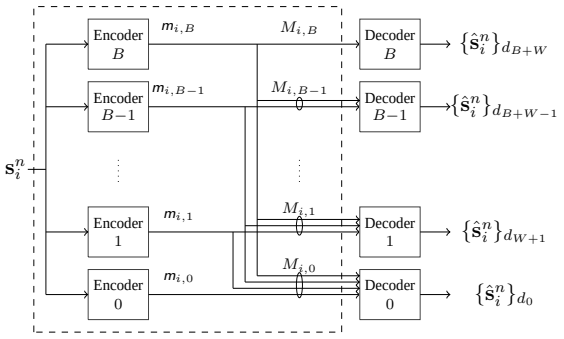

Fig. 14: $(B+1)$-layer coding scheme based on successive refinement (SR). Note that for each $k \in [0, B]$, $m_{i,k}$ is of rate $\tilde{R}_k$ and $M_{i,k}$ is of rate R_k. The dashed box represents the SR code.

The j-th layer uses indices

$$(M_{i,j})_l \triangleq \{(m_{i,j})_l, \ldots, (m_{i,B})_l\} \tag{191}$$

for reproduction and the associated rate with layer j is given by:

$$R_j = \begin{cases} \sum_{k=0}^{B} \tilde{R}_k = \frac{1}{2}\log(\frac{1}{d_0}) & \text{for } j = 0 \\ \sum_{k=j}^{B} \tilde{R}_k = \frac{1}{2}\log(\frac{1}{d_{W+j}}) & \text{for } j \in \{1, 2, \ldots, B\}, \end{cases} \tag{192}$$

and the corresponding distortion associated with layer j equals d_0 for $j = 0$ and d_{W+j} for $j \in \{1, 2, \ldots, B\}$.

From Fig. 14 it is clear that for any i and $j \in \{0, \ldots, B\}$, the j-th layer $M_{i,j}$ is a subset of $j-1$-th layer $M_{i,j-1}$, i.e. $M_{i,j} \subseteq M_{i,j-1}$.

2) Layer Rearrangement (LR) and Binning: In this stage the encoder rearranges the outputs of the SR blocks associated with different layers to produce an auxiliary set of sequences as follows[3].

$$\mathbf{c}_i \triangleq \begin{pmatrix} M_{i,0} \\ M_{i-1,1} \\ M_{i-2,2} \\ \vdots \\ M_{i-B,B} \end{pmatrix} \tag{193}$$

In the definition of (193) we note that $M_{i,0}$ consists of all the refinement layers associated with the source sequence at time i. It can be viewed as the "innovation symbol" since it is independent of all past symbols. It results in a distortion of d_0. The symbol $M_{i-1,1}$ consists of all refinement layers of the source sequence at time $i-1$, except the last layer and results in a distortion of d_1. Recall that $M_{i-1,1} \subseteq M_{i-1,0}$. In a similar fashion $M_{i-B,B}$ is associated with the source sequence at time $i-B$ and results in a distortion of d_B. Fig. 15 illustrates a schematic of these auxiliary codewords.

Note that as shown in Fig. 14 the encoder at each time generates r independent auxiliary codewords $(\mathbf{c}_i)_1, \ldots, (\mathbf{c}_i)_r$. Let $\mathbf{c}_i^r$ be the set of all r codewords. In the final step, the encoder generates f_i, the bin index associated with the codewords $\mathbf{c}_i^r$ and transmit this through the channel. The bin indices are randomly and independently assigned to all the codewords beforehand and are revealed to both encoder and decoder.

3) Decoding and Rate Analysis: To analyze the decoding process, first consider the simple case where the actual codewords $\mathbf{c}_i^r$ defined in (193), and not the assigned bin indices, are transmitted through the channel. In this case, whenever the channel packet is not erased by the channel, the decoder has access to the codewords $\mathbf{c}_i^r$. According to the problem setup, at anytime i outside the error propagation window,

[3]We suppress the index l in (191) for compactness.

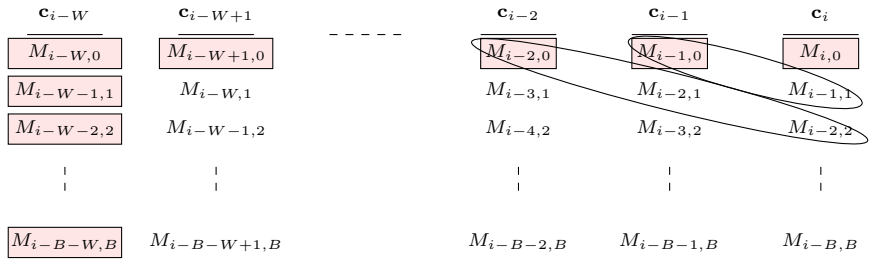

Fig. 15: Schematic of the auxiliary codewords defined in (193). The codewords are temporally correlated in a diagonal form depicted using ellipses. In particular, as shown in Fig. 14, $M_{i-j,j} \subseteq M_{i-j,j-1}$. Based on this diagonal correlation structure, the codewords depicted in the boxes are sufficient to know all the codewords .

when the decoder is interested in reconstructing the original source sequences, it has access to the past $W+1$ channel packets, i.e. $(f_{i-W}, \ldots, f_{i-1}, f_i)$. Therefore, the codewords $(\mathbf{c}_i^r, \mathbf{c}_{i-1}^r, \ldots, \mathbf{c}_{i-W}^r)$ are known to the decoder. Now consider the following claim.

Claim 1. *The decoder at each time i is able to reconstruct the source sequences within required distortion vector if either the sequences $(\mathbf{c}_i^r, \mathbf{c}_{i-1}^r, \ldots, \mathbf{c}_{i-W}^r)$ or $(\hat{\mathbf{t}}_{i-1}^{n\cdot r}, \mathbf{c}_i^r)$ is available.* □

Proof: Fig. 15 shows a schematic of the codewords. First consider the case where $(\mathbf{c}_i^r, \mathbf{c}_{i-1}^r, \ldots, \mathbf{c}_{i-W}^r)$ is known. According to (193) the decoder also knows $(M_{i,0}^r, M_{i-1,0}^r, \ldots, M_{i-W,0}^r)$. Therefore, according to SR structure depicted in Fig. 14, the source sequences $(s_i^{nr}, s_{i-1}^{nr}, \ldots, s_{i-W}^{nr})$ are each known within distortion d_0. This satisfies the original distortion constraint as $d_0 \leq d_k$ for each $k \in \{1, \ldots, W\}$. In addition, since $\mathbf{c}_{i-W}$ is known, according to (193), $(M_{i-W-1,1}^r, M_{i-W-2,2}^r, \ldots, M_{i-B-W,B}^r)$ is known and according to SR structure depicted in Fig. 14 the source sequences $(s_{i-W-1}^{nr}, s_{i-W-2}^{nr}, \ldots, s_{i-B-W}^{nr})$ are known within distortion $(d_{W+1}, d_{W+2}, \ldots, d_{B+W})$ which satisfies the distortion constraint. Now consider the case where $\hat{\mathbf{t}}_{i-1}^n$ and $\mathbf{c}_i^r$ are available, i.e. $\mathbf{t}_{i-1}^{nr}$ is already reconstructed within the required distortion vector, the decoder is able to reconstruct $\hat{\mathbf{t}}_i^{nr}$ from $\hat{\mathbf{t}}_{i-1}^{nr}$ and $\mathbf{c}_i^r$. In particular, from M_i^r the source sequence s_i^{nr} is reconstructed within distortion d_0. Also reconstruction of s_{i-k}^{nr} within distortion d_{k-1} is already available from $\hat{\mathbf{t}}_i$ for $k \in [1, B+W]$ which satisfies the distortion constraint as $d_{k-1} \leq d_k$. ■

Thus we have shown that if actual codewords $\mathbf{c}_i^r$ defined in (193) are transmitted the required distortion constraints are satisfied. It can be verified from (193) and (192) that the rate associated with the $\mathbf{c}_i^r$ is given by

$$R_{\mathcal{C}} = \sum_{k=0}^{B} R_k = \frac{1}{2}\log\left(\frac{1}{d_0}\right) + \sum_{j=1}^{B} \frac{1}{2}\log\left(\frac{1}{d_{W+j}}\right) \quad (194)$$

Thus compared to the achievable rate (25) in Theorem 2 we are missing the factor of $\frac{1}{W+1}$ in the second term. To reduce the rate, note that, as shown in Fig. 15 and based on definition of the auxiliary codewords in (193), there is a strong temporal correlation among the consecutive codewords. We therefore bin the set of all sequences $\mathbf{c}_i^r$ into 2^{nrR} bins as in Section V-C. The encoder, upon observing $\mathbf{c}_i^r$, only transmits its bin index f_i through the channel. We next describe the decoder and compute the minimum rate required to reconstruct $\mathbf{c}_i^r$.

Outside the error propagation window, one of the following cases can happen as discussed below. We claim that in either case the decoder is able to reconstruct $\mathbf{c}_i^r$ as follows.

- In the first case, the decoder has already recovered $\mathbf{c}_{i-1}^r$ and attempts to recover $\mathbf{c}_i^r$ given $(f_i, \mathbf{c}_{i-1}^r)$. This succeeds with high probability if

$$\begin{aligned} nR &\geq H(\mathbf{c}_i|\mathbf{c}_{i-1}) && (195)\\ &= H(M_{i,0}, M_{i-1,1}, \ldots, M_{i-B,B}|\mathbf{c}_{i-1}) && (196)\\ &= H(M_{i,0}, M_{i-1,1}, \ldots, M_{i-B,B}|M_{i-1,0}, M_{i-2,1}, \ldots, \\ &\quad \ldots M_{i-B,B-1}, M_{i-B-1,B}) && (197)\\ &= H(M_{i,0}) && (198)\\ &= nR_0 && (199) \end{aligned}$$

  where we use (193) in (196) and (197), and the fact that layer j is a subset of layer $j-1$ i.e., $M_{i-j,j} \subseteq M_{i-j,j-1}$ in (198). Thus the reconstruction of $\mathbf{c}_i^r$ follows since the choice of (25) satisfies (199). Thus according to the second part of Claim 1, the decoder is able to reconstruct $\hat{\mathbf{t}}_i^{n\cdot r}$.
- In the second case we assume that the decoder has not yet successfully reconstructed $\mathbf{c}_{i-1}^r$ but is required to reconstruct $\mathbf{c}_i^r$. In this case $\mathbf{c}_i^r$ is the first sequence to be recovered following the end of the error propagation window. Our proposed decoder uses $(f_i, f_{i-1}, \ldots, f_{i-W})$ to simultaneously reconstruct $(\mathbf{c}_i^r, \ldots, \mathbf{c}_{i-W}^r)$. This suc-

ceeds with high probability provided:

$$\begin{aligned}
&n(W+1)R \\
&\geq H(\mathbf{c}_{i-W}, \mathbf{c}_{i-W+1}, \ldots, \mathbf{c}_i) \\
&= H(\mathbf{c}_{i-W}, M_{i-W+1,0}, M_{i-W+2,0}, \ldots, M_{i,0}) \quad (200)\\
&= H(\mathbf{c}_{i-W}) + \sum_{k=1}^{W} H(M_{i-W+k,0}) \quad (201)\\
&= H(M_{i-W,0}, M_{i-W-1,1}, \ldots, M_{i-B-W,B}) \\
&\quad + \sum_{k=1}^{W} H(M_{i-W+k,0}) \\
&= n\sum_{k=1}^{B} R_k + n(W+1)R_0 \quad (202)
\end{aligned}$$

where in (200) we use the fact that the sub-symbols satisfy $M_{i,j+1} \subseteq M_{i,j}$ as illustrated in Fig. 15. In particular, in computing the rate in (200) all the sub-symbols in $\mathbf{c}_{i-W}$ and the sub-symbols $M_{j,0}$ for $j \in [i-W+1, i]$ need to be considered. From (199), (202) and (192), the rate R is achievable if

$$\begin{aligned}
R &\geq R_0 + \frac{1}{W+1}\sum_{k=1}^{B} R_k \quad (203)\\
&= \frac{1}{2}\log\left(\frac{1}{d_0}\right) + \frac{1}{2(W+1)}\sum_{k=1}^{B}\log\left(\frac{1}{d_{W+k}}\right). \quad (204)
\end{aligned}$$

as required. Thus, the rate constraint in (204) is sufficient for the decoder to recover the codewords $(\mathbf{c}_i^r, \ldots, \mathbf{c}_{i-W}^r)$ right after the error propagation window and to reconstruct $\hat{\mathbf{t}}_i^{n\cdot r}$ according to Claim 1.

Thus, the rate constraint in (204) is sufficient for the decoder to succeed in reconstructing the source sequences within required distortion constraints at the anytime i outside error propagation window. This completes the justification of the upper bound in Theorem 2.

C. Converse for Theorem 2

We need to show that for any sequence of codes that achieve a distortion tuple $(d_0, \ldots, d_{W+B})$ the rate is lower bounded by (204). As in the proof of Theorem 1, we consider a burst erasure of length B spanning the time interval $[t-B-W, t-W-1]$. Consider,

$$\begin{aligned}
(W+1)nR &\geq H([f]_{t-W}^t) \\
&\geq H([f]_{t-W}^t | [f]_0^{t-B-W-1}, s_{-1}^n) \quad (205)
\end{aligned}$$

where the last step follows from the fact that conditioning reduces entropy. We need to lower bound the entropy term in (205). Consider

$$\begin{aligned}
&H([f]_{t-W}^t | [f]_0^{t-B-W-1}, s_{-1}^n) \\
&= I([f]_{t-W}^t; \mathbf{t}_t^n | [f]_0^{t-B-W-1}, s_{-1}^n) + \\
&\quad H([f]_{t-W}^t | [f]_0^{t-B-W-1}, \mathbf{t}_t^n, s_{-1}^n) \quad (206)\\
&= h(\mathbf{t}_t^n | [f]_0^{t-B-W-1}, s_{-1}^n) - h(\mathbf{t}_t^n | [f]_0^{t-B-W-1}, [f]_{t-W}^t, s_{-1}^n) + \\
&\quad H([f]_{t-W}^t | [f]_0^{t-B-W-1}, \mathbf{t}_t^n, s_{-1}^n) \\
&= h(\mathbf{t}_t^n) - h(\mathbf{t}_t^n | [f]_0^{t-B-W-1}, [f]_{t-W}^t, s_{-1}^n) + \\
&\quad H([f]_{t-W}^t | [f]_0^{t-B-W-1}, \mathbf{t}_t^n, s_{-1}^n) \quad (207)
\end{aligned}$$

where (207) follows since $\mathbf{t}_t^n = (s_{t-B-W}^n, \ldots, s_t^n)$ is independent of $([f]_0^{t-B-W-1}, s_{-1}^n)$ as the source sequences s_i^n are generated i.i.d. . By expanding $\mathbf{t}_t^n$ we have that

$$h(\mathbf{t}_t^n) = h(s_{t-B-W}^n, \ldots, s_{t-W-1}^n) + h(s_{t-W}^n, \ldots, s_t^n), \quad (208)$$

and

$$\begin{aligned}
&h(\mathbf{t}_t^n | [f]_0^{t-B-W-1}, [f]_{t-W}^t, s_{-1}^n) \\
&= h(s_{t-B-W}^n, \ldots, s_{t-W-1}^n | [f]_0^{t-B-W-1}, [f]_{t-W}^t, s_{-1}^n) + \\
&\quad h\left(s_{t-W}^n, \ldots, s_t^n | [f]_0^{t-B-W-1}, [f]_{t-W}^t, s_{t-B-W}^n, \right. \\
&\qquad \left. \ldots, s_{t-W-1}^n, s_{-1}^n\right) \quad (209)
\end{aligned}$$

We next establish the following claim whose proof is in Appendix G.

Lemma 11. *The following two inequalities holds.*

$$\begin{aligned}
&h(s_{t-B-W}^n, \ldots, s_{t-W-1}^n) - \\
&\quad h(s_{t-B-W}^n, \ldots, s_{t-W-1}^n | [f]_0^{t-B-W-1}, [f]_{t-W}^t, s_{-1}^n) \\
&\qquad \geq \sum_{i=1}^{B} \frac{n}{2}\log\left(\frac{1}{d_{W+i}}\right) \quad (210)
\end{aligned}$$

$$\begin{aligned}
&h(s_{t-W}^n, \ldots, s_t^n) - \\
&\quad h\left(s_{t-W}^n, \ldots, s_t^n | [f]_0^{t-B-W-1}, [f]_{t-W}^t, s_{t-B-W}^n, \right. \\
&\qquad \left. \ldots, s_{t-W-1}^n, s_{-1}^n\right) \\
&\quad + H([f]_{t-W}^t | [f]_0^{t-B-W-1}, \mathbf{t}_t^n, s_{-1}^n) \\
&\qquad \geq \frac{n(W+1)}{2}\log\left(\frac{1}{d_0}\right) \quad (211)
\end{aligned}$$

□

Proof: See Appendix G. ■

From (207), (208), (209), (210) and (211), we can write

$$\begin{aligned}
&H\left([f]_{t-W}^t | [f]_0^{t-B-W-1}, s_{-1}^n\right) \geq \\
&\qquad \frac{n}{2}\sum_{i=1}^{B}\log\left(\frac{1}{d_{W+i}}\right) + \frac{n(W+1)}{2}\log\left(\frac{1}{d_0}\right). \quad (212)
\end{aligned}$$

Substituting (212) into (205) and taking $n \to \infty$, we recover

$$R \geq \frac{1}{2}\log_2\left(\frac{1}{d_0}\right) + \frac{1}{2(W+1)}\sum_{j=1}^{B}\log_2\left(\frac{1}{d_{W+j}}\right). \quad (213)$$

as required.

D. Illustrative Suboptimal Schemes

We compare the optimal lossy rate-recovery function with the following suboptimal schemes.

1) Still-Image Compression: In this scheme, the encoder ignores the decoder's memory and at time $i \geq 0$ encodes the source $\mathbf{t}_i$ in a memoryless manner and sends the codewords through the channel. The rate associated with this scheme is

$$R_{\text{SI}}(\mathbf{d}) = I(\mathbf{t}_i; \hat{\mathbf{t}}_i) = \sum_{k=0}^{K} \frac{1}{2} \log\left(\frac{1}{d_k}\right) \tag{214}$$

In this scheme, the decoder is able to recover the source whenever its codeword is available, i.e. at all the times except when the erasure happens.

2) Wyner-Ziv Compression with Delayed Side Information: At time i the encoders assumes that $\mathbf{t}_{i-B-1}$ is already reconstructed at the receiver within distortion $\mathbf{d}$. With this assumption, it compresses the source $\mathbf{t}_i$ according to Wyner-Ziv scheme and transmits the codewords through the channel. The rate of this scheme is

$$R_{\text{WZ}}(B, \mathbf{d}) = I(\mathbf{t}_i; \hat{\mathbf{t}}_i | \hat{\mathbf{t}}_{i-B-1}) = \sum_{k=0}^{B} \frac{1}{2} \log\left(\frac{1}{d_k}\right) \tag{215}$$

Note that, if at time i, $\hat{\mathbf{t}}_{i-B-1}$ is not available, $\hat{\mathbf{t}}_{i-1}$ is available and the decoder can still use it as side-information to construct $\hat{\mathbf{t}}_i$ since $I(\mathbf{t}_i; \hat{\mathbf{t}}_i | \hat{\mathbf{t}}_{i-B-1}) \geq I(\mathbf{t}_i; \hat{\mathbf{t}}_i | \hat{\mathbf{t}}_{i-1})$.

As in the case of Still-Image Compression, the Wyner-Ziv scheme also enables the recovery of each source sequence except those with erased codewords.

3) Predictive Coding plus FEC: This scheme consists of predictive coding followed by a Forward Error Correction (FEC) code to compensate the effect of packet losses of the channel. As the contribution of B erased codewords need to be recovered using $W+1$ available codewords, the rate of this scheme can be computed as follows.

$$R_{\text{FEC}}(B, W, \mathbf{d}) = \frac{B+W+1}{W+1} I(\mathbf{t}_i; \hat{\mathbf{t}}_i | \hat{\mathbf{t}}_{i-1}) \tag{216}$$

$$= \frac{B+W+1}{2(W+1)} \log\left(\frac{1}{d_0}\right) \tag{217}$$

4) GOP-Based Compression: This scheme consists of predictive coding where the synchronization sources (I-frames) are inserted periodically to prevent error propagation. The synchronization frames are transmitted with the rate $R_1 = I(\mathbf{t}_i; \hat{\mathbf{t}}_i)$ and the rest of the frames are transmitted at the rate $R_2 = I(\mathbf{t}_i; \hat{\mathbf{t}}_i | \hat{\mathbf{t}}_{i-1})$ using predictive coding. Whenever the erasure happens the decoder fails to recover the source sequences until the next synchronization source and then the decoder becomes synced to the encoder. In order to guarantee the recovery of the sources, the synchronization frames have to be inserted with the period of at most $W+1$. This results in the following average rate expression.

$$R = \frac{1}{(W+1)} I(\mathbf{t}_i; \hat{\mathbf{t}}_i) + \frac{W}{(W+1)} I(\mathbf{t}_i; \hat{\mathbf{t}}_i | \hat{\mathbf{t}}_{i-1}) \tag{218}$$

$$= \frac{1}{2(W+1)} \sum_{k=0}^{K} \log(\frac{1}{d_k}) + \frac{W}{2(W+1)} \log(\frac{1}{d_0}) \tag{219}$$

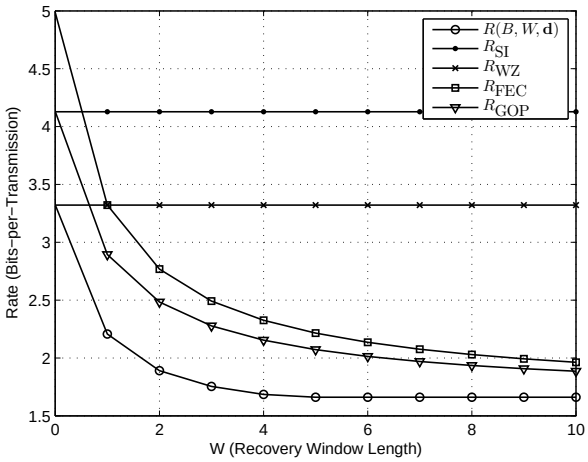

Fig. 16: Comparison of rate-recovery of suboptimal systems to minimum possible rate-recovery function for different recovery window length W. We assume $K = 5$, $B = 2$ and a distortion vector $\mathbf{d} = (0.1, 0.25, 0.4, 0.55, 0.7, .85)$.

In Fig. 16, we compare the result in Theorem 2 with the described schemes. It can be observed from Fig. 16 that except when $W = 0$ none of the other schemes are optimal. The *Predictive Coding plus FEC* scheme, which is a natural separation based scheme and the *GOP-based* compression scheme are suboptimal even for relatively large values of W. Also note that the *GOP-based* compression scheme reduces to *Still-Image* compression for $W = 0$.

X. Conclusions

We presented a real-time streaming scenario where a sequence of source vectors must be sequentially encoded, and transmitted over a burst erasure channel. The source vectors must be reconstructed with zero delay at the destination. However those sequences that occur during the erasure burst or a period of length W following the burst need not be reconstructed. We assume that the source vectors are sampled i.i.d. across the spatial dimension and from a first-order, stationary, Markov process across the temporal dimension. We study the minimum achievable compression rate, which we define to be the rate-recovery function in our setup.

For the case of discrete sources and lossless recovery, we establish upper and lower bounds on the rate-recovery function and observe that they coincide for the special cases when $W = 0$ and $W \to \infty$. More generally both our upper and lower bound expressions can be expressed as the rate of predictive coding plus another term that decreases at-least inversely with W. For the restricted class of memoryless encoders and symmetric sources, we establish that a binning based scheme is optimal. For the case of Gauss-Markov sources and a quadratic distortion measure, we establish upper and lower bounds on the minimum rate when $W = 0$ and observe that these bounds coincide in the high-resolution regime. The achievability is based on a quantize and binning scheme, but the analysis is a non-trivial extension of the lossless case as the reconstruction sequences at the destination

do not form a Markov chain. We also study another setup involving independent Gaussian sources and a sliding-window reconstruction constraint where the rate-recovery function is attained using a successive refinement coding scheme.

We believe that the present work can be extended in a number of directions. The focus in this paper has been on causal encoders and zero-delay decoders. It is interesting to consider more general encoders with finite-lookahead and decoders with delay constraint. Some such extensions have been recently considered in [36]. Secondly, the paper considers only the case of burst-erasure channels. It may be interesting to consider channels that introduce both burst erasures and isolated erasures as considered recently in the channel coding context [21]. Thirdly, our present setup assumes that within the recovery period, a complete outage is declared, and no reconstruction is necessary. Finally our paper only addressed the case of lossless recovery for discrete sources. Extensions to lossy reconstruction, analogous to the case of Gaussian sources, will require characterization of the worst-case erasure sequence for a general source model, which appears challenging. This may be further generalized by considering partial recovery with a higher distortion during the recovery period. Such extensions will undoubtedly lead to a finer understanding of tradeoffs between compression rate and error propagation in video transmission systems.

Appendix A
Proof of Corollary 1

We want to show the following equality.

$$R^+(B,W) = H(s_1|s_0) + \frac{1}{W+1} I(s_B; s_{B+1}|s_0) = \frac{1}{W+1} H(s_{B+1}, s_{B+2}, \ldots, s_{B+W+1}|s_0) \tag{220}$$

According to the chain rule of entropies, the term in (220) can be written as

$$\begin{aligned} &H(s_{B+1}, s_{B+2}, \ldots, s_{B+W+1}|s_0) && (221)\\ &= H(s_{B+1}|s_0) + \sum_{k=1}^{W} H(s_{B+k+1}|s_0, s_{B+1}, \ldots, s_{B+k}) \\ &= H(s_{B+1}|s_0) + WH(s_1|s_0) && (222)\\ &= H(s_{B+1}|s_0) - H(s_{B+1}|s_B, s_0) + H(s_{B+1}|s_B, s_0) \\ &\quad + WH(s_1|s_0) && (223)\\ &= H(s_{B+1}|s_0) - H(s_{B+1}|s_B, s_0) + H(s_{B+1}|s_B) \\ &\quad + WH(s_1|s_0) && (224)\\ &= I(s_{B+1}; s_B|s_0) + (W+1)H(s_1|s_0) && (225)\\ &= (W+1)R^+(B,W) && (226) \end{aligned}$$

where (222) follows from the Markov property

$$(s_0, s_{B+1}, \ldots, s_{B+k-1}) \to s_{B+k} \to s_{B+k+1} \tag{227}$$

for any k and from the stationarity of the sources which for each k implies that

$$H(s_{B+k+1}|s_{B+k}) = H(s_1|s_0). \tag{228}$$

Note that in (223) we add and subtract the same term and (224) also follows from the Markov property of (227) for $k = 0$.

Appendix B
Proof of Lemma 4

Define $q_k \triangleq 2^{\frac{2}{n} h(s_k^n | f^k, s_{-1}^n)}$. We need to show that

$$q_k \geq \frac{2\pi e(1-\rho^2)}{2^{2R} - \rho^2} \left(1 - \left(\frac{\rho^2}{2^{2R}}\right)^k\right) \tag{229}$$

Consider the following entropy term.

$$\begin{aligned} &h(s_k^n | [f]_0^k, s_{-1}^n) = h(s_k^n | [f]_0^{k-1}, s_{-1}^n) - I(f_k; s_k^n | [f]_0^{k-1}, s_{-1}^n) \\ &= h(s_k^n | [f]_0^{k-1}, s_{-1}^n) - \\ &\qquad H(f_k | [f]_0^{k-1}, s_{-1}^n) + H(f_k | s_k^n, [f]_0^{k-1}, s_{-1}^n) \\ &\geq h(s_k^n | [f]_0^{k-1}, s_{-1}^n) - H(f_k) && (230)\\ &\geq \frac{n}{2} \log\left(\rho^2 2^{\frac{2}{n} h(s_{k-1}^n | [f]_0^{k-1}, s_{-1}^n)} + 2\pi e(1-\rho^2)\right) - nR && (231) \end{aligned}$$

where (230) follows from the fact that conditioning reduces entropy and (231) follows from the Entropy Power Inequality similar to (101). Thus

$$q_k \geq \frac{\rho^2}{2^{2R}} q_{k-1} + \frac{2\pi e(1-\rho^2)}{2^{2R}}. \tag{232}$$

By repeating the iteration in (232), we have

$$\begin{aligned} q_k &\geq (\frac{\rho^2}{2^{2R}})^k q_0 + \frac{2\pi e(1-\rho^2)}{2^{2R}} \sum_{l=0}^{k-1} (\frac{\rho^2}{2^{2R}})^l && (233)\\ &\geq \frac{2\pi e(1-\rho^2)}{2^{2R} - \rho^2} \left(1 - \left(\frac{\rho^2}{2^{2R}}\right)^k\right), && (234) \end{aligned}$$

where (234) follows from the fact $0 < \frac{\rho^2}{2^{2R}} < 1$ for any $\rho \in (0,1)$ and $R > 0$. This completes the proof.

Appendix C
Proof of (235) and (236)

We need to show (112) and (113), i.e. we need to establish the following two inequities for each $k \in [1 : t - B']$

$$h(u_t | [u]_0^{t-B'-k-1}, [u]_{t-k}^{t-1}, s_{-1}) \leq h(u_t | [u]_0^{t-B'-k}, [u]_{t-k+1}^{t-1}, s_{-1}) \tag{235}$$

$$h(s_t | [u]_0^{t-B'-k-1}, [u]_{t-k}^{t}, s_{-1}) \leq h(s_t | [u]_0^{t-B'-k}, [u]_{t-k+1}^{t}, s_{-1}). \tag{236}$$

We first establish the following Lemmas.

Lemma 12. *Consider random variables $\{X_0, X_1, X_2, Y_1, Y_2\}$ that are jointly Gaussian, $X_k \sim \mathcal{N}(0,1), k \in \{0,1,2\}$, $X_0 \to X_1 \to X_2$ and that for $j \in \{1,2\}$ we have:*

$$X_j = \rho_j X_{j-1} + N_j, \tag{237}$$

$$Y_j = X_j + Z_j. \tag{238}$$

Assume that $Z_j \sim \mathcal{N}(0, \sigma_z^2)$ are independent of all random variables and likewise $N_j \sim \mathcal{N}(0, 1-\rho_j^2)$ for $j \in \{1,2\}$ are also independent of all random variables. The structure of correlation is sketched in Fig. 17. Then we have that:

$$\sigma^2_{X_2}(X_0, Y_2) \leq \sigma^2_{X_2}(X_0, Y_1) \tag{239}$$

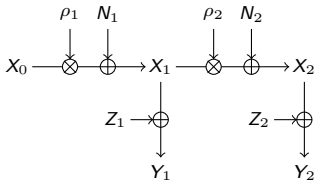

Fig. 17: Relationship of the Variables for Lemma 12.

where $\sigma^2_{X_2}(X_0, Y_j)$ denotes the minimum mean square error of estimating X_2 from $\{X_0, Y_j\}$.

Proof: By applying the standard relation for the MMSE estimation error we have (see e.g. [32])

$$\sigma^2_{X_2}(X_0, Y_1) = E[X_2^2] - \begin{pmatrix} E[X_2Y_1] & E[X_2X_0] \end{pmatrix} \begin{pmatrix} E[Y_1^2] & E[X_0Y_1] \\ E[X_0Y_1] & E[X_0^2] \end{pmatrix}^{-1} \begin{pmatrix} E[X_2Y_1] \\ E[X_2X_0] \end{pmatrix} \tag{240}$$

$$= 1 - \rho_2^2 \begin{pmatrix} 1 & \rho_1 \end{pmatrix} \begin{pmatrix} 1+\sigma_z^2 & \rho_1 \\ \rho_1 & 1 \end{pmatrix}^{-1} \begin{pmatrix} 1 \\ \rho_1 \end{pmatrix} \tag{241}$$

$$= 1 - \frac{\rho_1^2\rho_2^2\sigma_z^2 - \rho_1^2\rho_2^2 + \rho_2^2}{1+\sigma_z^2-\rho_1^2} \tag{242}$$

where we use the fact that $E[X_0^2] = 1$, $E[Y_1^2] = 1+\sigma_z^2$, $E[X_0Y_1] = \rho_1$, $E[X_2X_0] = \rho_0\rho_1$ and $E[X_2Y_1] = \rho_2$. In a similar fashion it can be shown that:

$$\sigma^2_{X_2}(X_0, Y_2) = 1 - \begin{pmatrix} 1 & \rho_1\rho_2 \end{pmatrix} \begin{pmatrix} 1+\sigma_z^2 & \rho_1\rho_2 \\ \rho_1\rho_2 & 1 \end{pmatrix}^{-1} \begin{pmatrix} 1 \\ \rho_1\rho_2 \end{pmatrix} \tag{243}$$

$$= 1 - \frac{\rho_1^2\rho_2^2\sigma_z^2 - \rho_1^2\rho_2^2 + 1}{1+\sigma_z^2-\rho_1^2\rho_2^2} \tag{244}$$

To establish (239) we only need to show that,

$$\frac{\rho_1^2\rho_2^2\sigma_z^2 - \rho_1^2\rho_2^2 + 1}{1+\sigma_z^2-\rho_1^2\rho_2^2} \geq \frac{\rho_1^2\rho_2^2\sigma_z^2 - \rho_1^2\rho_2^2 + \rho_2^2}{1+\sigma_z^2-\rho_1^2} \tag{245}$$

It is equivalent to showing

$$\frac{1+\sigma_z^2-\rho_1^2}{1+\sigma_z^2-\rho_1^2\rho_2^2} \geq \frac{\rho_1^2\rho_2^2\sigma_z^2 - \rho_1^2\rho_2^2 + \rho_2^2}{\rho_1^2\rho_2^2\sigma_z^2 - \rho_1^2\rho_2^2 + 1} \tag{246}$$

or equivalently

$$1 - \frac{\rho_1^2(1-\rho_2^2)}{1+\sigma_z^2-\rho_1^2\rho_2^2} \geq 1 - \frac{1-\rho_2^2}{\rho_1^2\rho_2^2\sigma_z^2 - \rho_1^2\rho_2^2 + 1} \tag{247}$$

which is equivalent to showing

$$\frac{\rho_1^2}{1+\sigma_z^2-\rho_1^2\rho_2^2} \leq \frac{1}{\rho_1^2\rho_2^2\sigma_z^2 - \rho_1^2\rho_2^2 + 1}. \tag{248}$$

However note that (248) can be immediately verified since the left hand side has the numerator smaller than the right hand side and the denominator greater than the right hand side whenever $\rho_i^2 \in (0,1)$. This completes the proof. ■

Lemma 13. *Consider the Gauss-Markov source model* (11) *and the test channel in Prop. 3. For a fixed t, $k \in [1,t]$ and a set $\Omega \subseteq [t-k, t]$, consider two sets of random variables $\mathcal{W}_1$ and $\mathcal{W}_2$ each jointly Gaussian with s_{t-k} such that the following Markov property holds:*

$$\mathcal{W}_1 \to s_{t-k} \to \{s_t, \mathbf{u}_\Omega\} \tag{249}$$

$$\mathcal{W}_2 \to s_{t-k} \to \{s_t, \mathbf{u}_\Omega\} \tag{250}$$

If the MMSE error in s_{t-k} satisfies , $\sigma^2_{t-k}(\mathcal{W}_1) \leq \sigma^2_{t-k}(\mathcal{W}_2)$ then we have

$$h(s_t|\mathcal{W}_1, \mathbf{u}_\Omega) \leq h(s_t|\mathcal{W}_2, \mathbf{u}_\Omega), \qquad \forall \Omega \subseteq [t-k, t] \tag{251}$$

$$h(u_t|\mathcal{W}_1, \mathbf{u}_\Omega) \leq h(u_t|\mathcal{W}_2, \mathbf{u}_\Omega), \qquad \forall \Omega \subseteq [t-k, t-1]. \tag{252}$$

Proof: Since the underlying random variables are jointly Gaussian, we can express the MMSE estimates of s_{t-k} from $\mathcal{W}_j$, $j \in \{1,2\}$ as follows (see e.g. [32])

$$\hat{s}_{t-k}(\mathcal{W}_1) = \alpha_1 s_{t-k} + e_1 \tag{253}$$

$$\hat{s}_{t-k}(\mathcal{W}_2) = \alpha_2 s_{t-k} + e_2 \tag{254}$$

where $e_1 \sim \mathcal{N}(0, E_1)$ and $e_2 \sim \mathcal{N}(0, E_2)$ are Gaussian random variables both independent of s_{t-k}. Furthermore the constants in (253) and (254) are given by

$$\alpha_j = 1 - \sigma^2_{t-k}(\mathcal{W}_j) \tag{255}$$

$$E_j = \sigma^2_{t-k}(\mathcal{W}_j)(1 - \sigma^2_{t-k}(\mathcal{W}_j)) \tag{256}$$

for $j = 1, 2$. To establish (251), we have

$$h(s_t|\mathcal{W}_1, \mathbf{u}_\Omega) = h(s_t|\hat{s}_{t-k}(\mathcal{W}_1), \mathbf{u}_\Omega) \tag{257}$$

$$= h(s_t|\alpha_1 s_{t-k} + e_1, \mathbf{u}_\Omega) \tag{258}$$

$$\leq h(s_t|\alpha_2 s_{t-k} + e_2, \mathbf{u}_\Omega) \tag{259}$$

$$= h(s_t|\hat{s}_{t-k}(\mathcal{W}_2), \mathbf{u}_\Omega) \tag{260}$$

$$= h(s_t|\mathcal{W}_2, \mathbf{u}_\Omega) \tag{261}$$

where (257) and (261) follows from the following Markov property.

$$\mathcal{W}_1 \to \hat{s}_{t-k}(\mathcal{W}_1) \to \{s_t, u_\Omega\} \tag{262}$$

$$\mathcal{W}_2 \to \hat{s}_{t-k}(\mathcal{W}_2) \to \{s_t, u_\Omega\} \tag{263}$$

(258) and (260) follows from (253) and (254) and (259) follows from the fact that $\sigma^2_{t-k}(\mathcal{W}_1) \leq \sigma^2_{t-k}(\mathcal{W}_2)$ implies that

$$\frac{E_1}{\alpha_1^2} \leq \frac{E_2}{\alpha_2^2} \tag{264}$$

Thus the only difference between (258) and (259) is that the variance of the independent noise component in the first term is smaller in the former. Clearly we obtain a better estimate of s_t in (258), which justifies the inequality in (259).

Eq. (252) can be established as an immediate consequence of (251). Since the noise z_t in the test channel is Gaussian and independent of all other random variables, we have

$$\mathrm{Var}(u_t|\mathcal{W}_j, \mathbf{u}_\Omega) = \mathrm{Var}(s_t|\mathcal{W}_j, \mathbf{u}_\Omega) + \sigma_z^2 \tag{265}$$

where the notation $\mathrm{Var}(a|\mathcal{W})$ indicates the noise variance of estimating a from $\mathcal{W}$. As a result,

$$h(u_t|\mathcal{W}_j, \mathbf{u}_\Omega) = \frac{1}{2}\log\left(2^{2h(s_t|\mathcal{W}_j, \mathbf{u}_\Omega)} + 2\pi e\sigma_z^2\right). \tag{266}$$

Thus (251) immediately imples (252). ∎

We now establish (235) and subsequently establish (236) in a similar fashion. Consider the following two steps.

1) First by applying Lemma 12 we show.

$$\sigma^2_{t-k}([u]_0^{t-B'-k-1}, u_{t-k}, s_{-1}) \leq \sigma^2_{t-k}([u]_0^{t-B'-k-1}, u_{t-B'-k}, s_{-1}), \quad (267)$$

i.e., knowing $\{[u]_0^{t-B'-k-1}, u_{t-k}, s_{-1}\}$ rather than $\{[u]_0^{t-B'-k-1}, u_{t-B'-k}, s_{-1}\}$, improves the estimate of the source s_{t-k}. Let $\hat{s}_{t-B'-k}([u]_0^{t-B'-k-1}, s_{-1})$ be the MMSE estimator of $s_{t-B'-k}$ given $([u]_0^{t-B'-k-1}, s_{-1})$.

Note that $\hat{s}_{t-B'-k}([u]_0^{t-B'-k-1}, s_{-1})$ is a sufficient statistic of $s_{t-B'-k}$ given $\{[u]_0^{t-B'-k-1}, s_{-1}\}$ and thus we have that:

$$\{[u]_0^{t-B'-k-1}, s_{-1}\} \rightarrow \hat{s}_{t-B'-k}([u]_0^{t-B'-k-1}, s_{-1}) \rightarrow s_{t-B'-k} \rightarrow s_{t-k}. \quad (268)$$

Therefore, by application of Lemma 12 for $X_0 = \hat{s}_{t-B'-k}([u]_0^{t-B'-k-1}, s_{-1})$, $X_1 = s_{t-B'-k}$, $Y_1 = u_{t-B'-k}$, $X_2 = s_{t-k}$ and $Y_2 = u_{t-k}$, we have

$$\begin{aligned}
&\sigma^2_{t-k}([u]_0^{t-B'-k-1}, u_{t-k}, s_{-1}) \\
&= \sigma^2_{t-k}(\hat{s}_{t-B'-k}([u]_0^{t-B'-k-1}, s_{-1}), u_{t-k}) && (269)\\
&\leq \sigma^2_{t-k}(\hat{s}_{t-B'-k}([u]_0^{t-B'-k-1}, s_{-1}), u_{t-B'-k}) && (270)\\
&= \sigma^2_{t-k}([u]_0^{t-B'-k-1}, u_{t-B'-k}, s_{-1}). && (271)
\end{aligned}$$

where (269) and (271) both follow from (268). This completes the claim in (267).

2) In the second step, we apply Lemma 13 for

$$\begin{aligned}
\mathcal{W}_1 &= \{[u]_0^{t-B'-k-1}, u_{t-k}, s_{-1}\} && (272)\\
\mathcal{W}_2 &= \{[u]_0^{t-B'-k-1}, u_{t-B'-k}, s_{-1}\} && (273)\\
\Omega &= [t-k+1, t-1] && (274)
\end{aligned}$$

we have

$$h\left(u_t \mid [u]_0^{t-B'-k-1}, [u]_{t-k}^{t-1}, s_{-1}\right) \leq h\left(u_t \mid [u]_0^{t-B'-k}, [u]_{t-k+1}^{t-1}, s_{-1}\right) \quad (275)$$

and again by applying Lemma 13 for $\mathcal{W}_1$ and $\mathcal{W}_2$ in (272) and (273) and $\Omega = [t-k+1, t]$, we have

$$h\left(s_t \mid [u]_0^{t-B'-k-1}, [u]_{t-k}^{t}, s_{-1}\right) \leq h\left(s_t \mid [u]_0^{t-B'-k}, [u]_{t-k+1}^{t}, s_{-1}\right) \quad (276)$$

This establishes (235) and (236) and equivalently (112) and (113).

Appendix D
Proof of Lemma 8

For reader's convenience, we first repeat the statement of the Lemma. Consider the two sets $A, B \subseteq \mathbb{N}$ each of size r as $A = \{a_1, a_2, \cdots, a_r\}$, $B = \{b_1, b_2, \cdots, b_r\}$ such that $1 \leq a_1 < a_2 < \cdots < a_r$ and $1 \leq b_1 < b_2 < \cdots < b_r$ and for any $i \in \{1, \ldots, r\}$, $a_i \leq b_i$. Then the test channel (106) satisfies the following:

$$\begin{aligned}
h(s_t|\mathbf{u}_A, s_{-1}) &\geq h(s_t|\mathbf{u}_B, s_{-1}), \quad \forall t \geq b_r && (277)\\
h(u_t|\mathbf{u}_A, s_{-1}) &\geq h(u_t|\mathbf{u}_B, s_{-1}), \quad \forall t > b_r. && (278)
\end{aligned}$$

We first prove (277) by induction as follows. The proof of (278) follows directly from (277) as discussed at the end of this section.

• First we show that (277) is true for $r = 1$, i.e. given $0 \leq a_1 \leq b_1$ and for all $t \geq b_1$ we need to show

$$h(s_t \mid u_{a_1}, s_{-1}) \geq h(s_t \mid u_{b_1}, s_{-1}). \quad (279)$$

We apply Lemma 12 in Appendix C for $\{X_0, X_1, X_2, Y_1, Y_2\} = \{s_{-1}, s_{a_1}, s_{b_1}, u_{a_1}, u_{b_1}\}$ which results in

$$h(s_{b_1}|u_{a_1}, s_{-1}) \geq h(s_{b_1}|u_{b_1}, s_{-1}) \quad (280)$$

Thus (279) holds for $t = b_1$. For any $t > b_1$ we can always express $s_t = \rho^{t-b_1} s_{b_1} + \tilde{n}$ where $\tilde{n} \sim \mathcal{N}(0, 1-\rho^{2(t-b_1)})$ and also we can express $s_{b_1} = \hat{s}_{b_1}(u_j, s_{-1}) + w_j$ for $j \in \{a_1, b_1\}$ where $w_j \sim \mathcal{N}(0, \sigma^2_{b_1}(u_j, s_{-1}))$ is the MMSE estimation error. For $j \in \{a_1, b_1\}$, we have

$$s_t = \rho^{t-b_1}\hat{s}_{b_1}(u_j, s_{-1}) + \rho^{t-b_1} w_j + \tilde{n}. \quad (281)$$

Then we have

$$\begin{aligned}
\sigma^2_t(u_{a_1}, s_{-1}) &= \rho^{2(t-b_1)}\sigma^2_{b_1}(u_{a_1}, s_{-1}) + 1 - \rho^{2(t-b_1)} && (282)\\
&\geq \rho^{2(t-b_1)}\sigma^2_{b_1}(u_{b_1}, s_{-1}) + 1 - \rho^{2(t-b_1)} && (283)\\
&= \sigma^2_t(u_{b_1}, s_{-1}) && (284)
\end{aligned}$$

where (283) immediately follows from (280). Thus (284) establishes (279) and the proof of the base case is now complete.

• Now assume that (277) is true for r, i.e. for the sets A_r, B_r of size r satisfying $a_i \leq b_i$ for $i \in \{1, \cdots, r\}$ and any $t \geq b_r$,

$$h(s_t|\mathbf{u}_{A_r}, s_{-1}) \geq h(s_t|\mathbf{u}_{B_r}, s_{-1}) \quad (285)$$

We show that the lemma is also true for the sets $A_{r+1} = \{A_r, a_{r+1}\}$ and $B_{r+1} = \{B_r, b_{r+1}\}$ where $a_r \leq a_{r+1}$, $b_r \leq b_{r+1}$ and $a_{r+1} \leq b_{r+1}$. We establish this in two steps.

1) We show that

$$h(s_t|\mathbf{u}_{A_{r+1}}, s_{-1}) \geq h(s_t|\mathbf{u}_{A_r}, u_{b_{r+1}}, s_{-1}). \quad (286)$$

By application of Lemma 12 for

$$\{X_0, X_1, X_2, Y_1, Y_2\} = \{\hat{s}_{a_r}(\mathbf{u}_{A_r}, s_{-1}), s_{a_{r+1}}, s_{b_{r+1}}, u_{a_{r+1}}, u_{b_{r+1}}\} \quad (287)$$

we have

$$h(s_{b_{r+1}}|\hat{s}_{a_r}(\mathbf{u}_{A_r}, s_{-1}), u_{a_{r+1}}) \geq h(s_{b_{r+1}}|\hat{s}_{a_r}(\mathbf{u}_{A_r}, s_{-1}), u_{b_{r+1}}) \quad (288)$$

Thus (286) holds for $t = b_{r+1}$. For $t \geq b_{r+1}$ we can use the argument analogous to that leading to (284). We omit the details as they are completely analogous. This establishes (286).

2) Next we show that

$$h(\mathsf{s}_t|\mathbf{u}_{A_r}, u_{b_{r+1}}, \mathsf{s}_{-1}) \geq \tag{289}$$
$$h(\mathsf{s}_t|\mathbf{u}_{B_{r+1}}, \mathsf{s}_{-1}). \tag{290}$$

First note that based on the induction hypothesis in (285) for $t = b_{r+1}$ we have

$$h(\mathsf{s}_{b_{r+1}}|\mathbf{u}_{A_r}, \mathsf{s}_{-1}) \geq h(\mathsf{s}_{b_{r+1}}|\mathbf{u}_{B_r}, \mathsf{s}_{-1}) \tag{291}$$

and equivalently

$$\sigma^2_{b_{r+1}}(\mathbf{u}_{A_r}, \mathsf{s}_{-1}) \geq \sigma^2_{b_{r+1}}(\mathbf{u}_{B_r}, \mathsf{s}_{-1}) \tag{292}$$

Now by application of Lemma 13 for $k = t - b_r$ and

$$\mathcal{W}_1 = \{\mathbf{u}_{B_r}, \mathsf{s}_{-1}\} \tag{293}$$
$$\mathcal{W}_2 = \{\mathbf{u}_{A_r}, \mathsf{s}_{-1}\} \tag{294}$$
$$\Omega = \{b_{r+1}\} \tag{295}$$

and noting that $\mathcal{W}_j \to \mathsf{s}_{b_r} \to (\mathsf{s}_{b_{r+1}}, u_\Omega)$ for $j = 1, 2$ we have

$$h(\mathsf{s}_t|\mathbf{u}_{A_r}, u_{b_{r+1}}, \mathsf{s}_{-1}) \geq h(\mathsf{s}_t|\mathbf{u}_{B_r}, u_{b_{r+1}}, \mathsf{s}_{-1}) \tag{296}$$

which is equivalent to (290).

Combining (286) and (290) we have $h(\mathsf{s}_t|\mathbf{u}_{A_{r+1}}, \mathsf{s}_{-1}) \geq h(\mathsf{s}_t|\mathbf{u}_{B_{r+1}}, \mathsf{s}_{-1})$ which shows that (277) is also true for $r+1$.

This completes the induction and the proof of (277) for general r.

Finally note that (277) implies (278) as follows.

$$h(u_t|\mathbf{u}_{A_r}, \mathsf{s}_{-1}) = \frac{1}{2}\log\left(2^{2h(\mathsf{s}_t|\mathbf{u}_{A_r}, \mathsf{s}_{-1})} + 2\pi e\sigma_z^2\right) \tag{297}$$
$$\geq \frac{1}{2}\log\left(2^{2h(\mathsf{s}_t|\mathbf{u}_{B_r}, \mathsf{s}_{-1})} + 2\pi e\sigma_z^2\right) \tag{298}$$
$$= h(u_t|\mathbf{u}_{B_r}, \mathsf{s}_{-1}) \tag{299}$$

where (297) follows from the fact that the noise in the test channel is independent. Also (298) follows from (277). This completes the proof.

Appendix E
Proof of Lemma 9

We prove each part separately as follows.

1) For any feasible set Ω_t with size θ we have

$$\lambda_t(\Omega_t) = I(\mathsf{s}_t; u_t|\mathbf{u}_{\Omega_t}, \mathsf{s}_{-1})$$
$$= h(u_t|\mathbf{u}_{\Omega_t}, \mathsf{s}_{-1}) - h(u_t|\mathsf{s}_t)$$
$$\leq h(u_t|\mathbf{u}_{\Omega_t^\star(\theta)}, \mathsf{s}_{-1}) - h(u_t|\mathsf{s}_t) \tag{300}$$
$$= I(\mathsf{s}_t; u_t|\mathbf{u}_{\Omega_t^\star(\theta)}, \mathsf{s}_{-1})$$
$$= \lambda_t(\Omega_t^\star(\theta)) \tag{301}$$

where (300) follows from the application of Lemma 8 with $A = \Omega_t^\star(\theta)$ and $B = \Omega_t$, which by construction of $\Omega_t^\star(\theta)$ clearly satisfy the required condition. Also note that

$$\frac{1}{2}\log\left(2\pi e\gamma_t(\Omega_t)\right) = h(\mathsf{s}_t|u_t, \mathbf{u}_{\Omega_t}, \mathsf{s}_{-1})$$
$$\leq h(\mathsf{s}_t|u_t, \mathbf{u}_{\Omega_t^\star(\theta)}, \mathsf{s}_{-1}) \tag{302}$$
$$= \frac{1}{2}\log\left(2\pi e\gamma_t(\Omega_t^\star(\theta))\right) \tag{303}$$

where (302) follows from Lemma 8 for the sets $A = \{\Omega_t^\star(\theta), t\}$ and $B = \{\Omega_t, t\}$. Thus we have $\gamma_t(\Omega_t) \leq \gamma_t(\Omega_t^\star(\theta))$.

2) We next argue that both $\lambda_t(\Omega_t^\star(\theta))$ and $\gamma_t(\Omega_t^\star(\theta))$ attain their maximum values with the minimum possible θ. Recall from Part 1 that when the number of erasures $n_e = t - \theta$ is fixed, the worst case sequence must have all erasure positions as close to t as possible. Thus if $n_e \leq B$ the worst case sequence consists of a single burst spanning $[t - n_e, t - 1]$. If $B < n_e \leq 2B$, the worst case sequence must have two burst erasures spanning $[t-n_e-L, t-B-L-1]\cup[t-B, t-1]$. More generally the worst case sequence will consist of a sequence of burst erasures each (except possibly the first one) of length B separated by a guard interval of length L. Thus the non-erased indices associated with decreasing values of θ are nested, i.e. $\theta_1 \leq \theta_2$ implies that $\Omega_t^\star(\theta_1) \subseteq \Omega_t^\star(\theta_2)$. Further note that adding more elements in the non-erased indices $\Omega_t^\star(\cdot)$ can only decrease both $\lambda_t(\cdot)$ and $\gamma_t(\cdot)$, i.e. $\Omega_t^\star(\theta_1) \subseteq \Omega_t^\star(\theta_2)$ implies that $\lambda_t(\Omega_t^\star(\theta_1)) \geq \lambda_t(\Omega_t^\star(\theta_2))$ and $\gamma_t(\Omega_t^\star(\theta_1)) \geq \gamma_t(\Omega_t^\star(\theta_2))$. Thus the worst case $\Omega_t^\star(\theta)$ must constitute the minimum possible value of θ. The formal proof, which is analogous to the second part of Lemma 6 will be skipped.

3) This property follows from the fact that in steady state the effect of knowing s_{-1} vanishes. In particular we show below that $\lambda_{t+1}(\Omega_{t+1}^\star) \geq \lambda_t(\Omega_t^\star)$ and $\gamma_{t+1}(\Omega_{t+1}^\star) \geq \gamma_t(\Omega_t^\star)$.

$$\lambda_{t+1}(\Omega_{t+1}^\star)$$
$$= I(\mathsf{s}_{t+1}; u_{t+1}|\mathbf{u}_{\Omega_{t+1}^\star}, \mathsf{s}_{-1})$$
$$= h(u_{t+1}|\mathbf{u}_{\Omega_{t+1}^\star}, \mathsf{s}_{-1}) - h(u_{t+1}|\mathsf{s}_{t+1})$$
$$\geq h(u_{t+1}|\mathbf{u}_{\Omega_{t+1}^\star}, \mathsf{s}_{-1}, \mathsf{s}_0) - h(u_{t+1}|\mathsf{s}_{t+1}) \tag{304}$$
$$= h(u_{t+1}|\mathbf{u}_{\Omega_{t+1}^\star\setminus\{0\}}, \mathsf{s}_0) - h(u_{t+1}|\mathsf{s}_{t+1}) \tag{305}$$
$$= h(u_t|\mathbf{u}_{\Omega_t^\star}, \mathsf{s}_{-1}) - h(u_t|\mathsf{s}_t) \tag{306}$$
$$= I(\mathsf{s}_t; u_t|\mathbf{u}_{\Omega_t^\star}, \mathsf{s}_{-1})$$
$$= \lambda_t(\Omega_t^\star) \tag{307}$$

where (304) follows from the fact that conditioning reduces the differential entropy. Also in (305) the notation $\Omega_{t+1}^\star\setminus\{0\}$ indicates the set $\Omega_{t+1}^\star$ when the index 0 is excluded if $0 \in \Omega_{t+1}^\star$. It can be easily verified that the set $\Omega_t^\star$ is equivalent to the set obtained by left shifting the elements of the set $\Omega_{t+1}^\star\setminus\{0\}$ by one. Then (305) follows from this fact and the following Markov property.

$$\{u_0, \mathsf{s}_{-1}\} \to \{\mathbf{u}_{\Omega_{t+1}^\star\setminus\{0\}}, \mathsf{s}_0\} \to u_{t+1} \tag{308}$$

Eq. (306) follows from the time-invariant property of source model and the test channel. Also note that

$$\frac{1}{2}\log\left(2\pi e\gamma_{t+1}(\Omega_{t+1}^\star)\right) = h(\mathsf{s}_{t+1}|u_{t+1}, \mathbf{u}_{\Omega_{t+1}^\star}, \mathsf{s}_{-1})$$
$$\geq h(\mathsf{s}_{t+1}|u_{t+1}, \mathbf{u}_{\Omega_{t+1}^\star}, \mathsf{s}_{-1}, \mathsf{s}_0) \tag{309}$$
$$= h(\mathsf{s}_{t+1}|u_{t+1}, \mathbf{u}_{\Omega_{t+1}^\star\setminus\{0\}}, \mathsf{s}_0) \tag{310}$$
$$= h(\mathsf{s}_t|u_t, \mathbf{u}_{\Omega_t^\star}, \mathsf{s}_{-1}) \tag{311}$$
$$= \frac{1}{2}\log\left(2\pi e\gamma_t(\Omega_t^\star)\right) \tag{312}$$

where (309) follows from the fact that conditioning reduces the differential entropy, (310) follows from the following Markov property

$$\{u_0, s_{-1}\} \to \{\mathbf{u}_{\Omega^\star_{t+1}\setminus\{0\}}, u_{t+1}, s_0\} \to s_{t+1} \tag{313}$$

and (311) again follows from the time-invariant property of source model and the test channel.

Appendix F
Proof of Lemma 10

We need to show

$$I(s_t; u_t|\tilde{s}_{t-L-B}, [u]_{t-L-B+1}^{t-B-1}) \geq \lim_{t\to\infty} \lambda_t(\Omega_t^\star) = \lim_{t\to\infty} I(s_t; u_t|\mathbf{u}_{\Omega_t^\star}, s_{-1}) \tag{314}$$

$$\sigma_t^2(\tilde{s}_{t-L-B}, [u]_{t-L-B+1}^{t-B-1}, u_t) \geq \lim_{t\to\infty} \gamma_t(\Omega_t^\star) = \lim_{t\to\infty} \sigma_t^2(\mathbf{u}_{\Omega_t^\star}, u_t, s_{-1}) \tag{315}$$

For any $t > L + B$, we can write

$$\begin{aligned}
\lambda_t(\Omega_t^\star) &= I(s_t; u_t|\mathbf{u}_{\Omega_t^\star}, s_{-1}) && (316)\\
&= I(s_t; u_t|\mathbf{u}_{\Omega^\star_{t-L-B}}, [u]_{t-L-B+1}^{t-B-1}, s_{-1}) && (317)\\
&= I(s_t; u_t|\hat{s}_{t-L-B}(\mathbf{u}_{\Omega^\star_{t-L-B}}, s_{-1}), [u]_{t-L-B+1}^{t-B-1}) && (318)\\
&\leq I(s_t; u_t|\tilde{\alpha}s_{t-L-B} + \tilde{e}, [u]_{t-L-B+1}^{t-B-1}) && (319)\\
&= I(s_t; u_t|s_{t-L-B} + e, [u]_{t-L-B+1}^{t-B-1})\\
&= I(s_t; u_t|\tilde{s}_{t-L-B}, [u]_{t-L-B+1}^{t-B-1}) && (320)\\
&= R^+_{\text{GM-ME}}(L, B, D) && (321)
\end{aligned}$$

where (317) follows from the structure of $\Omega_t^\star$ in Lemma 9, (318) follows from the Markov relation

$$\{\mathbf{u}_{\Omega^\star_{t-L-B}}, s_{-1}\} \to \{\hat{s}_{t-L-B}(\mathbf{u}_{\Omega^\star_{t-L-B}}, s_{-1}), [u]_{t-L-B+1}^{t-B-1}\} \to s_t \tag{322}$$

and in (319) we introduce $\tilde{\alpha} = 1 - D$ and $\tilde{e} \sim \mathcal{N}(0, D(1-D))$. This follows from the fact that the estimate $\hat{s}_{t-L-B}(\mathbf{u}_{\Omega^\star_{t-L-B}}, s_{-1})$ satisfies the average distortion constraint of D. In (320) we re-normalize the test channel so that $e \sim \mathcal{N}(0, D/(1-D))$. Taking the limit of (321) when $t \to \infty$, results in (314). Also note that

$$\begin{aligned}
\gamma_t(\Omega_t^\star) &= \sigma_t^2(\mathbf{u}_{\Omega_t^\star}, u_t, s_{-1})\\
&= \sigma_t^2(\mathbf{u}_{\Omega^\star_{t-L-B}}, [u]_{t-L-B+1}^{t-B-1}, u_t, s_{-1})\\
&= \sigma_t^2(\hat{s}_{t-L-B}(\mathbf{u}_{\Omega^\star_{t-L-B}}, s_{-1}), [u]_{t-L-B+1}^{t-B-1}, u_t) && (323)\\
&\leq \sigma_t^2(\tilde{\alpha}s_{t-L-B} + \tilde{e}, [u]_{t-L-B+1}^{t-B-1}, u_t) && (324)\\
&= \sigma_t^2(s_{t-L-B} + e, [u]_{t-L-B+1}^{t-B-1}, u_t) && (325)\\
&= \sigma_t^2(\tilde{s}_{t-L-B}, [u]_{t-L-B+1}^{t-B-1}, u_t) && (326)
\end{aligned}$$

where (323) follows from the following Markov property (322) and (324) again follows from the fact that the estimate $\hat{s}_{t-L-B}(\mathbf{u}_{\Omega^\star_{t-L-B}}, s_{-1})$ satisfies the distortion constraint. All the constants and variables in (324) and (325) are as defined before. Again, taking the limit of (326) when $t \to \infty$ results in (315).

According to (321) and (326) if we choose the noise in the test channel σ_z^2 to satisfy

$$\sigma_t^2(\tilde{s}_{t-L-B}, [u]_{t-L-B+1}^{t-B-1}, u_t) = D \tag{327}$$

then the test channel and the rate $R^+_{\text{GM-ME}}(L, B, D)$ defined in (321) both satisfy rate and distortion constraints in (168) and (169) and therefore $R^+_{\text{GM-ME}}(L, B, D)$ is achievable.

Appendix G
Proof of Lemma 11

We first show that (210) which is repeated in (328) at the top of next page. From the fact that conditioning reduces the differential entropy, we can lower bound the left hand side in (328) by

$$\sum_{i=0}^{B-1} \big(h(s_{t-B-W+i}^n) - h(s_{t-B-W+i}^n|[f]_0^{t-B-W-1}, [f]_{t-W}^t, s_{-1}^n)\big) \tag{329}$$

We show that for each $i = 0, 1, \ldots, B-1$

$$h(s_{t-B-W+i}^n) - h(s_{t-B-W+i}^n|[f]_0^{t-B-W-1}, [f]_{t-W}^t, s_{-1}^n) \geq \frac{n}{2}\log\left(\frac{1}{d_{B+W-i}}\right), \tag{330}$$

which then establishes (328). Recall that since there is a burst erasure between time $t \in [t-B-W, t-W-1]$ the receiver is required to reconstruct

$$\hat{\mathbf{t}}_t^n = \left[\hat{s}_t^n, \ldots, \hat{s}_{t-B-W}^n\right] \tag{331}$$

with a distortion vector $(d_0, \ldots, d_{B+W})$ i.e., a reconstruction of $\hat{s}_{t-B-W+i}^n$ is desired with a distortion of d_{B+W-i} for $i = 0, 1, \ldots, B+W$ when the decoder is revealed $([f]_0^{t-B-W-1}, [f]_{t-W}^t)$. Hence

$$\begin{aligned}
&h(s_{t-B-W+i}^n) - h(s_{t-B-W+i}^n|[f]_0^{t-B-W-1}, [f]_{t-W}^t, s_{-1}^n)\\
&\quad= h(s_{t-B-W+i}^n) - h\left(s_{t-B-W+i}^n|[f]_0^{t-B-W-1}, [f]_{t-W}^t, s_{-1}^n, \{\hat{s}_{t-B-W+i}^n\}_{d_{B+W-i}}\right) && (332)\\
&\quad\geq h(s_{t-B-W+i}^n) - h(s_{t-B-W+i}^n|\{\hat{s}_{t-B-W+i}^n\}_{d_{B+W-i}}) && (333)\\
&\quad\geq h(s_{t-B-W+i}^n) - h(s_{t-B-W+i}^n - \{\hat{s}_{t-B-W+i}^n\}_{d_{B+W-i}}) && (334)
\end{aligned}$$

Since we have that

$$E\left[\frac{1}{n}\sum_{j=1}^{n}(s_{t-B-W+i,j} - \hat{s}_{t-B-W+i,j})^2\right] \leq d_{B+W-i} \tag{335}$$

It follows from standard arguments that [29, Chapter 13] that

$$h(s_{t-B-W+i}^n - \{\hat{s}_{t-B-W+i}^n\}_{d_{B+W-i}}) \leq \frac{n}{2}\log 2\pi e(d_{B+W-i}). \tag{336}$$

Substituting (336) into (334) and the fact that $h(s_{t-B-W+i}^n) = \frac{n}{2}\log 2\pi e$ establishes (330).

$$h(\boldsymbol{s}_{t-B-W}^n,\ldots,\boldsymbol{s}_{t-W-1}^n)-h(\boldsymbol{s}_{t-B-W}^n,\ldots,\boldsymbol{s}_{t-W-1}^n|[f]_0^{t-B-W-1},[f]_{t-W}^t,\boldsymbol{s}_{-1}^n)\geq\sum_{i=1}^{B}\frac{n}{2}\log(\frac{1}{d_{W+i}}) \tag{328}$$

$$\begin{aligned}&h(\boldsymbol{s}_{t-W}^n,\ldots,\boldsymbol{s}_t^n)-h(\boldsymbol{s}_{t-W}^n,\ldots,\boldsymbol{s}_t^n|[f]_0^{t-B-W-1},[f]_{t-W}^t,\boldsymbol{s}_{t-B-W}^n,\ldots,\boldsymbol{s}_{t-W-1}^n,\boldsymbol{s}_{-1}^n)\\&+H([f]_{t-W}^t|[f]_0^{t-B-W-1},\mathbf{t}_t^n,\boldsymbol{s}_{-1}^n)\geq\frac{n(W+1)}{2}\log(\frac{1}{d_0})\end{aligned} \tag{337}$$

Now we establish (211) which is repeated in (337) at the top of next page. Since $(\boldsymbol{s}_{t-W}^n,\ldots,\boldsymbol{s}_t^n)$ are independent we can express the left-hand side in (337) as:

$$\begin{aligned}&I\left(\boldsymbol{s}_{t-W}^n,\ldots,\boldsymbol{s}_t^n;[f]_{t-W}^t\,|[f]_0^{t-B-W-1},\boldsymbol{s}_{t-B-W}^n,\right.\\&\quad\left.\ldots,\boldsymbol{s}_{t-W-1}^n,\boldsymbol{s}_{-1}^n\right)\\&+H([f]_{t-W}^t|[f]_0^{t-B-W-1},\mathbf{t}_t^n,\boldsymbol{s}_{-1}^n)\end{aligned} \tag{338}$$

$$=H([f]_{t-W}^t|[f]_0^{t-B-W-1},\boldsymbol{s}_{t-B-W}^n,\ldots,\boldsymbol{s}_{t-W-1}^n,\boldsymbol{s}_{-1}^n) \tag{339}$$

$$\begin{aligned}&\geq H([f]_{t-W}^t|[f]_0^{t-W-1},\boldsymbol{s}_{t-B-W}^n,\ldots,\boldsymbol{s}_{t-W-1}^n,\boldsymbol{s}_{-1}^n)\\&\geq I\left([f]_{t-W}^t;\boldsymbol{s}_{t-W}^n,\ldots,\boldsymbol{s}_t^n|[f]_0^{t-W-1},\boldsymbol{s}_{t-B-W}^n,\right.\\&\quad\left.\ldots,\boldsymbol{s}_{t-W-1}^n,\boldsymbol{s}_{-1}^n\right)\end{aligned} \tag{340}$$

The above mutual information term can be bounded as follows:

$$\begin{aligned}&h(\boldsymbol{s}_{t-W}^n,\ldots,\boldsymbol{s}_t^n|[f]_0^{t-W-1},\boldsymbol{s}_{t-B-W}^n,\ldots,\boldsymbol{s}_{t-W-1}^n,\boldsymbol{s}_{-1}^n)\\&\quad-h(\boldsymbol{s}_{t-W}^n,\ldots,\boldsymbol{s}_t^n|[f]_0^t,\boldsymbol{s}_{t-B-W}^n,\ldots,\boldsymbol{s}_{t-W-1}^n,\boldsymbol{s}_{-1}^n)\\&=h(\boldsymbol{s}_{t-W}^n,\ldots,\boldsymbol{s}_t^n)\\&\quad-h(\boldsymbol{s}_{t-W}^n,\ldots,\boldsymbol{s}_t^n|[f]_0^t,\boldsymbol{s}_{t-B-W}^n,\ldots,\boldsymbol{s}_{t-W-1}^n,\boldsymbol{s}_{-1}^n)\end{aligned} \tag{341}$$

$$\geq h(\boldsymbol{s}_{t-W}^n,\ldots,\boldsymbol{s}_t^n)-h(\boldsymbol{s}_{t-W}^n,\ldots,\boldsymbol{s}_t^n|\{\hat{\boldsymbol{s}}_{t-W}^n\}_{d_0},\ldots,\{\hat{\boldsymbol{s}}_t^n\}_{d_0}) \tag{342}$$

$$\begin{aligned}&\geq\sum_{i=0}^{W}\left(h(\boldsymbol{s}_{t-W+i}^n)-h(\boldsymbol{s}_{t-W+i}^n-\{\hat{\boldsymbol{s}}_{t-W+i}^n\}_{d_0})\right)\\&\geq\sum_{i=0}^{W}\frac{n}{2}\log(\frac{1}{d_0})=\frac{n(W+1)}{2}\log(\frac{1}{d_0})\end{aligned} \tag{343}$$

where (341) follows from the independence of $(\boldsymbol{s}_{t-W}^n,\ldots,\boldsymbol{s}_t^n)$ from the past sequences, and (342) follows from the fact that given the entire past $[f]_0^t$ each source sub-sequence needs to be reconstructed with a distortion of d_0 and the last step follows from the standard approach in the proof of the rate-distortion theorem. This establishes (337).

This completes the proof.

REFERENCES

[1] Y. Wang, S. Wenger, J. Wen, and A. Katsaggelos, "Error resilient video coding techniques," *IEEE Signal Processing Magazine*, vol. 17, no. 4, pp. 61–82, 2000.

[2] W. Tan and A. Zakhor, "Video multicast using layered FEC and scalable compression," *IEEE Transactions on Circuits and Systems for Video Technology*, vol. 11, pp. 373–386, 2001.

[3] Y. Huang, Y. Kochman, and G. Wornell, "Causal transmission of colored source frames over a packet erasure channel," in *DCC*, 2010, pp. 129–138.

[4] S. S. Pradhan and K. Ramchandran, "Distributed source coding using syndromes (DISCUS): Design and construction," *IEEE Trans. Inform. Theory*, vol. 49, pp. 626–643, Mar. 2003.

[5] J. Wang, V. Prabhakaran, and K. Ramchandran, "Syndrome-based robust video transmission over networks with bursty losses," in *ICIP*, Atlanta, GA, 2006.

[6] H. S. Witsenhausen, "On the structure of real-time source coders," *Bell Syst. Tech. J.*, vol. 58, no. 6, pp. 1437–1451, Jul-Aug 1979.

[7] D. Teneketzis, "On the structure of optimal real-time encoders and decoders in noisy communication," *IEEE Trans. Inform. Theory*, vol. 52, no. 9, pp. 4017–4035, sep 2006.

[8] H. Asnani and T. Weissman, "Real-time coding with limited lookahead," *IEEE Trans. Inform. Theory*, vol. 59, no. 6, pp. 3582–3606, 2013.

[9] H. Viswanathan and T. Berger, "Sequential coding of correlated sources," *IEEE Trans. Inform. Theory*, vol. 46, no. 1, pp. 236 –246, jan 2000.

[10] W. H. Equitz and T. M. Cover, "Successive refinement of information," *IEEE Trans. Inform. Theory*, vol. 37, pp. 269–275, Mar. 1991.

[11] J. Wang and X. Wu, "Information flows in video coding," in *Data Compression Conference (DCC)*, 2010, pp. 149–158.

[12] N. Ma and P. Ishwar, "On delayed sequential coding of correlated sources," *IEEE Trans. Inform. Theory*, vol. 57, pp. 3763–3782, 2011.

[13] L. Song, J. Chen, J. Wang, and T. Liu, "Gaussian robust sequential and predictive coding," *IEEE Trans. Inform. Theory*, vol. 59, no. 6, pp. 3635–3652, 2013.

[14] S. Y. Chung, "On the construction of some capacity approaching coding schemes," Ph.D. dissertation, Mass. Instit. of Tech., 2000.

[15] X. Chen and E. Tuncel, "Zero-delay joint source-channel coding for the Gaussian Wyner-Ziv problem," in *ISIT*, 2011, pp. 2929–2933.

[16] T. Arildsen, M. N. Murthi, S. V. Andersen, and S. H. Jensen, "On predictive coding for erasure channels using a Kalman framework," *IEEE Trans. Signal Processing*, vol. 57, no. 11, pp. 4456–4466, 2009.

[17] C. Chang, "Streaming source coding with delay," Ph.D. dissertation, U. C. Berkeley, 2007.

[18] S. Draper, C. Chang, and A. Sahai, "Sequential random binning for streaming distributed source coding," in *Proc. Int. Symp. Inform. Theory*, 2005, pp. 1396–1400.

[19] R. G. Gallager, *Information Theory and Reliable Communication*. John Wiley and Sons, 1968.

[20] E. Martinian, "Dynamic information and constraints in source and channel coding," Ph.D. dissertation, Mass. Instit. of Tech., 2004.

[21] A. Badr, A. Khisti, W. Tan, and J. Apostolopoulos, "Streaming codes for channels with burst and isolated erasures," in *Proc. IEEE INFOCOMM*, June 2013.

[22] O. Tekin, T. Ho, H. Yao, and S. Jaggi, "On erasure correction coding for streaming," in *ITA*, 2012, pp. 221–226.

[23] D. Leong and T. Ho, "Erasure coding for real-time streaming," in *ISIT*, 2012.

[24] D. Aldous, "Reversible Markov chains and random walks on graphs (Chapter 3)," unpublished notes, available at http://www.stat.berkeley.edu/∼aldous/RWG/book.html, Sep. 2002.

[25] Y. Oohama, "Gaussian multiterminal source coding," *IEEE Trans. Inform. Theory*, vol. 43, no. 6, pp. 1912–1923, 1997.

[26] I. Csiszàr and J. Korner, "Towards a general theory of source networks," *IEEE Trans. Inform. Theory*, vol. 26, no. 2, pp. 155 – 165, mar 1980.

[27] T. M. Cover, "A proof of the data compression theorem of Slepian and Wolf for ergodic sources," *IEEE Trans. Inform. Theory*, vol. IT-21, no. 2, pp. 226–228, 1995.

[28] D. Slepian and J. K. Wolf, "Noiseless coding of correlated information sources," *IEEE Trans. Inform. Theory*, vol. 19, pp. 471–480, July 1973.

[29] T. M. Cover and J. A. Thomas, *Elements of Information Theory*. John Wiley and Sons, 1991.

[30] S. Tavildar, P. Viswanath, and A. B. Wagner, "The Gaussian many-help-one distributed source coding problem," *IEEE Trans. Inform. Theory*, vol. 56, no. 1, pp. 564–581, 2010.
[31] H. V. Poor, *An Introduction to Signal Detection and Estimation*, 2*nd Ed.* NewYork: Springer Verlag.
[32] A. S. Willsky, G. W. Wornell, and J. H. Shapiro, *Stochastic Processes, Detection and Estimation*. 6.432 Course Notes, Department of Electrical Engineering and Computer Science, MIT, 2003.
[33] S. Tung, "Multiterminal source coding," Ph.D. dissertation, Cornell University, 1978.
[34] F. Etezadi and A. Khisti, "Prospicient real-time coding of Markov sources over burst erasure channels: Lossless case," in *Proc. Data Compression Conf.*, Apr. 2012.
[35] B. Rimoldi, "Successive refinement of information: Characterization of the achievable rates," *IEEE Trans. Inform. Theory*, vol. 40, pp. 253–259, Jan. 1994.
[36] F. Etezadi and A. Khisti, "Sequential transmission of Markov sources over burst erasure channels," in *International Zurich Seminar*, 2014.